A STUDY OF CHROMATIN STRUCTURE

by

CATHERINE HSIAO-YIN CHANG

A dissertation submitted to the Graduate Faculty in Biochemistry in partial fulfillment of the requirements for the degree of Doctor of Philosophy, The City University of New York.

1976

This manuscript has been read and accepted for the Graduate Faculty in Biochemistry in satisfaction of the dissertation requirement for the degree of Doctor of Philosophy.

2-20-76
Date

Chairman of Examining Committee

2-20-76
Date

Executive Officer

Liont Cohn

R.A. Eckhardt

Aaron Lukton

Joseph Kraus

TABLE OF CONTENTS

ACKNOWLEDGMENTS

I wish to express my sincere thanks to Dr. H. J. Li for his constant help and advice given in the course of this research.

I would also like to thank my committee members Dr. Ronald Eckhardt and Dr. Aaron Lukton for their kind help.

A special thanks is due Dr. Irving Listowsky for being so understanding during the writing and completion of this thesis.

Special thanks is also due Manny Weiskopf and Zoi Evagelinou for their invaluable collaboration in the polylysine and trypsin work used in this thesis.

I would also like to thank our laboratory group: Peggy, Regina, Sharon, Robert and Michael for all the advice and comraderie given during those informal discussion periods.

And finally George, who gave me moral and intellectual support and help in countless ways through the difficult times.

LIST OF TABLES

LIST OF FIGURES

Page

Page

page

CHAPTER I

INTRODUCTION

One approach to the elucidation of gene regulation in eukaryotic cells is through the study of the chromatin in these cells. In this dissertation physical biochemical methods were chosen to study chromatin. The interactions between the different components of chromatin, and the interactions of various polypeptides with DNA, used as models for chromatin, were studied. General introductions to various topics covered in the experimental section are given here.

I. Chromatin

Chromatin, the interphase chromosome of eukaryotic nuclei, is composed of DNA, histones, nonhistone proteins and RNA (1, 2). The role of these components and their interactions with each other in chromatin is examined in detail below.

a. Histones

Histones, the basic proteins in chromatin, have been the most extensively studied. Despite the vast amount of work done on the histones their exact role

in chromatin is still not fully understood. There are five main histones all having 25% to 30% of basic amino acids. The lysine rich histones are H1 and H5, the slightly lysine rich histones are H2A and H2B, and the arginine rich histones are H3 and H4. The molecular weights of all histones with the exception of H1 and H5 are approximately 10,000 daltons (3). Histones H1 and H5 have an average molecular weight of 20,000 daltons (4,5).

All typical histones lack tryptophane and, with the exception of the arginine rich H3, cysteine. The basic amino acids are distributed unevenly in the histone molecules; they are mainly concentrated at the amino half of the molecules, except histone H1, which has the more basic amino acids at the carboxyl half of the molecule. Histone H4, the smallest of the histones, is the most conserved during evolution. Calf thymus histone H4 differs from pea seedling histone only in two amino acids (6). Histone H4 is also rich in glycine and has its amino terminal residue acetylated (7). Histone H3 is the only histone having cysteine (8, 9). There is a relatively high concentration of alanine residues in histone H3 sequence (10). Histone H3 as well as histones H2A and H2B are also highly conserved. The lysine rich histone H1 (and H5 in erythrocytes of birds) is heterogeneous and the number of its subfractions varies between individual tissues in the same animal as well as between

various species (11, 12). As mentioned above, the charge distribution in this histone is opposite to that of the other histones with the basic residues clustered at the carboxyl terminus. The amino terminal residue of this histone is also acetylated (13).

Studies of template activity suggest that histones are **repressors** of DNA genes (14, 15). However the simple structure of histones, their lack of tissue specificity (16, 17), their nonspecific interaction with DNA (18) indicate the need of additional factors in controlling the repressive action of histones. The structural differences between each histone and modification of their amino acids (e.g. acetylation, phosphorylation, methylation) make each histone differ in their effects on DNA conformation (19, 20) and the thermodynamic stability of the histone-DNA complexes. Monod et al. (21) suggested that inducer-repressor molecules in bacteria are most likely allosteric. An allosteric repressor has two binding sites, one binds the operator and the other binds the inducer. Because their interactions with DNA are non-specific histones cannot function as regulatory repressors for specific gene in eukaryotic cells. It is more likely that the histones associate with large segments of DNA, perhaps determined by cytodifferentiation, to remain transcriptionally inactive.

b. Nonhistone proteins

In contrast to histones, the nonhistone proteins are extremely heterogeneous. Using urea or SDS gel electrophoresis several investigators reported as many as thirty bands in nonhistone proteins preparation from various tissues (22-25). The molecular weights of the nonhistone proteins range from 10,000 to 300,000 daltons (22). The amino acid composition of nonhistone proteins showed an excess of acidic amino acids, so they are sometimes known as nuclear acidic proteins. Nonhistone proteins also exhibit extensive tissue and species specificity (26, 27).

From DNA-RNA hybridization studies, the tissue specificity of RNA synthesized in vitro using native and reconstituted chromatin templates depends on the origin of the nonhistone proteins (28, 29). Although conditions used in the experiments did not allow the hybridization of non-repetitive RNA species (30) it is quite likely that tissue specific transcription of unique RNA is also regulated by the nonhistone proteins. Another piece of evidence that supports this role of nonhistone proteins in chromatin comes from studies of the binding of hormone-receptor complexes to chromatin of target tissue (31, 32, 33). Chromatin from target tissue (chick oviduct for example) of a specific hormone such as estradiol, will bind to the complex of the hormone with its cyto-

plasmic protein. Chromatin from nontarget tissues cannot bind the hormone-receptor complex efficiently. The binding specificity appears to be determined by a fraction of the nonhistone proteins, since it can be transferred to the chromatin of nontarget tissues by reconstituting this nonhistone protein fraction to this chromatin.

c. Chromosomal RNA

Another macromolecule which may be related to tissue specific transcription is chromosomal RNA. Huang and Bonner (34) first reported the presence in chromatin of a new RNA species called chromosomal RNA (cRNA). The cRNA-nonhistone protein complex associate with histones, probably by hydrogen bonding, since they can be dissociated by guanidine hydrochloride (35). In chromatin the cRNA is resistant to RNAase digestion, probably because it exists in a hybrid with complementary DNA. The cRNA is small, about 40 to 60 nucleotides long, and contains 5-10% of dihydroxypyrimidine in addition to the common bases (36). It hybridizes to native DNA sequences and is species (37) and tissue (38) specific. Recent studies showed that cRNA could be derived from a high molecular weight nuclear heterogeneous RNA (39).

Although it is still not clear how tissue specific restriction of DNA genes works, it is certain that the interactions of the three components of chromatin, histones, nonhistone proteins and cRNA with each other and with DNA are essential. Therefore, it is important to understand

the interaction of DNA with these proteins.

d. DNA

It is known from circular dichroism (40) and X-ray diffraction (41) that DNA in aqueous solution exists primarily in the B-conformation, which is one of the several double-helical states of DNA defined by fiber X-ray diffraction. Table 1 gives the different parameters for B-form, A-form and C-form DNA. Briefly, the B-form is characterized by an overall diameter of about 20Å with stacked base pairs in which the bases lie perpendcular to the helix axis and are slightly twisted relative to one another. The interbase hydrogen-bonding pattern is that first defined by Watson and Crick (42). The helix axis passes approximately through the N-H...N imino hydrogen bond, and the helix is right handed with 10 base pairs per turn and a rise per residue of 3.4Å. The distance between C_1' carbon atoms in the deoxyribose rings of the opposite (antiparallel) chain is about 11Å. The grooves in the double helix structure are depressions between the negatively charged hydrophilic sugar-phosphate backbones. In the B-form the grooves are unequal in size, the large (major) groove being about 22Å across, measured between phosphates in the direction of the helix axix, while the small (minor) groove is about 12Å across. The grooves are both approximately 7Å in depth measured from the surface of the enveloping cylinder (43).

Table 1

Dimensions of DNA in different forms*

DNA, salt	Residues per turn	Pitch Å	Translation per turn	Angle between perpendicular to helix axis and base (°)	Dihedral angle between base plane (°)
A form, Na 75% r.h.	11	28.15	2.55	20	16
B form, Na 92% r.h.	10	34.6	3.46	-	-
B form, Li 66% r.h.	10	33.7	3.37	2	5
C form, Li	9.3	31	3.32	6	10

* Davis, D.R., (1967) Ann. Rev. Biochem. 36, 321

In the fiber (or gel) state the B-form of DNA is easily converted to the A-form or the C-form. The A-form is seen at decreased relative humidity with counterions other than lithium. The C-form is observed for Li-DNA salts at relative humidities of 66% or less. In the A-form the base pairs are tilted about 20° from the perpendicular to the helix axis and are displaced outward from the axis. There are 11 base pairs per turn with a rise per residue of 2.82Å. This form is very similar to the structure of double stranded RNA at 100% relative humidity. The C-form resembles B-form but has only 9.3 base pairs per turn and a rise per residue of 3.32Å.

The interconversion of B-form to A- and C- (and perhaps others) structures by varying humidity or counterion types in fibers suggests that the B-form can also be easily deformed to other structures by perturbants in solution. The structural changes that occur when proteins such as histones, other chromosomal proteins and synthetic polypeptides bind to DNA can be one way of studying the interaction of these proteins to DNA.

II. Chromatin Structure

Another approach to the study of the interactions between various components of chromatin is through elucidation of the structure of chromatin. Tuan and Bonner (44) observed that in high ionic strength media the conformations of histones approximate those found in histone-DNA complexes as measured by ORD. If this is so, DNA obviously can

superimpose considerable conformation on histone structure, including formation of α-helix in the very basic regions. Estimates of the helix content (ordered structure) of histones in nucleohistone vary from 18% to 41% for histone-DNA complexes, as high as 59% for histone H2A and H2B and as low as 13% for histone H1 (45). The structure of DNA is also markedly affected by histones in nucleohistones. This was studied by Fasman et al. (46, 47), Leffak et al. (48), Hwan et al. (49), Permogorov et al. (50) and Simpson and Sober (51) among amany others. CD, ORD, X-ray diffraction and flow dichroism techniques were used. The complexes used for the experiments were partially dehistonized chromatin or reconstituted nucleohistones. Although these studies agree that histones affect DNA structure, these is considerable disagreement as to which histone is responsible for the observed effects. Most studies agree that histone H1 does not affect chromatin structure, although it may be involved in crosslinking of chromatin molecules (52). Currently, two structures of chromatin have been proposed. One is the supercoil structure of chromatin proposed by Richards et al. (53), and Richards and Pardon (54) form X-ray diffraction work. The other is the beaded structure of chromatin proposed by Olins and Olins (55) based on electronmicroscopy. Recent data from histone-histone interaction (56), nuclease and trypsin digestion (57) and neutron diffraction (58) favor the second model. In this dissertation the problem of chromatin structure

is approached by studying the interactions of model polypeptides such as polylysine and protamine with DNA and with chromatin.

III. Polypeptide-DNA interactions

Basicity is the most obvious common feature of histone and protamines the two proteins which form the most prominent complexes with DNA. The charge-charge interaction between histone and DNA is one the main driving forces for histone-DNA interaction. This conclusion has led to a number of model studies of interactions of DNA with cationic homopolypeptides, poly L-lysine and poly L-arginine (59, 60, 61), as well as different co-polymers (62, 63) with the idea that such studies should provide some interpretable information than could be derived from DNA-histone complexes themselves.

Early studies of binding between oligo- and polylylysine and nucleic acids were performed by Latt and Sober (64). They demonstrated a 1:1 lysine to phosphate stoichiometry for a number of synthetic and natural polyribonucleotides structures. Leng and Felsenfeld (65), and Shapiro et al. (66) were able to demonstrate that polylysine, under high salt conditions to minimize nonspecific interactions, preferentially and stoichiometrically precipitates (A+T)-rich DNA. This preferential binding could be reversed by the addition of tetramethylammonium ion (67). Polyarginine under the same conditons

preferentially binds to (G+C)-rich DNA. Olins et al. (68) used spectral and melting profile measurements to examine the structure and stability of several DNA-polypeptide complexes at low ionic strength, using complexes prepared by salt-annealing technique. These workers showed (A+T) preference by polylysine to DNA by demonstrating that the average T_m of the dA.T base pairs in the complexes were elevated more than that of dG.C pairs. These studies and selective precipitation measurements showed these interactions to be cooperative i.e. in the presence of excess DNA, the available polypeptides reacted with DNA in such a way that some of the DNA's are totally bound while the rest are free. The cooperativity can be caused by (a) conformational changes induced on DNA by the binding of the polypeptide, (b) a favorable direct interaction between adjacent bound peptide (an unlikely event). Support for the first alternative comes from hydrogen exchange experiments of DNA in the presence and absence of polylysine. These studies showed that the interaction with polylysine induces a conformational change in the DNA and results in moving about $\frac{1}{4}$ of the interbased hydrogen-bonded hydrogens into a rapidly exchanging class (69). Base tilting of DNA caused by polylysine binding is possible interpretation. This could explain the observed cooperativity since the partially tilted DNA segments adjacent to the complexed regions should provide more easily deformable sites for additional polylysine binding. One problem encountered

by researchers in all the above work with polylysine was the solubility of the polylysine-DNA complexes. The high light scattering present in the complexes caused ambiguity in the interpretation of the results of experiments using optical methods such as CD, ORD and absorption spectrum.

The above problem can be overcome by using a simple method of making polylysine-DNA complexes with slow and direct mixing (70). The binding of polylysine to DNA of these complexes is random. The resultant complexes have negligible light scattering with A_{320nm}/A_{260nm} less than 0.05. Optical properties of these complexes can be interpreted more easily. This dissertation includes research on polylysine-DNA and -chromatin complexes using the method of circular dichroism and thermal denaturation.

CHAPTER II

MATERIALS AND METHODS

Preparation of chromatin

Chromatin was prepared by the method of Shih and Bonner (71). Frozen calf thymus was minced and soaked in grinding medium (0.25M sucrose-0.01M Tris, pH 8.0). A 1 gram of tissue in 10 ml of solution was blended in a Waring blender at 30 volts for 3 minutes and 60 volts for 1 minute. The speed was adjusted by a variac. The solution was then filtered through 4 layers of cheese cloth and 2 layers of miracloth. After removal of tissue membranes by filtration the solutions was centrifuged at 6,000 rpm (Sorvall SS-34 rotor) for 10 minutes at 4°C. The pellets were collected, homogenized by a Dounce homogenizer with a teflon head in 0.01M Tris pH 8.0 and centrifuged again at 10,000 rpm for 10 minutes. This step was repeated until the supernatant became clear. The final nuclear pellets were homogenized (Dounce-teflon) layered on top of 1.7M sucrose in 0.01M Tris pH 8.0. This was centrifuged at 21,000 rpm for 2 hours using a

Beckman ultracentrifuge Model L2-65B (SW25.1 rotor). The sticky pellets obtained were homogenized and dialyzed in 15 volumes of 0.01M Tris pH 8.0 to remove the sucrose. The resulting preparation was pure chromatin.

Chromatin was also prepared by the method of Panyim (72). In this method pure nuclei were isolated first, then chromatin extracted by bursting the nuclei. Calf thymus were minced and soaked in grinding medium (0.25M sucrose-0.01M $MgCl_2$ pH 8.0), blended in a Waring blender at 30 volts for 3 minutes and 60 volts for 1 minute. The homogenate was filtered through 4 layers of cheese-cloth and 2 layers of miracloth. After filtration it was centrifuged at 3,000 rpm (Sorvall SS-34 rotor) for 5 minutes. The crude nuclei pellets were homogenized by a Dounce homogenizer with a teflon pestle in wash medium (0.025M sucrose-0.01M $MgCl_2$-(0.2%-0.5%)Triton X-100 pH 8.0). The homogenate was then centrifuged at 3,000 rpm for 10 minutes. This step was repeated until the supernatant remained clear. Usually 2-3 washings were sufficient. The crude pellets were homogenized in 2.2M sucrose-0.01M $MgCl_2$-(0.2%-0.5%)Triton X-100) and layered on top of 2.4M sucrose containing the same ionic components. This was centrifuged for 2½ hours at 23,000 rpm in a Beckman ultracentrifuge Model L2-65B (SW 27 rotor). The purified nuclei pellets obtained were washed twice in 0.25mM EDTA-0.01M Tris-0.05M sodium bisulfite and

centrifuged at 6,000 rpm for 10 minutes (Sorvall SS-34 rotor). Nuclei were then lysed in cold distilled water. In this method each step can be checked by means of a light microscope.

Soluble nucleohistones were obtained by shearing the chromatin in a Virtis "45" homogenizer at 60 volts for 1 minute. The resulting homogenate was centrifuged at 10,000 rpm for 10 minutes (Sorvall SS-34 rotor). The supernatant obtained was called sheared chromatin. Salt-treated nucleohistones were obtained by adding dropwise 4M NaCl to a constantly stirring solution of sheared chromatin. The solutions were allowed to stir in the cold (4° C) for ½ hour, then layered over 1.7M sucrose-0.01M Tris. The nucleohistone and salt-treated nucleohistone pellets were obtained by centrifugation for 24 hours at 36,000 rpm in a Beckman ultracentrifuge L2-65B (SW 41 rotor). The salt-treated nucleohistones were 0.35M NaCl-, 0.6M NaCl-, 1.0M NaCl-, 1.6M NaCl- and 2.5M NaCl-treated nucleohistones. The increase in NaCl concentration progressively remove more nuclear proteins. After carefully removing the dissociated proteins the nucleohistone pellets were dialyzed first into 0.01M Tris pH 8.0, then into 0.25mM EDTA, pH 8.0.

Thermal denaturation

The thermal denaturation of different nucleohistones

were made on a Gilford Spectrophotometer Model 2400-S at 260 nm. The heating rate was about 2/3°C/min. The derivatives of the melting profiles were calculated according to the equation of Li and Bonner (73):

$$\frac{dh_{260}(T)}{dT} = \frac{h_{260}(T+1) - h_{260}(T-1)}{2} \qquad (1)$$

where $h_{260}(T)$ is the hyperchromicity at 260 nm at temperature T.

Circular dichroism

The circular dichroism spectra of the samples were performed on a Durrum-Jasco Spectropolarimeter Model J-20 at room temperature. Circular Dichroism results were reported as $\Delta\varepsilon$:

$$\Delta\varepsilon = \varepsilon_L - \varepsilon_R$$

where ε_L and ε_R are molar extinction coefficient for the left- and right-handed circularly polarized light. The units of $\Delta\varepsilon_m$ are $M^{-1}cm^{-1}$ in nucleotides.

$$\Delta\varepsilon_m = \frac{\theta(\text{millidegree})}{33.05 \times C \times 1\ (\text{cm})}$$

Where: θ = ellipticity in millidegree
C = concentration (moles/liter)
1 = pathlength of light in cm.

Nucleotide concentration was determined on a Beckman spectrophotometer Model 25 using extinction coefficient $6500M^{-1}cm^{-1}$ for DNA at 260 nm.

CHAPTER III

CHROMATIN AND SALT-TREATED CHROMATIN

One approach to studying gene regulation of chromatin is through studying its structure and physical interactions of the various components of chromatin. Thermal denaturation had been used to study helix-coil transition in DNA (74, 75), and interactions between basic peptides and DNA (76), and histones and DNA (77). Since DNA is one of the major component in chromatin, thermal denaturation can also be used to study chromatin. The binding of basic proteins, such as polylysine, polyarginine, protamine and histones to DNA cause biphasic or multiphasic melting. The mechanism of melting of these complexes with DNA was clarified by Li (78) when a model of helix-coil transition of nucleoproteins was introduced. According to this model DNA base pairs in a complex stabilized and bound irreversibily by a protein melt independently from the neighboring free DNA base pairs if the stabilization energy is greater than the stacking energy. This model is used here to explain the results

obtained from thermal denaturation of chromatin and salt-treated chromatin.

Circular dichroism had been used by many workers to study conformation of DNA in different solvents (79, 80), the conformation of DNA-basic polypeptide complexes (81), of chromatin itself. Here, circular dichroism has also been used to study the conformation of chromatin. Using an equation derived in Chang et al. (82) the CD of histone-bound regions and -free regions in chromatin can be determined.

Experimental

Nucleohistone and different salt-treated nucleohistones were prepared as previously described. The histone contents of the salt-treated nucleohistones are shown in Table 2. The samples for thermal denaturation and circular dichroism studies had absorbances of about 0.65 at 260nm, or about $1x10^{-4}$M. The buffer used in all experiments was 0.25mM EDTA, pH 8.0.

The T_m's of the different samples were obtained by thermal denaturation on a Gilford spectrophotometer Model 2400-S. Derivatives of melting curves were obtained as previously described. The conformational changes of the nucleohistones were examined based upon circular dichroism spectra obtained on a Jasco spectropolarimeter. $\Delta\varepsilon_m$ of the samples were obtained as previously described.

Calf thymus DNA was purchased from Sigma Chemical Co. and purified by phenol extraction as well as the method of

Table 2

NaCl Extraction of Nucleohistone*

NaCl concentration	Histones extracted
0.35M	30% H1
0.6M	100% H1
1.0M	100% H1, 70% H2A and H2B
1.6M	100% H1, 100% H2A and H2B, 70% H111 and H1V
2.5M	100% H1, 100% H2A and H2B, 95% H111 and H1V.

*Ohlenbush, H.H., Olivera, B.M., Tuan, D., and Davidson, N., (1967) J. Mol. Biol. 25, 229

Marmur (83).

Acid extraction of histones from nucleohistones and salt-treated nucleohistones were done according to the procedure described in Li (78). For any given amount of nucleohistone (A_{260nm}= 10-20) in 0.01M Tris pH 8.0, H_2SO_4 was added to make a final concentration of 0.5N. The solutions were stirred at 4° C for 1 hour. Dissociated histones were separated from DNA and nonhistone proteins by centrifugation at 10,000 rpm for 10 minutes. 0.5N H_2SO_4 dissociated histones were determined spectrophotometrically by taking A_{230nm}=4.25 for 1mg/ml of histone solution. An average residue weight of approximately 110 was used for all histones without consideration of the slight variations. Histone contents of the nucleohistones were reported as amino acid residues per nucleotide. 0.5N H_2SO_4 dissociated all the histones and less than 5% of 230nm absorbing material could be extracted by 1.0N H_2SO_4 after it has been treated by 0.5N H_2SO_4.

Results

A. Thermal denaturation

a. Thermal denaturation of chromatin, sheared chromatin and nucleohistone

Pure chromatin as prepared by the method of Shih

and Bonner is extremely viscous and gives a high light scattering (A_{320nm}/A_{260nm} >10%). In our experiments chromatin was first sheared and centrifuged as described earlier. The supernatant obtained was called sheared chromatin (A_{320nm}/A_{260nm}=5.6%). Sheared chromatin was further purified by high speed centrifugation through 1.7M sucrose. The pellet obtained after redissolving in 0.25mM EDTA, pH 8.0, was called nucleohistone. The light scattering for nucleohistone is small (A_{320nm}/A_{260nm}=1.4%).

To test whether the size of chromatin affect its melting properties, thermal denaturation of pure chromatin, sheared chromatin and nucleohistone was measure. Fig 1a shows the derivative melting profiles of the three samples. The derivative curves as well as the maximum hyperchromicities of the three nucleohistones are different. Chromatin has h_{max}=25.2, sheared chromatin has h_{max}=29.1 and nucleohistone has h_{max}=33.3. The difference in the maximum hyperchromicities of the three samples is due to the difference in the light scattering. Pure chromatin has the highest light scattering and nucleohistone the lowest. Therefore, correcting for the difference in light scattering by normalizing the h_{max} of all the three samples to 33.3, normalized melting curves are determined and shown in Fig 1b. All three chromatins show similar melting profiles. Therefore,

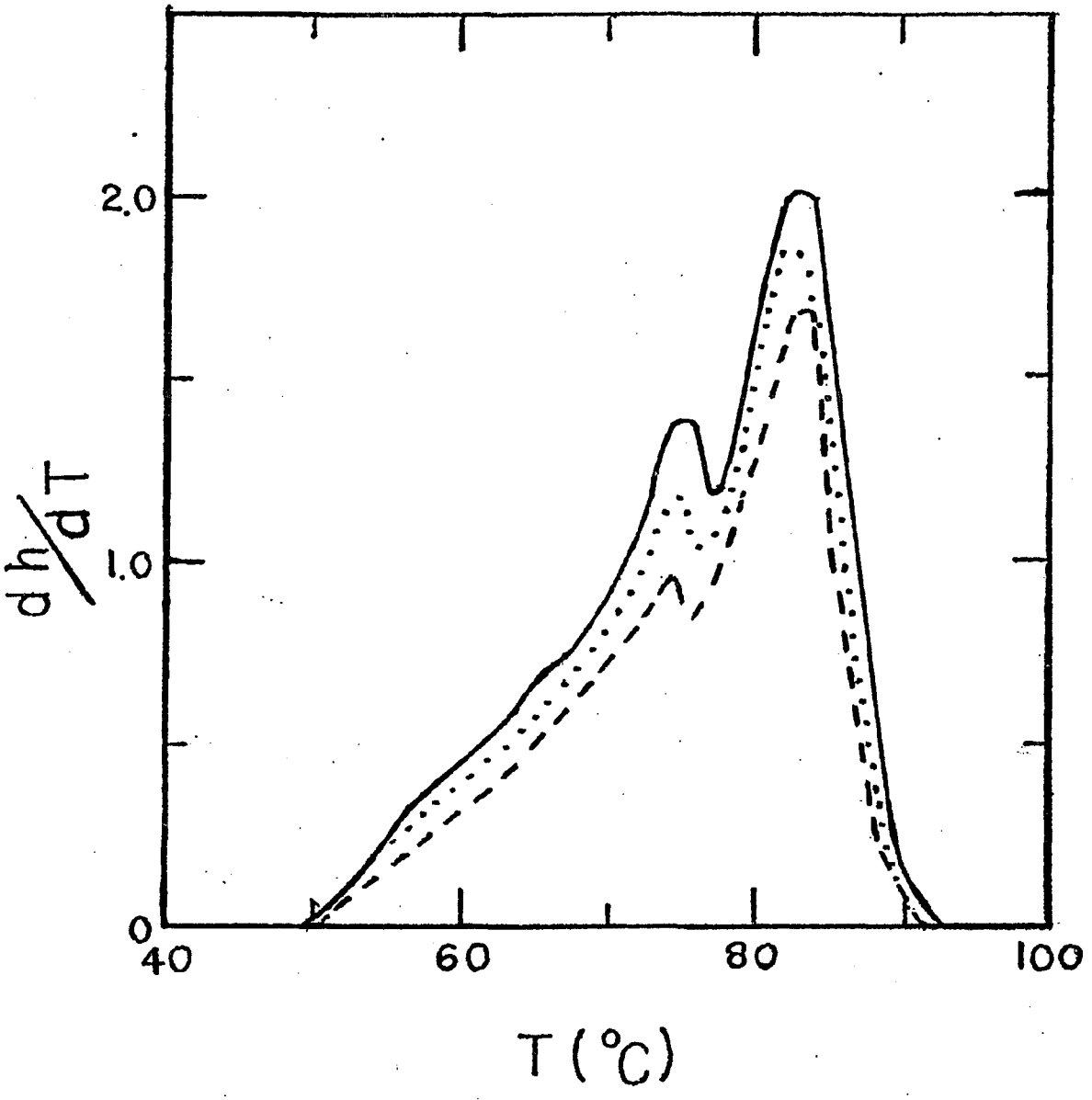

Fig 1a. Derivative melting profiles of purified chromatin (----), sheared chromatin (....) and nucleohistone (——). h_{max} is 25.2, 29.1 and 33.3 respectively. Buffer used was 0.25mM EDTA, pH 8.0

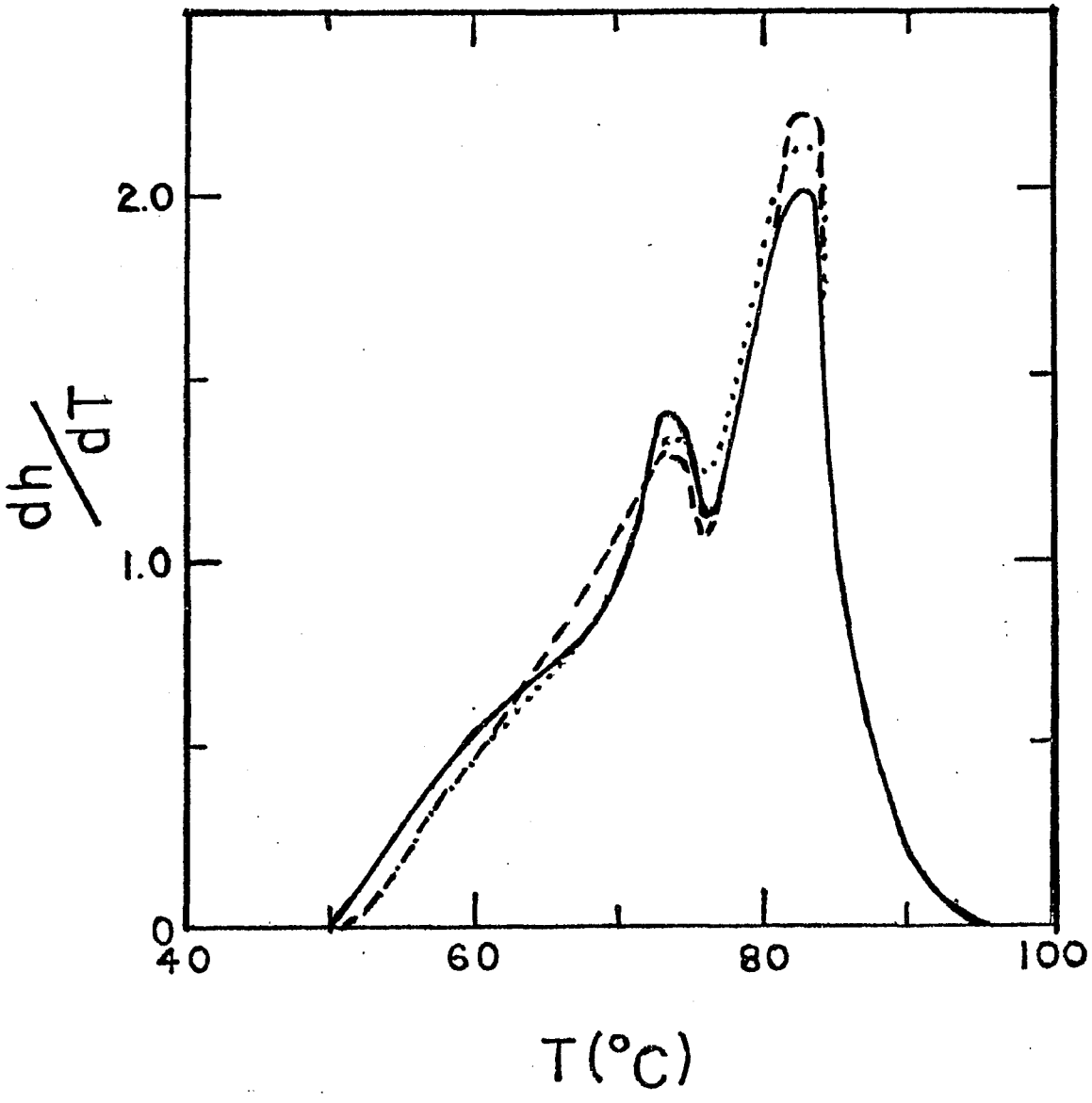

Fig 1b. Normalized derivative melting profiles of purified chromatin (- - -), sheared chromatin (...) and nucleohistone (——). h_{max} is 33.3 for all three curves. The buffer used is 0.25mM EDTA, pH 8.0

the size of the chromatin has no effect on its melting property. It is the ionic interaction between the phosphates of the DNA and the amino groups of the histones which mainly determines the melting properties of chromatin.

b. Thermal denaturation of nucleohistone and salt-treated nucleohistones

The salt-treated nucleohistones used here included 0.35M NaCl-, 0.6M NaCl-, 1.0M NaCl-, 1.6M NaCl-, and 2.5M NaCl-treated nucleohistones. All samples were in 0.25mM EDTA, pH 8.0. Derivative melting curves of nucleohistone and different salt-treated nucleohistones are shown in Fig 2. Calf thymus nucleohistone shows two melting bands at high temperature. One at 72°C and the other at 82°C. There is also a shoulder at 63°C designated as melting bands I+II. The melting at 72°C is designated melting band III and the melting at 82°C is melting band IV. Higher concentrations of NaCl removes increasing amounts of histones from nucleohistones. The melting curves of salt-treated nucleohistones show a decrease in area at melting bands III and IV and an increase in melting band I at 48°C. These results are interpreted to mean that melting bands III and IV represent the melting of DNA base pairs bound by histones and melting band I due to the melting of free DNA in nucleohistones. Melting band II may be due to the melting of DNA base pairs bound by nonhistone proteins or very short free DNA gaps

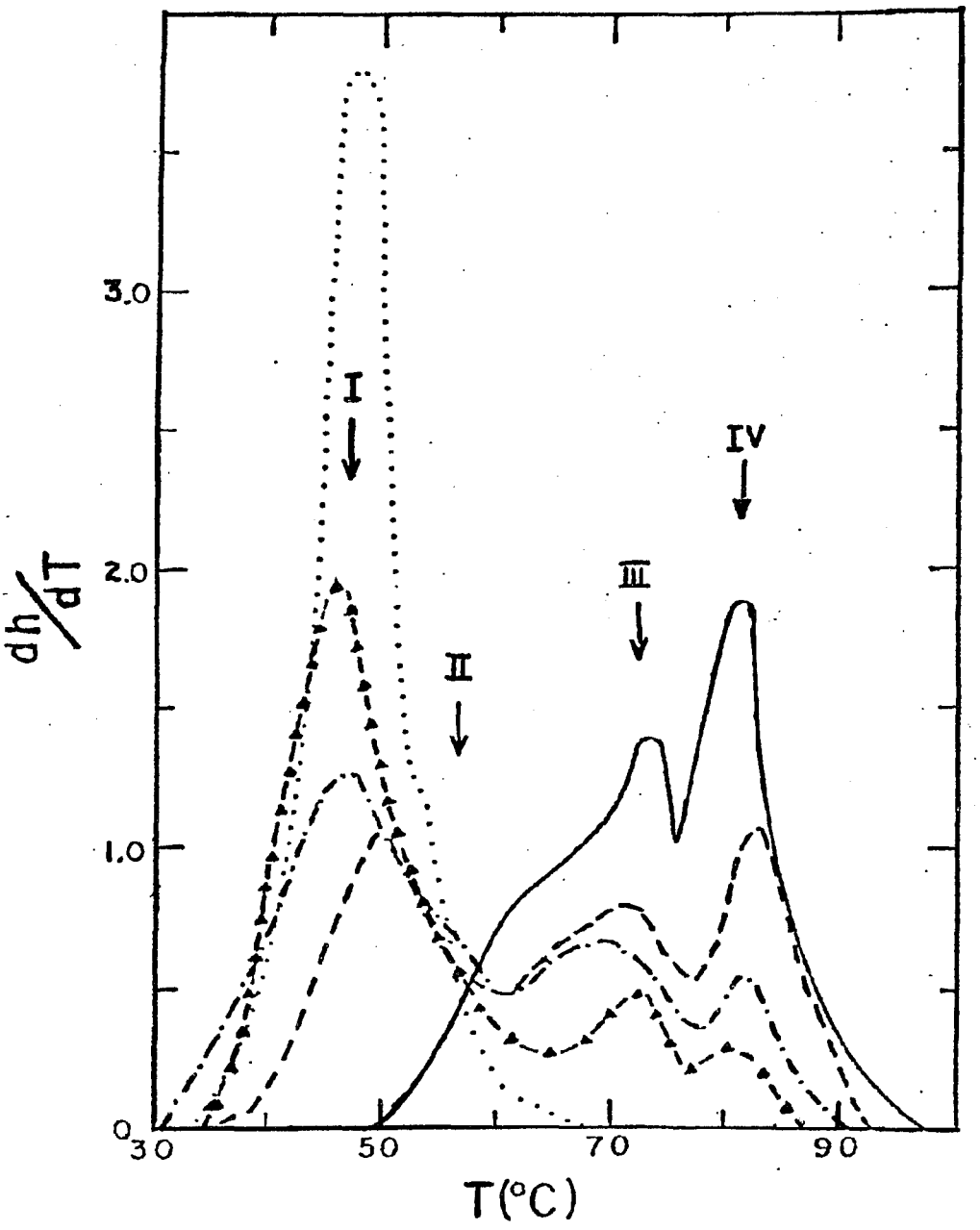

Fig 2. Derivative melting profiles of NaCl-treated Nucleohistones. NaCl concentration is 0 M (——), 0.6M (- - -), 1.6M (-.-), 2.5M (-▲-) and DNA (...). Buffer used was 0.25mM EDTA, pH 8.0

between adjacent histone-bound regions. Fig. 2 also shows the melting of pure calf thymus DNA at 48°C which corresponds to melting band I of nucleohistones. The histone-bound DNA base pairs having two T_m's at 72° and 82°C is explained by the fact that all five histones have uneven distribution in basic amino acid residues. Histones can be said to have two halves, the more basic half and the less basic half. The melting at 72°C is explained as due to the binding of DNA base pairs by the less basic half of histones and the melting at 82°C as due to melting of DNA base pairs bound the more basic half of histones (73).

c. <u>The number of amino acid residues of histones per nucleotide of DNA</u>

Since melting bands at 72° and 82°C correspond to melting of DNA base pairs bound by histones, the area of these two melting bands can be used to measure the fraction of DNA base pairs bound by histones. Using the equation derived in Li (78):

$$B_k = \frac{\beta_k A_k}{A_T} \qquad (3)$$

where B_k = the total amino acids of protein k/ nucleotide

A_k = the area under melting band k

A_T = h_{max} or total area of melting bands

β_k = average number of amino acids/ nucleotide of DNA bound by the protein k

In nucleohistones if B_H is the total amino acids of histones per nucleotide, then the above equation becomes:

$$B_H = \beta_H \frac{A_{TmIII} + A_{TmIV}}{A_T} \qquad (4)$$

B_H, the histone content of the nucleohistone and salt-treated nucleohistones was determined by acid extraction as described above. The fraction of DNA base pairs bound by histones was determined to be 79% for nucleohistone, 62% for 0.35M NaCl-treated nucleohistone, 57% for 0.6M NaCl-treated nucleohistone, 40% for 1.0M NaCl-treated nucleohistone and 20% for 1.6M NaCl-treated nucleohistone. By plotting the total histone content B_H against the fraction of area bound by histones the average number of amino acids of histone per nucleotide of DNA (β_H) can be determined from the slope of the plot as is shown in Fig. 3. The slope gives $\beta_H = 3.7 \pm 0.4$ amino acids of histone per nucleotide of DNA for calf thymus nucleohistones.

B. Circular dichroism

Fig. 4 shows the circular dichroism spectra of calf thymus DNA, nucleohistone and different salt-treated nucleohistones. The CD spectrum of nucleohistone is similar to that of earlier reports. As compared to the spectrum of pure DNA nucleohistone shows a decrease in

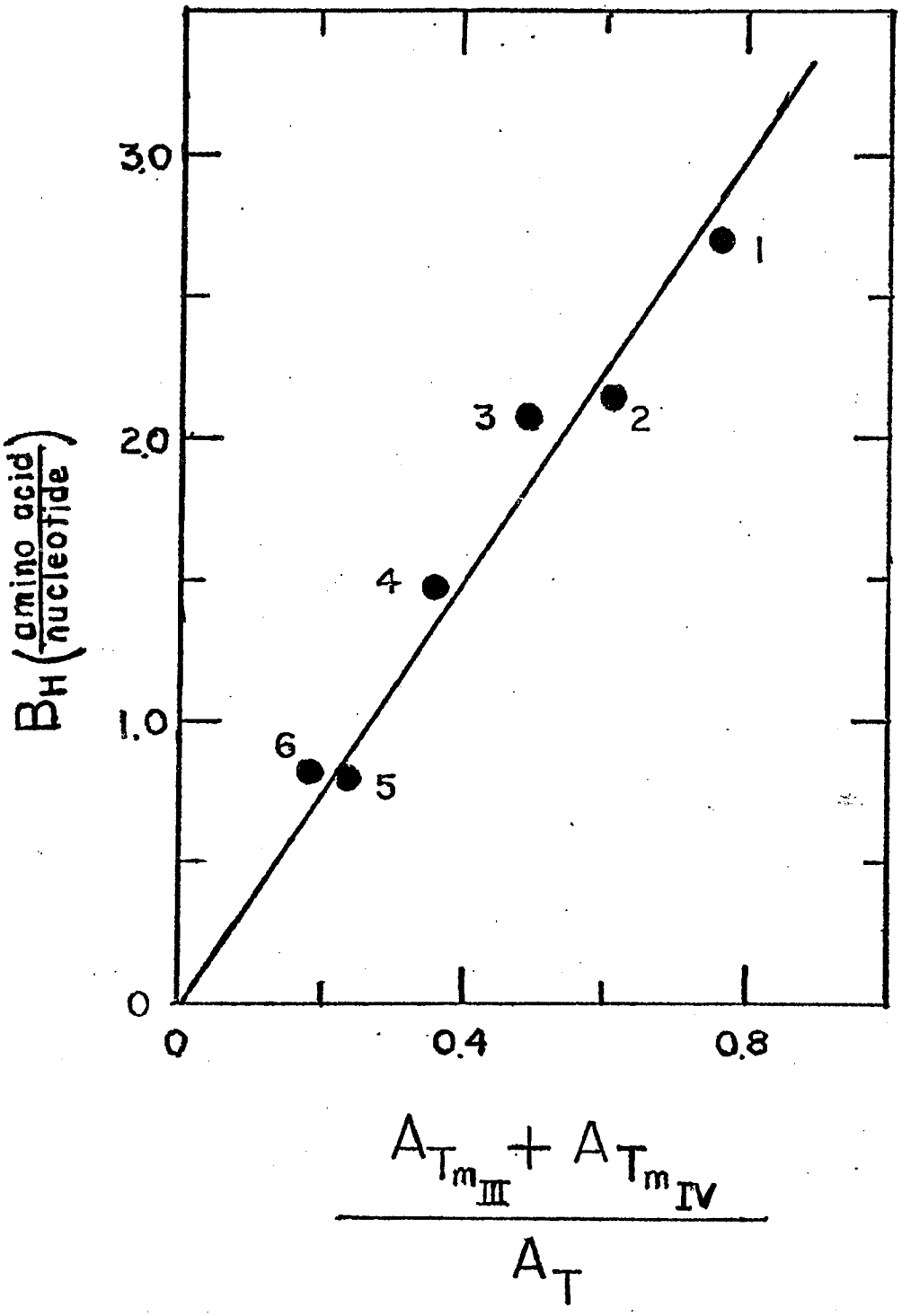

Fig 3. Linear relation between histone content and the area of melting band. Nucleohistones are, respectively, pretreated by NaCl of 0.0M(1), 0.35M (2), 0.6M (3), 1.0M (4), 1.6M (5) and 2.5M (6) in EDTA buffer of pH 8.0

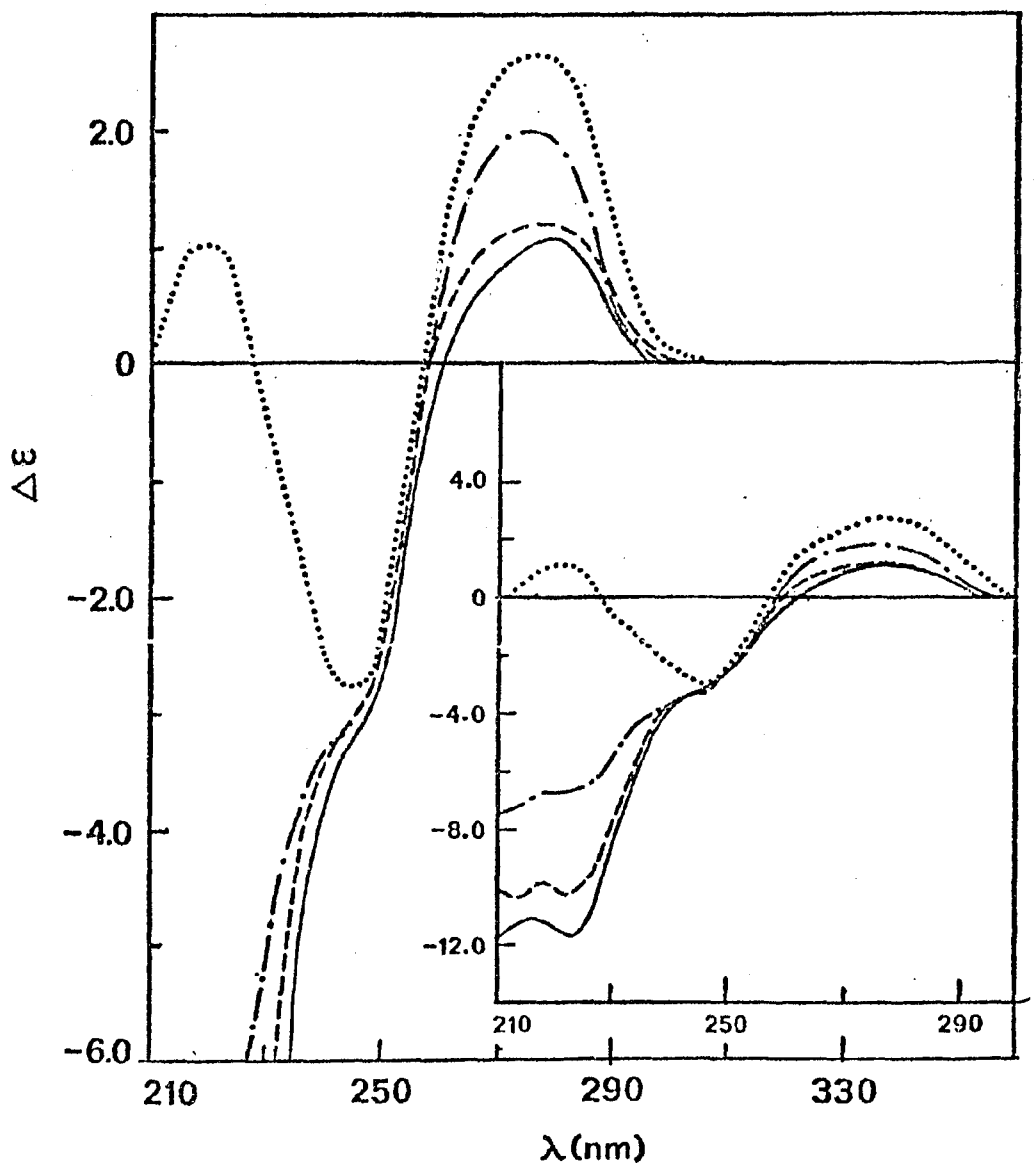

Fig 4. CD spectra of NaCl-treated nucleohistones. NaCl is 0.0M (——), 0.6M (- - -), and 1.6M (-.-). DNA (...)

the amplitude of the positive peak at 278nm from 2.5 for pure DNA to 1.0 for nucleohistone. The crossover point shows a red shift at 260.5nm as compared to 255nm for pure DNA. The large negative CD of nucleohistone at 220nm is contributed by the proteins. Table 3 gives the CD parameters of nucleohistones and different salt-treated nucleohistones. The removal of histones from nucleohistone by NaCl restores the CD spectrum to that of pure DNA by an increase in the amplitude of the positive peak at 278nm, a decrease of the negative peak at 220nm and a blue shift of the crossover at 255nm . From thermal denaturation the fraction of DNA base pairs bound by histones (F) can be computed as described earlier. To correlate the fraction of bound DNA base pairs and the circular dichroism changes as histones are removed from nucleohistone, a plot of F against $\Delta\varepsilon_{278nm}$ and $\Delta\varepsilon_{220nm}$ was made. Fig 5 shows that uncovering upto 50% of DNA in nucleohistone resulted in very little change in the amplitude of the positive peak at 278nm. In 0.6M NaCl-treated nucleohistone 50% of DNA is still bound by histones. Since 0.6M NaCl removes only histone H1, the above result implies that this histone has little effect on nucleohistone conformation. As other histones are removed by increasing the salt concentration the change in the amplitude of positive peak becomes more pronounced. The amplitude increases until it approaches that of pure DNA. The

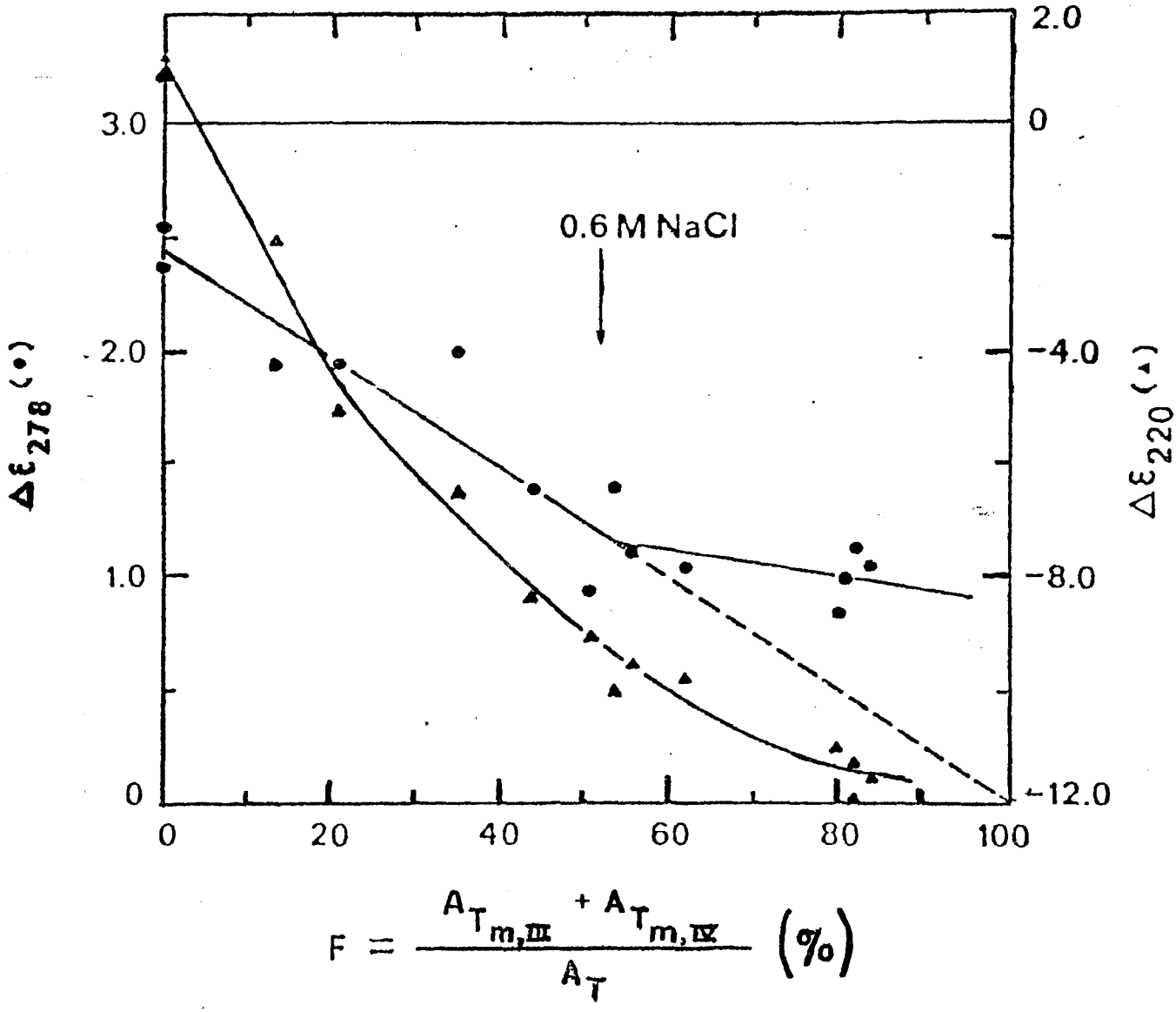

Fig 5. Dependence of $\Delta\varepsilon_{278}$ and $\Delta\varepsilon_{220}$ on the fraction of base pairs bound by histones (F).

Table 3

Circular Dichroism & Thermal Denaturation Parameters of Nucleohistones

Nucleohistones (NH)	$\frac{A_{TmIII}+A_{TmIV}}{A_T}$ (%)	$\Delta\varepsilon_{278}$	$\Delta\varepsilon_{220}$	λ_c
Native NH	81	0.99	-11.4	260.5
0.35M NaCl-NH	62	1.05	- 9.8	260.5
0.6M NaCl-NH	52	1.18	- 9.5	259.5
1.0M NaCl-NH	44	1.40	- 8.3	257.5
1.6M NaCl-NH	27	1.95	- 5.8	257.0
2.5M NaCl-NH	13	1.95	- 2.0	256.5
DNA	0	2.55	+ 1.0	255.5

linear relationship between histone content and the fraction of DNA bound is shown by a proportional decrease of the negative CD at 220nm which is reduced as more DNA base pairs becomes free of histones. Removal of histone H1 has the least effect on the negative CD at 220nm of nucleohistone.

The circular dichroism spectra of nucleohistone and partially dehistonized nucleohistones can be resolved into the CD of free DNA base pairs and the CD of bound base pairs by the following equation:

$$\Delta\varepsilon_m = (1-f)\Delta\varepsilon_o + f\Delta\varepsilon_b \qquad (5)$$

where $\Delta\varepsilon_m$ = measured CD

$\Delta\varepsilon_o$ = the CD of histone-free DNA base pairs

$\Delta\varepsilon_b$ = the CD of histone-bound base pairs

f = the fraction of base pairs bound by histones

Since f can be determined from thermal denaturation, $\Delta\varepsilon_o$ from the CD of pure DNA , $\Delta\varepsilon_b$, the CD of histone-bound base pairs can then be calculated. Fig.6 shows the calculated CD of the bound DNA base pairs. $\Delta\varepsilon_b$ is close to zero from 260nm to 300nm. The $\Delta\varepsilon_b^H$ for bound histones is calculated from the following equation derived in Pinkston and Li (62):

$$\Delta\varepsilon_m = \Delta\varepsilon_o + B_H \Delta\varepsilon_b^H \qquad (6)$$

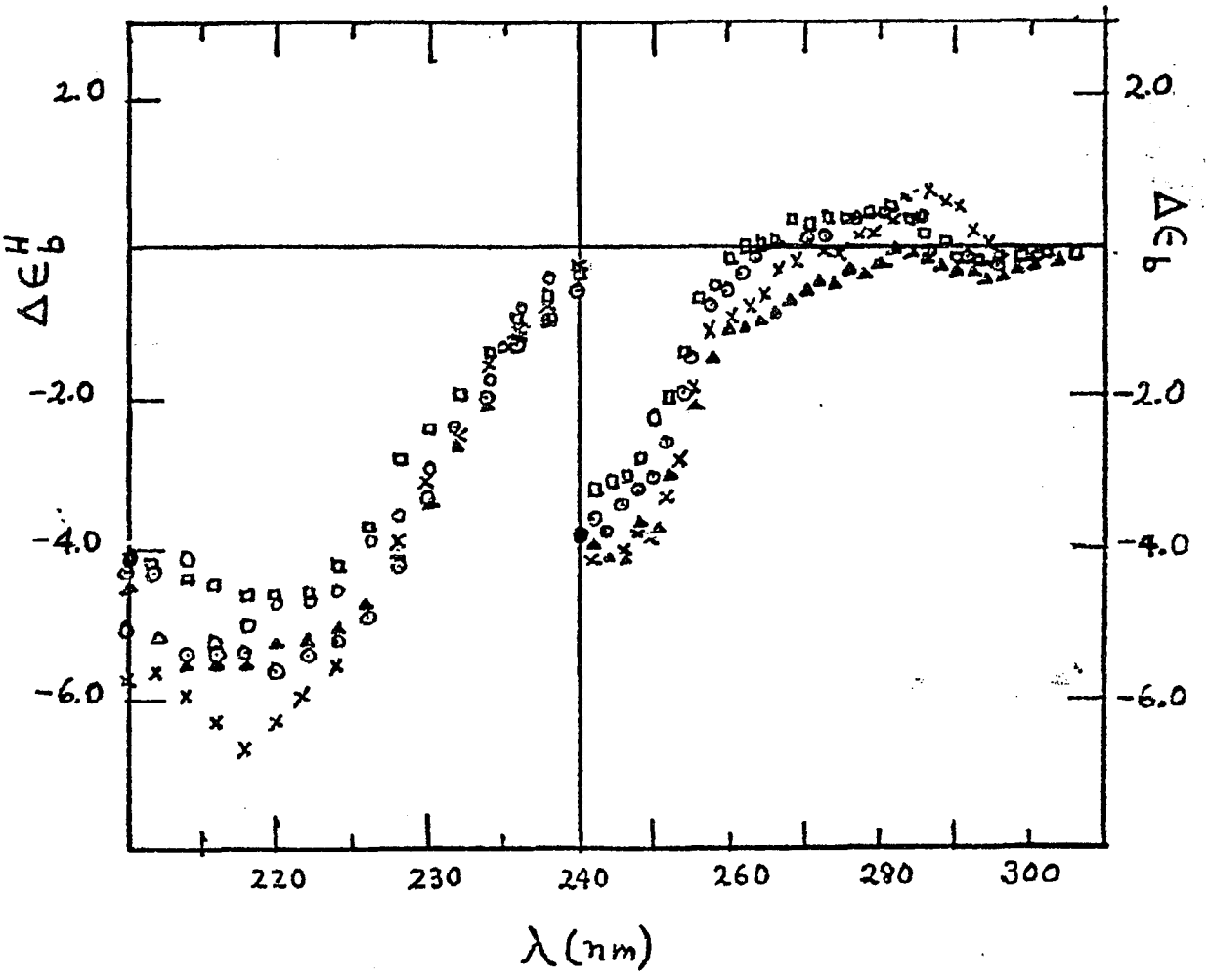

Fig 6. CD spectra of histone-bound DNA base pairs ($\Delta\epsilon_b$) and bound histones ($\Delta\epsilon_b^H$) of different NaCl-treated nucleohistones: 0 M (▲), 0.35M (●), 0.6M (□), 1.0M (⊖) and 2.5M (X). All samples are in 0.25mM EDTA, pH 8.0

As is seen in Fig. 6 theCD of the free DNA base pairs in nucleohistone and salt-treated nucleohistones is similar to that of DNA in the C-conformation (84). The CD of bound histones in all the nucleohistones appears similar within experimental error.

C. Effect of ionic strength on nucleohistone and salt-treated nucleohistones

a. Titration curve

Figure 7 shows the precipitation curves of nucleohistone and salt-treated nucleohistones by NaCl. Both nucleohistone and 0.35M NaCl-treated nucleohistone precipitate at 0.2M NaCl concentration. Only little precipitation occurs for 0.6M NaCl-treated nucleohistone and 1.6M NaCl treated nucleohistone is soluble in salt at all concentration. The results could be explained as a result of charge neutralization of the phosphates in DNA by histones, the more the neutralization the higher the tendency for precipitation in NaCl.

b. Thermal denaturation

Figs. 8 and 9 show the effect of ionic strength on the melting of nucleohistone and 2.5M NaCl-treated nucleohistone. The effect of increasing ionic strength on the T_m of pure DNA is a well known phenomenon (85). The free DNA regions in nucleohistones have a greater shift

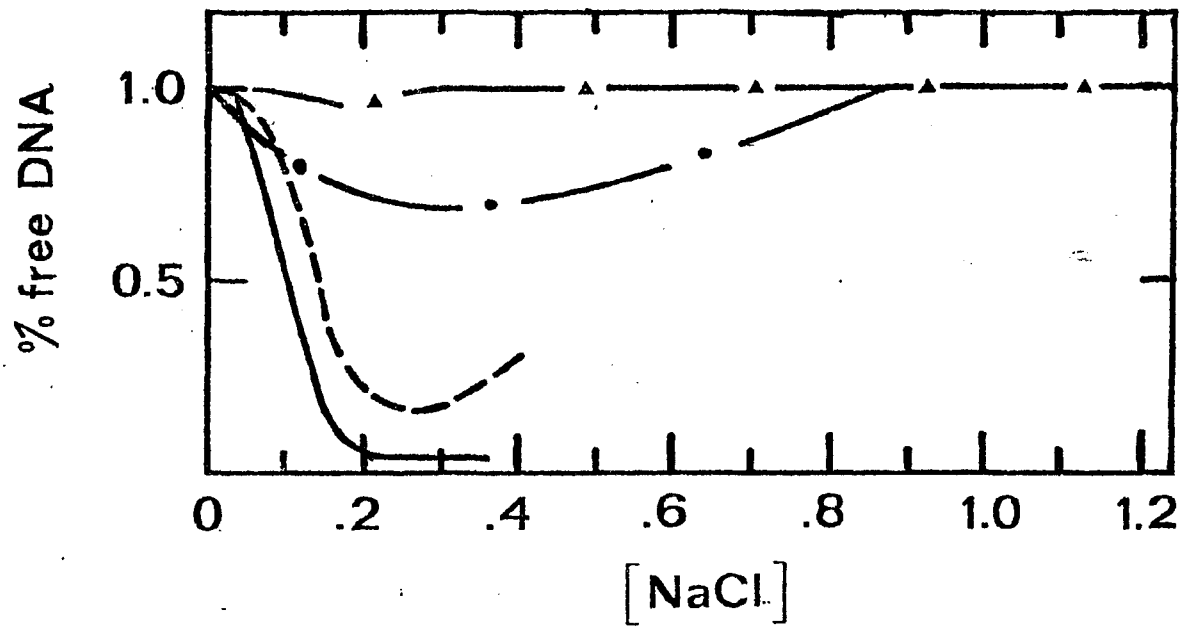

Fig 7. Titration curves of nucleohistones by NaCl. Nucleohistone (——), 0.35M NaCl-treated NH (---), 0.6M NaCl-treated NH (-●-) and 1.6M NaCl-treated NH (-▲-).
Buffer used for all samples was 0.25mM EDTA, pH 8.0

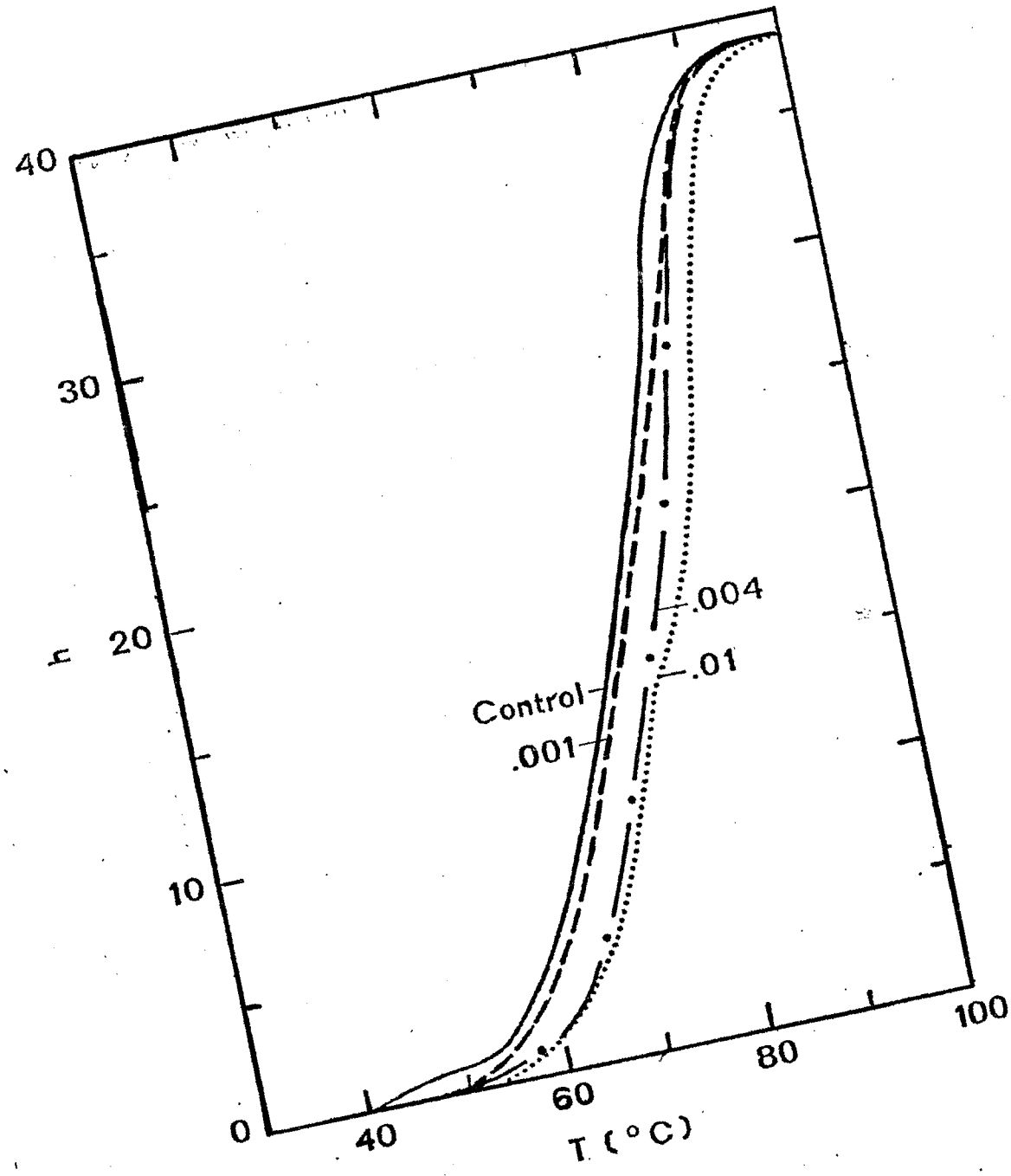

Fig 8. Melting curves of nucleohistones in NaCl. Control NH (——), 0.001M NaCl (– – –), 0.004M NaCl (–.–), and 0.01M NaCl (...)

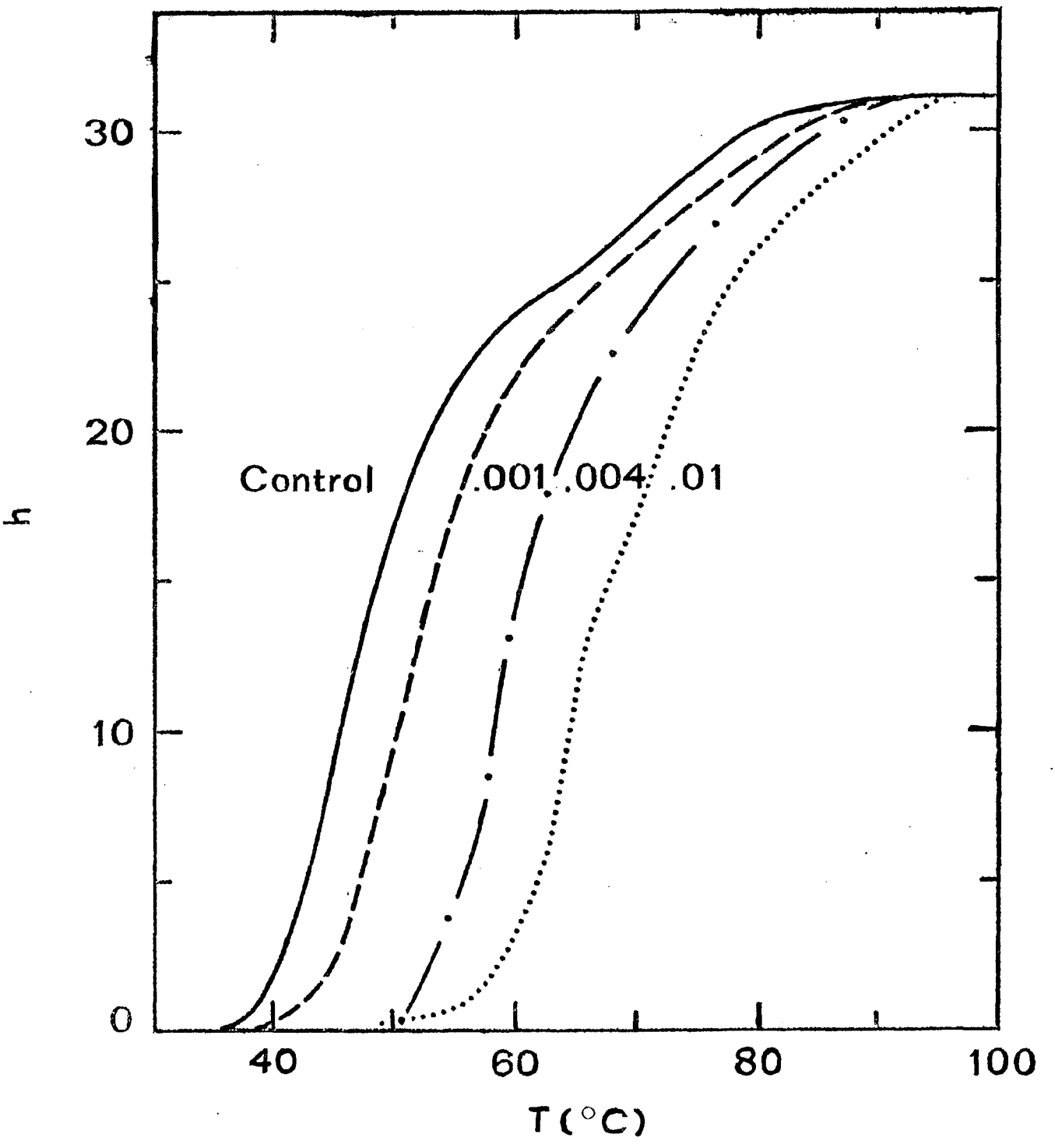

Fig 9. Melting curves of 2.5M NaCl-treated nucleohistone in NaCl. Control (——), 0.001M NaCl (---), 0.004M NaCl (-.-) and 0.01M NaCl (...). Buffer used was 0.25mM EDTA, pH 8.0

in T_m at increasing ionic strength. This is especially true of 2.5M NaCl-treated nucleohistone, the shift is greatest on T_{mI} of free DNA regions and the on T_{mIII} and T_{mIV} of histone-bound DNA base pairs.

c. Circular dichroism

Figs. 10, 11 and 12 show the effect of ionic strength on the circular dichroism of nucleohistone and two salt-treated nucleohistones. In all the three cases increase in NaCl concentration causes a slight decrease of the amplitude of the positive peak at 278nm and also a reduction of the negative trough at 220nm. The decrease in the amplitude of the positive peak can be explained as a result of dehydration in DNA by NaCl. Previously, a large negative CD (Ψ-CD) of DNA near 270 nm has been reported for reconstituted histone H1-DNA complexes at 0.15M NaCl and was interpreted as a real conformational effect of DNA in chromatin at physiological ionic strength (47). The CD results shown in Figs 10-12 dispute this interpretation, Ψ-CD does not occur in nucleohistone or NaCl-treated nucleohistones in physiological ionic strength. Ψ-CD must be a result of some type of structure of DNA complex very different from that of DNA in chromatin.

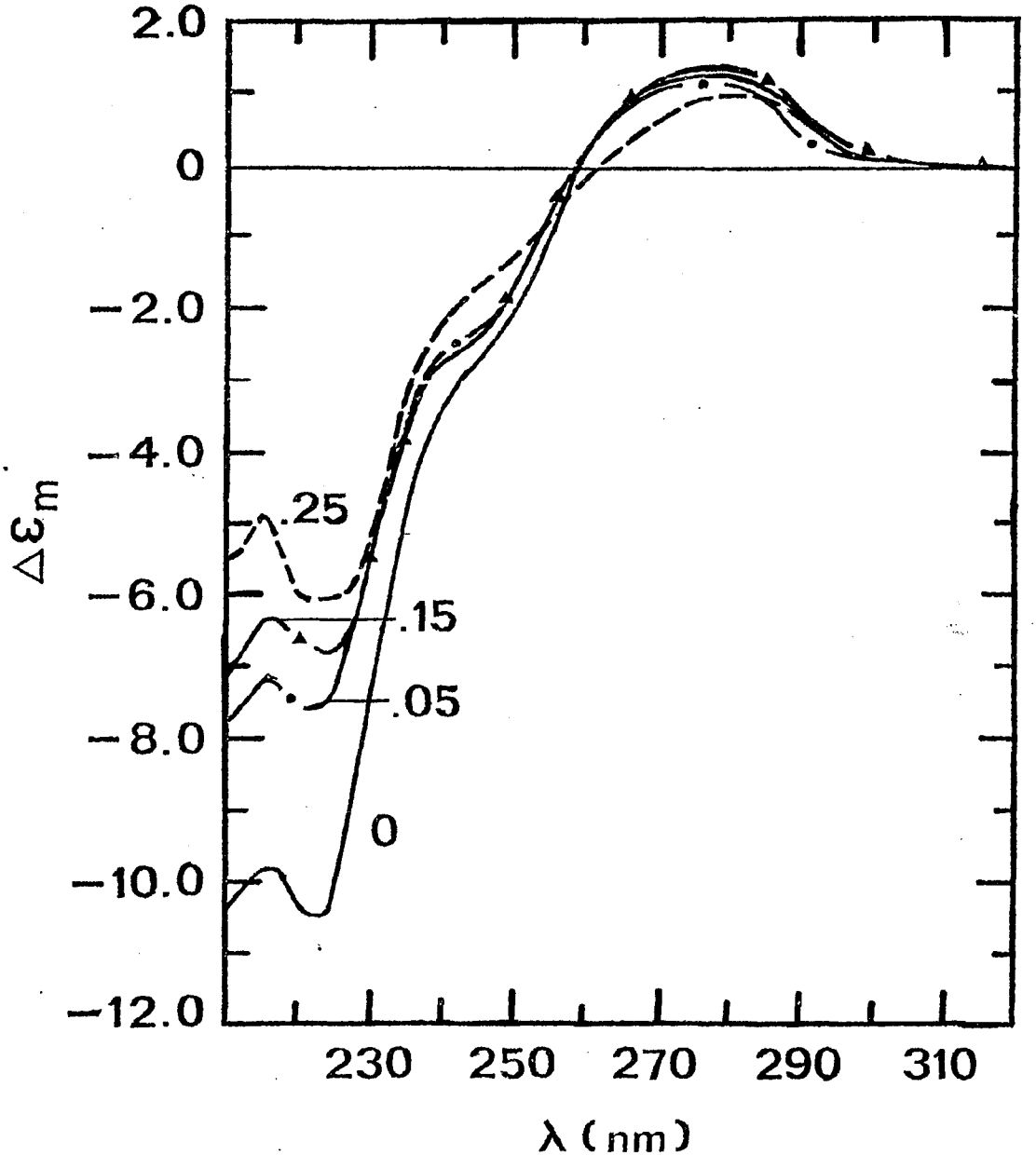

Fig.10. CD spectra of nucleohistone in NaCl. Control NH (——), 0.05M NaCl (-.-), 0.15M NaCl(-Δ-), and 0.25M NaCl (---)
All samples were made in 0.25mM EDTA buffer, pH 8.0

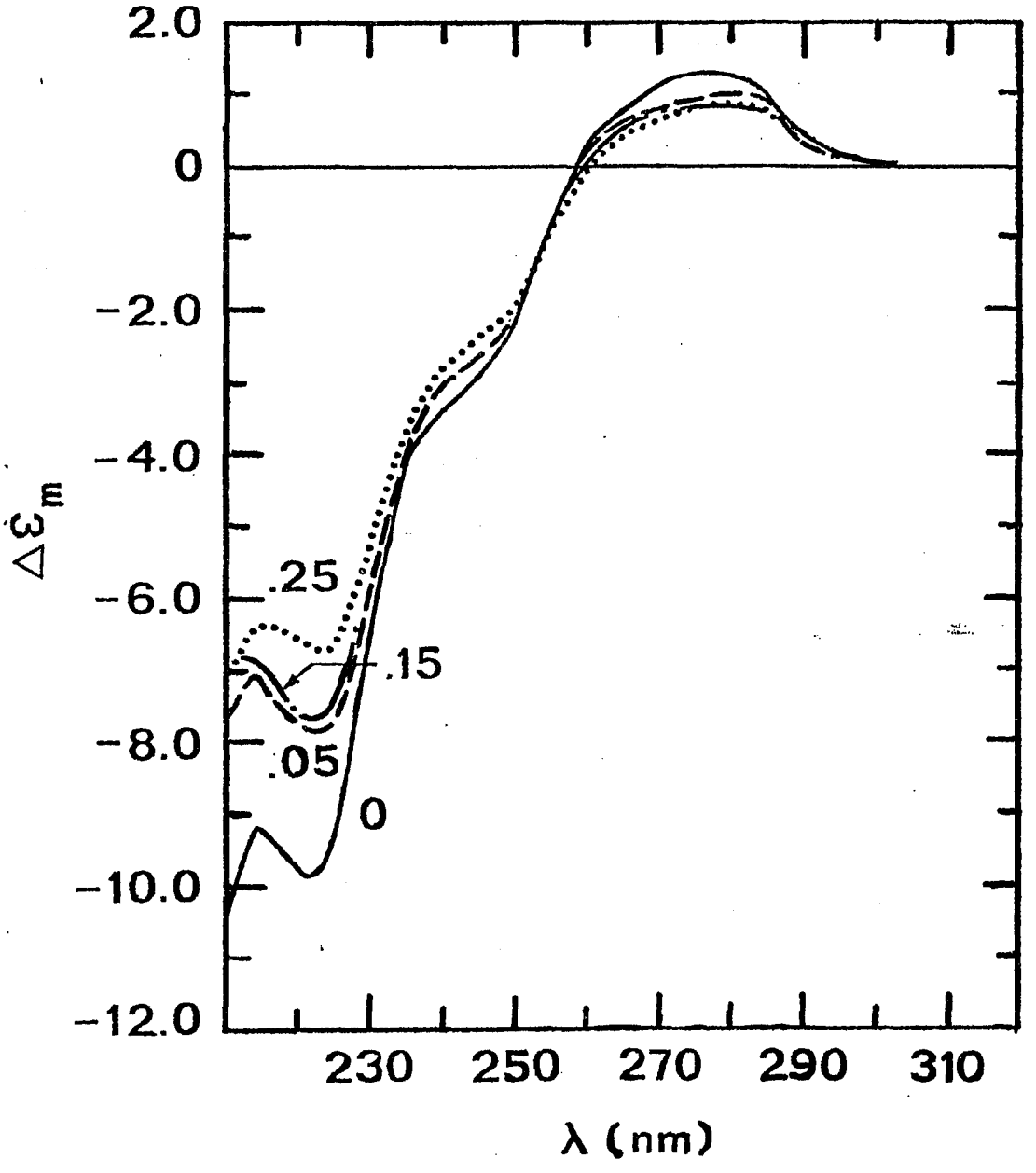

Fig 11. CD spectra of 0.6M NaCl-treated NH in NaCl. Control (——), 0.05M (---), 0.15M (-.-) and 0.25M (...) (Buffer: 0.25mM EDTA, pH 8.0)

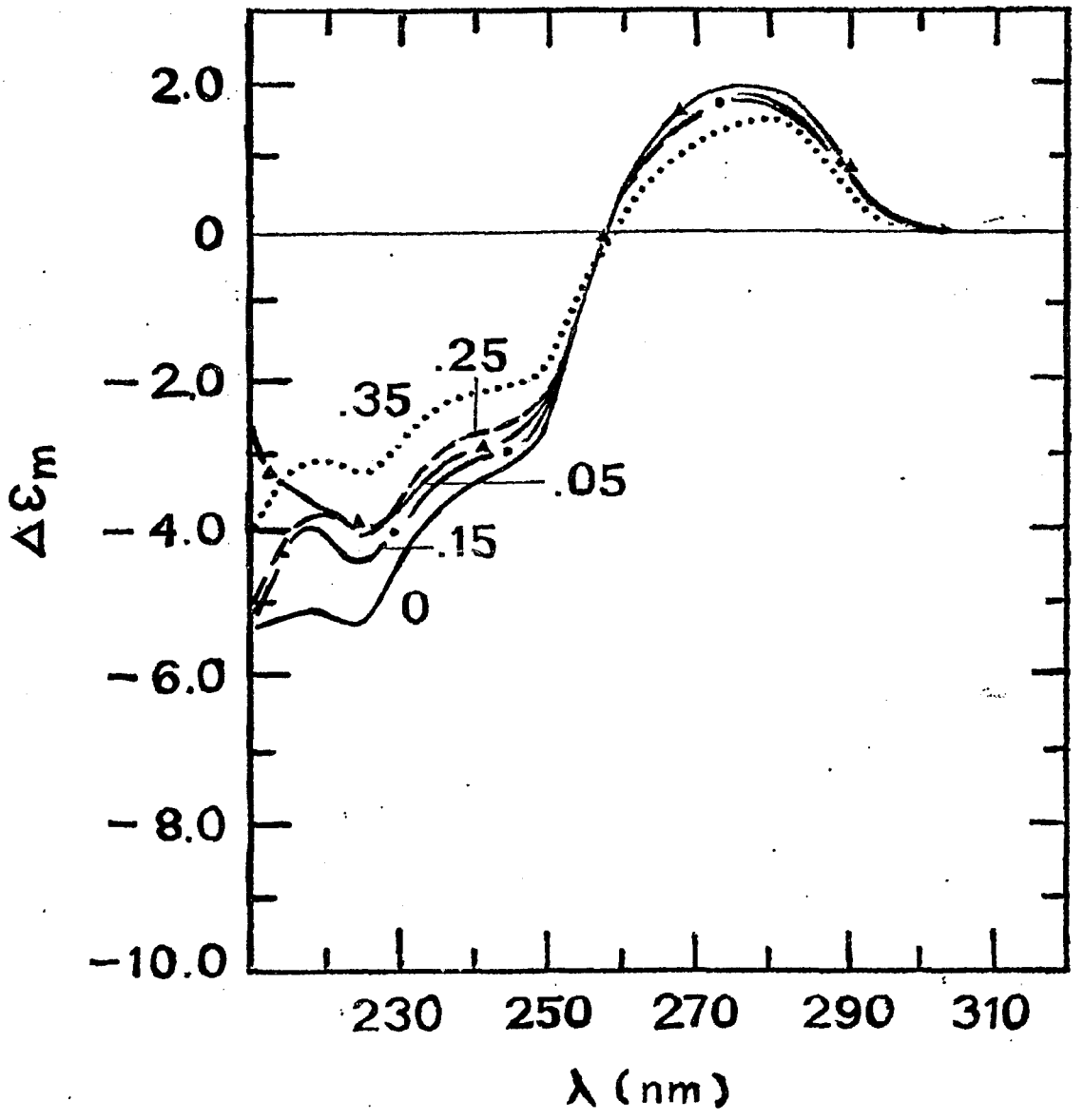

Fig 12. CD spectra of 1.6M NaCl-treated NH in NaCl. Control (——), 0.05M(-▲-), 0.15M(-.-), 0.25M(---) and 0.35M(...)
(Buffer: 0.25mM EDTA, pH 8.0)

Discussion

Primary interactions between proteins and DNA are ionic interaction, hydrogen bonding and hydrophobic interaction. These interactions cause a change in the conformation of both proteins and DNA. Removal of histones restores the CD of nucleohistone to that of DNA. The linear relationship shown in Fig. 5 suggests that conformational effect on DNA bound by histones is a localized event rather than a result of the formation of higher order structure such as supercoil (51). Thermal denaturation also measures thermal stability of histone-bound base pairs and is independent of the supercoil because partial removal of of histones reduces only the amplitude but not the characteristic melting bands of histone-bound regions (Fig 2). In addition, melting properties are also independent of the size of chromatin before or after shearing.

The earlier interpretation of melting bands III and IV as caused by the binding of the less basic and the more basic halves of histones (73) has been supported by the works of Leffak et al. (48), Hwan et al. (49), and Yu et al. (86) in our laboratory. Melting bands similar to melting bands III and IV in nucleohistone could be regenerated in DNA complexed with histone H2B (48), H5 (49) or H3+H4 (86). It is also supported by

the work of Ansevin et al. (87) and Li et al. (88) on trypsin digestion of chromatin. Trypsin digested chromatin shows preferential reduction of melting band IV which was explained by Li et al. (88) as a preferential digestion of the more basic regions of histones by trypsin. This interpretation was recently confirmed by Weintraub and Van Lente using peptide mapping and electrophoresis (57).

Thermal denaturation also show that 80% of chromatin is bound by nucleoproteins. This result is in agreement with values obtained from template activity and DNA-RNA hybridization results (89, 90). The size of free DNA regions in chromatin is unknown. However, due to the absence of T_{mI} in chromatin the presence of long stretches of uncovered DNA regions is unlikely. The result that in chromatin there are 3.5 amino acid residues per nucleotide of DNA in the bound regions agrees with that obtained from pea-bud chromatin (73). This means that one histone H2B with 125 amino acid residues will bind 15 base pairs and one histone H1 with 216 amino acid residues will bind 31 base pairs. Furthermore, there is less shielding of histone-bound regions in chromatin as compared to that in polylysine-DNA complexes, as the T'_m of polylysine-DNA is 100°C which is much higher than T_{mIII} and T_{mIV} in nucleohistones.

Histone H1 has the least effect on the conformation

of DNA in chromatin as shown in Fig 5. After histone H1 has been removed by 0.6M NaCl the extrapolation to 100% binding of other histones shows an average CD of zero in the histone-bound base pairs in chromatin which is close to the C-conformation. In other words, the average conformation of DNA complexed by whole histones minus H1 is close to the C-type. But the above results is only an average CD of the histone-bound regions in chromatin. The next chapter on polylysine-nucleohistone complexes will show that the DNA base pairs in melting band III and melting band IV have different CD spectra.

CHAPTER IV

POLYLYSINE-DNA, -CHROMATIN, AND -SALT TREATED NUCLEOHISTONE COMPLEXES

Polylysine, a basic polypeptide, had been used as a probe for chromatin structure (82), and as a model system for basic proteins when they interact with DNA (64, 65, 68). Thermal denaturation and circular dichroism were used in this study of the interaction in polylysine-DNA and polylysine-nucleohistones complexes. Polylysine binding to nucleohistone was also used as a probe to study the distribution of electrostatic charges along the chromatin molecule.

Experimental

Poly L- lysine hydrochloride, molecular weights 170,000 and 15,500 daltons was purchased from Schwarz/ Mann. It was dialyzed against 0.25mM EDTA, pH 8.0 and the concentration obtained afterwards was determined by the ninhydrin method using lysine hydrochloride as the standard. Polylysine-DNA and polylysine nucleohistone

complexes were made by direct and dropwise mixing of polylysine at 5 x 10^{-4}M to a DNA or nucleohistone solution of 1 x 10^{-4}M concentration. The resulting solutions were centrifuged for 10 minutes at 10,000 rpm(Sorvall SS-34 rotor) at 4°C and the supernatant collected for measurement. The input ratio of poly L-lysine to DNA and nucleohistones was computed as the number of lysine per nucleotide of DNA.

Results

a. Titration curves

A slow addition of polylysine directly to DNA results in irreversible complexes with polylysine scattered along the DNA molecules. These complexes are soluble until a certain input ratio of lysine/nucleotide is reached. Fig. 13 shows the titration curves of polylysine-DNA, -nucleohistone,-0.6M NaCl-treated nucleohistone, and -1.6M NaCl-treated nucleohistone complexes. Precipitation occurs sharply within a small range of lysine/nucleotide ratio. The mid-point of titration or precipitation is 0.52, 0.66, 0.81 and 1.02 for calf thymus nucleohistone, 0.6M NaCl-treated nucleohistone, 1.6M NaCl-treated nucleohistone and pure DNA. The precipitation point of lysine/nucleotide of 1.0 is expected for polylysine-DNA complexes where one lysine neutralized one phosphate of DNA. 50% of the DNA of

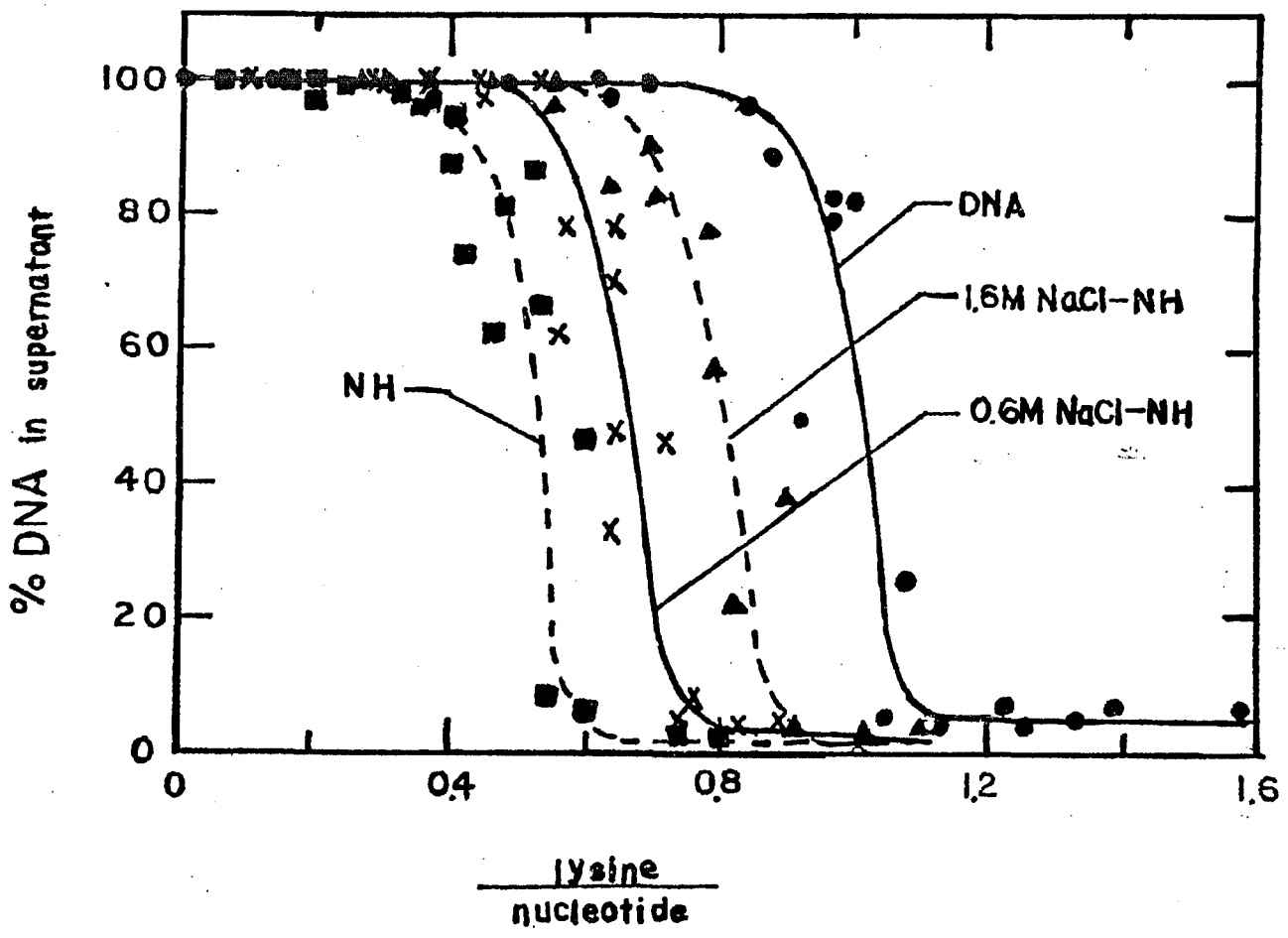

Fig 13. Titration curves of nucleohistones by polylysine. Nucleohistone (■), 0.6M NaCl-treated nucleohistone (×), 1.6M NaCl-treated nucleohistone (▲) and DNA (●). Buffer: 0.25mM EDTA, pH 8.0

nucleohistone is accessible for polylysine binding. As more DNA are exposed by removing histones more DNA base pairs are accessible to polylysine binding, this is shown by the increase in the precipitation point with the salt-treated nucleohistones.

b. Thermal denaturation of polylysine-DNA, -nucleohistone and salt-treated nucleohistone complexes

Derivative melting profiles of polylysine-DNA complexes (polylysine MW=170,000 daltons) is shown in Fig. 14. Pure DNA in 0.25mM EDTA, pH 8.0 has a melting band at 48°C. DNA base pairs bound by polylysine have a melting at 100°C. Increase in the lysine/nucleotide input ratio cause a decrease in the area of melting of free DNA region and an increase in the area of melting of bound DNA base pairs.

Thermal denaturation results of polylysine-nucleohistone and polylysine-1.6M NaCl-treated nucleohistone are shown in Fig. 15 and Fig. 16 respectively. In addition to the four melting bands (I, II, III and IV) in nucleohistone there is a fifth melting band at 95°- 99°C. This corresponds to the melting of DNA base pairs in nucleohistone covered by polylysine. Qualitatively, when more polylysine binds to nucleohistone or salt-treated nucleohistone the areas of melting bands I, II, and III decrease. The area of melting band IV does

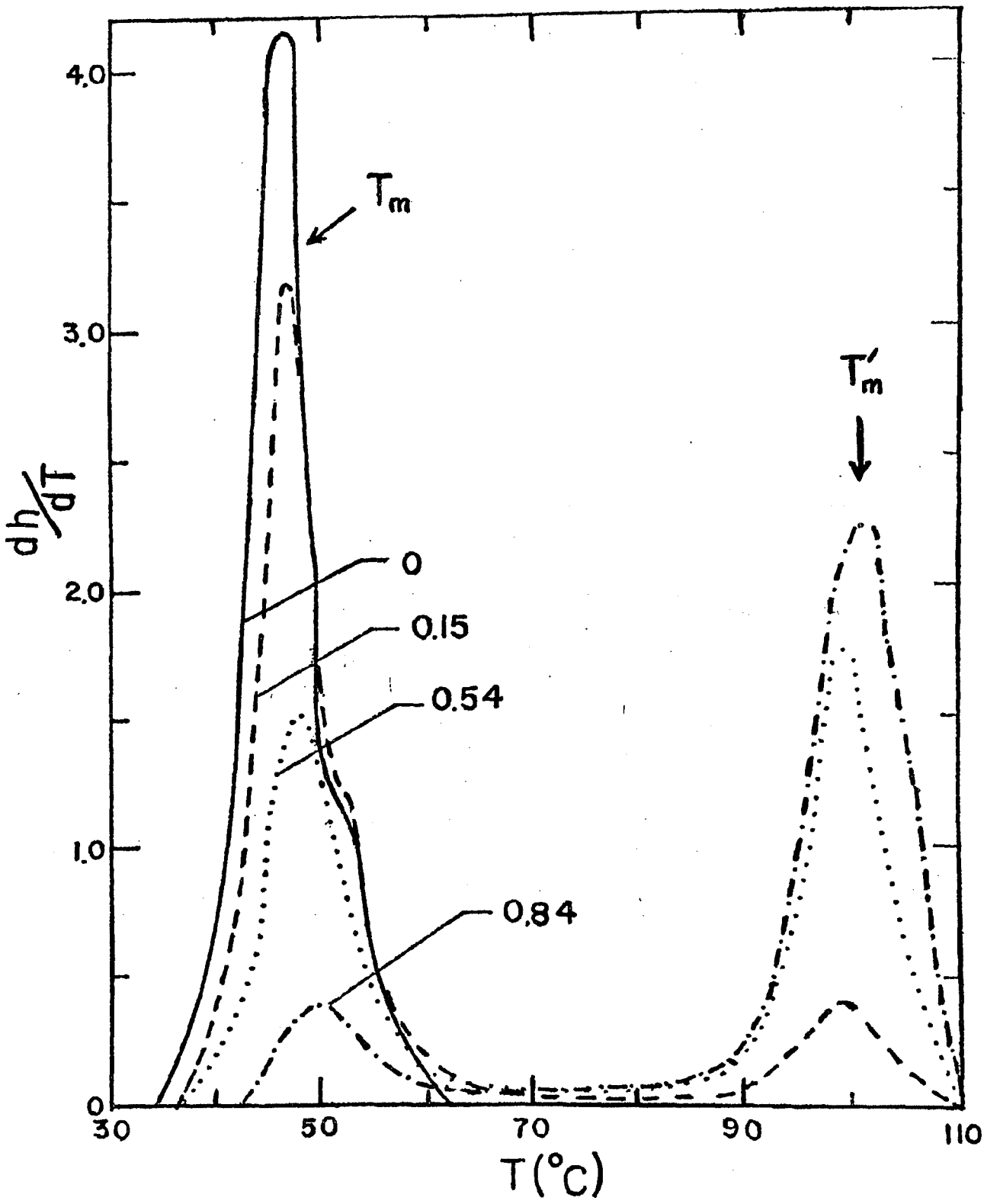

Fig 14. Derivative melting profiles of polylysine-DNA complexes. Input ratios of polylysine is given in the figure. Buffer: 0.25mM EDTA, pH 8.0

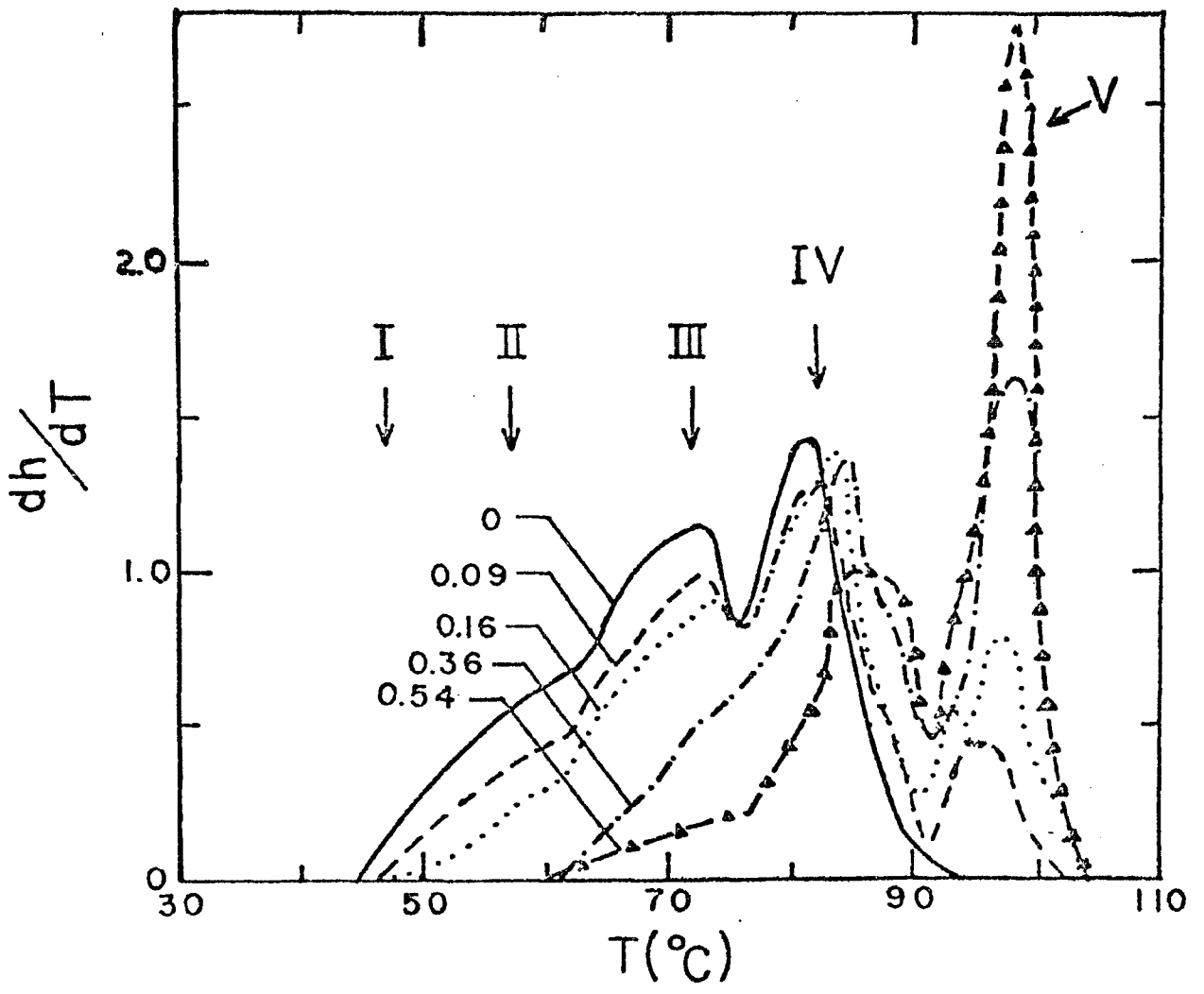

FIGURE 15: Derivative melting profiles of polylysine–nucleohistone complexes. Lysine/nucleotide ratios are given in the figure.

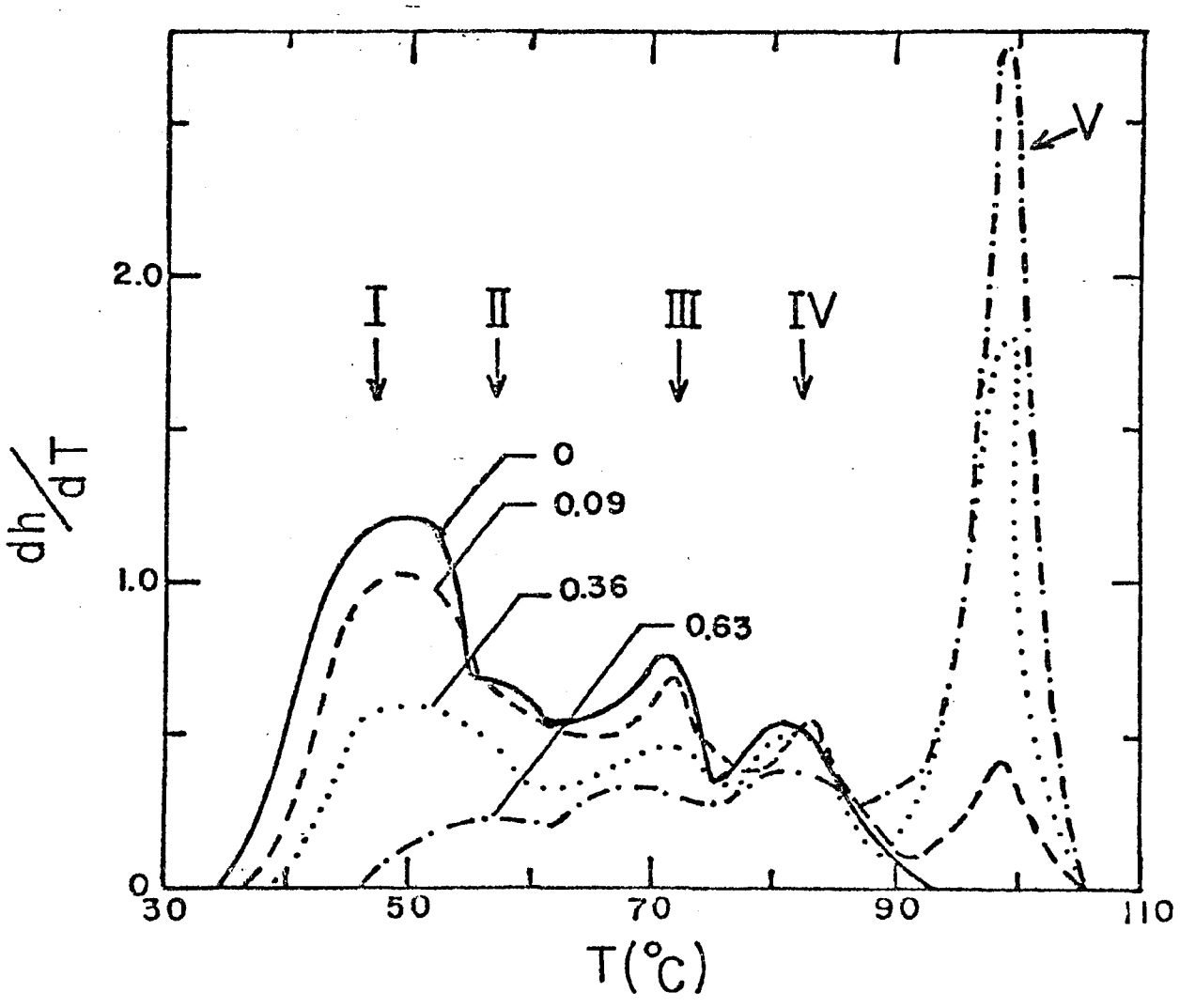

Fig 16. Derivative melting profiles of polylysine-1.6M NaCl-treated nucleohistone complexes. Input ratio of polylysine is given in the figure. Buffer: 0.25mM EDTA, pH 8.0

not change until a high input of lysine/nucleotide is reached. There is a gradual shift of T_{mIV} to higher temperature when the lysine/nucleotide input ratio is increased. From the previous chapter melting band I corresponds to the melting of free DNA regions, melting band II to DNA regions bound by nonhistone proteins or very short gaps of free DNA, and bands III and IV to DNA base pairs bound by the less basic and the more basic halves of histones. The melting profiles show qualitatively that the order of preference site of polylysine binding is : free DNA > nonhistone proteins bound DNA > less basic half of histone bound DNA > more basic half of histone bound DNA. This is consistant with one's expectation because accessibility of phosphates for polylysine binding also follow the same order. Fig. 17 and Fig. 18 show the quantitative comparison of this result.

Table 4 shows that the maximum hyperchromicity of polylysine-DNA complexes decrease with increasing binding of polylysine. The light scattering of these complexes made by direct and slow mixing is less than 5%. This is a major improvement because previous workers showed that high light scattering of polylysine-DNA complexes caused ambiguity in the interpretation of their results.

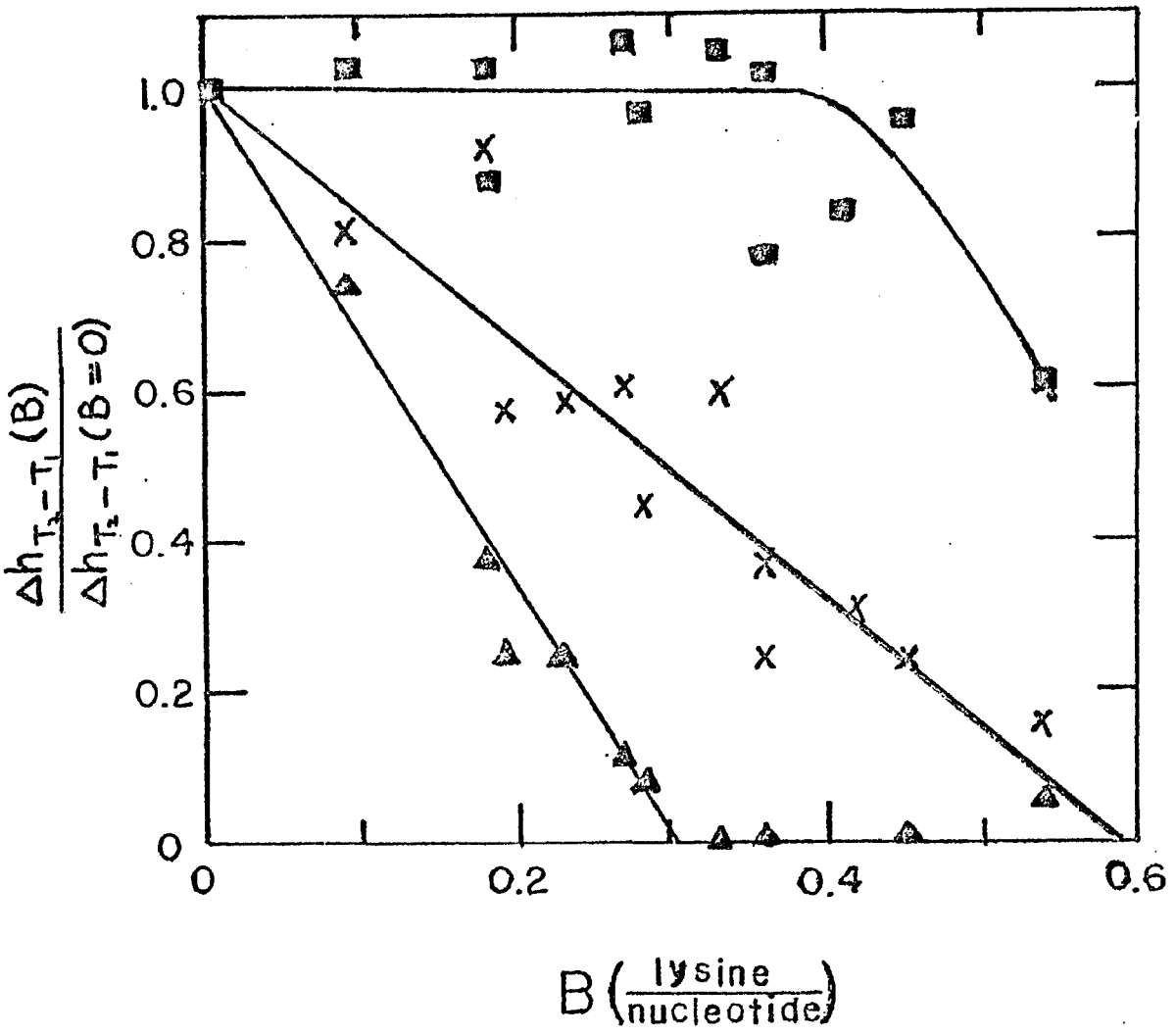

Fig 17. Decrease of hyperchromicity as a function of lysine/nucleotide ratio in polylysine-nucleohistone complexes. T_2-T_1 is 60°C-50°C (▲), 75°C-65°C (×), and 86°C-78°C (■). For B=0, Δh_{60-50} is 3.6, Δh_{75-65} is 9.6 and Δh_{86-78} is 9.7

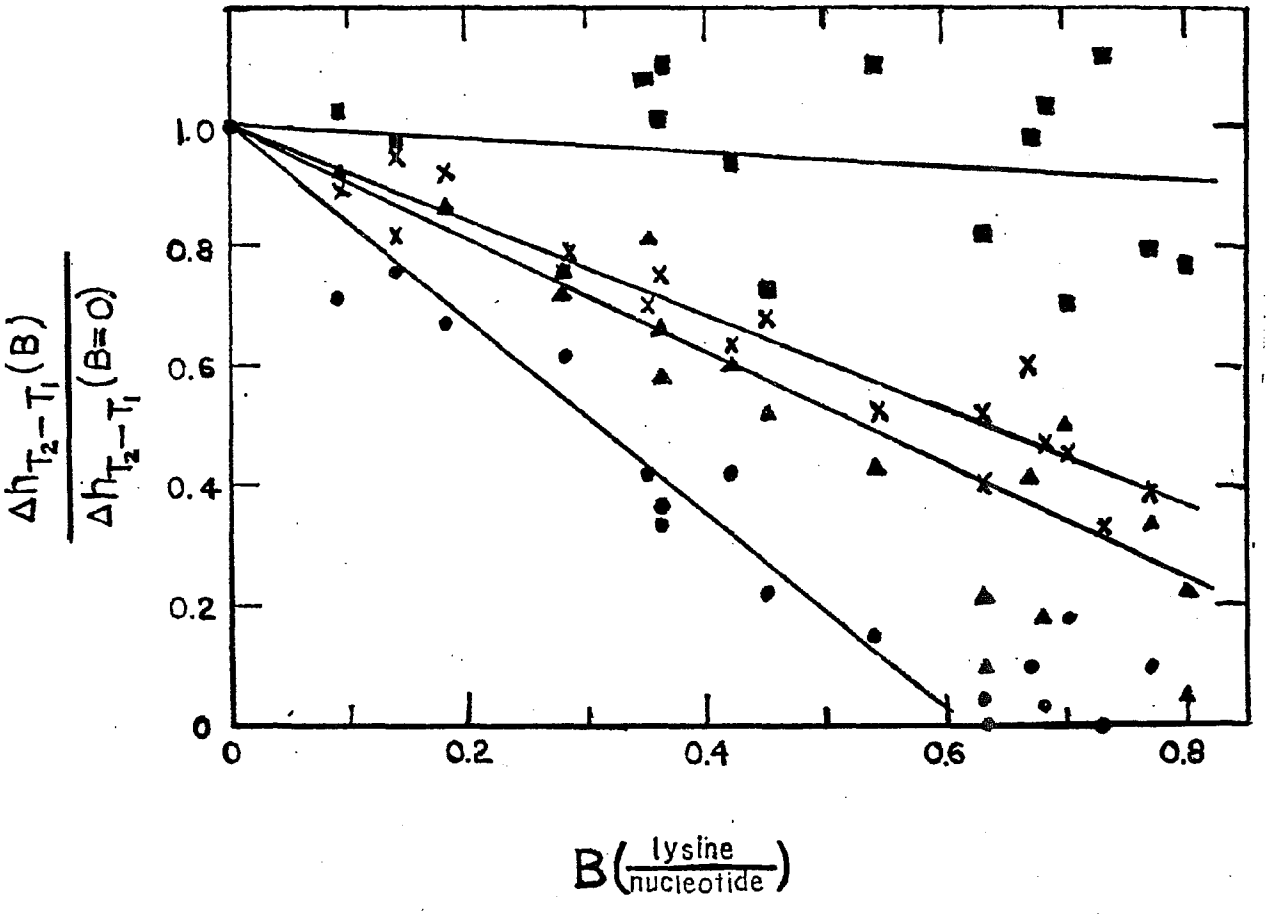

Fig 18. Decrease of hyperchromicity as a function of lysine/nucleotide ratio in polylysine-1.6M NaCl-treated nucleohistone complexes. T_2-T_1 is 50°C-30°C (●), 60°C-50°C (▲), 75°C-65°C (×), and 86°C-78°C (■). For B=0, $\Delta h_{50-30}=16.9$, $\Delta h_{60-50}=6.3$, $\Delta h_{75=65}=4.5$ and $\Delta h_{86-78}=2.9$

Table 4

Hyperchromicities of Polylysine-DNA Complexes

Lysine/ Nucleotide	A_{260} in Supernatant	h_{max}(%)	A_{320}/A_{260} 30°	A_{320}/A_{260} 110°
0	0.648	35.9	0.022	0.016
0.09	0.645	35.8	0.019	0.022
0.18	0.647	34.9	0.009	0.007
0.36	0.653	32.5	0.031	0.023
0.63	0.640	32.0	0.037	0.039
0.90	0.669	30.0	0.035	0.034

c. Quantitative analysis of polylysine binding to nucleohistone, salt-treated nucleohistones and DNA

Since the hyperchromicity of polylysine-bound regions are lower than that of free DNA regions, the equation:

$$B_k = \beta_k \frac{A_k}{A_T}$$

used in the previous chapter for nucleohistone and salt-treated nucleohistones can not be used to compute the average lysine residues/nucleotide in polylysine-bound regions in these nucleohistones. The above equation can be used in those cases where the hyperchromicity of the free DNA region is the same as that of protein-bound regions. Li et al. (91) derived an equation for the analysis of the complexes.

Let h_b = hyperchromicity of base pairs bound by polylysine

h_f = hyperchromicity of free DNA base pairs

A_b = area of melting bands of polylysine-bound base pairs

A_f = area of melting band of polylysine-free base pairs

In polylysine-nucleohistone complexes $A_b=A_V$ the area of melting band V. In polylysine-DNA complexes $A_b=A_{T_m}$. If A_T is the total melting area then:

$$A_T = A_b + A_f \qquad (7)$$

$A_b = h_b F$ where F=fraction of base pairs tightly bound by polylysine with T_m corresponding to that of A_b

then $A_f = h_f(1-F)$ (8)

where 1-F is the fraction of base pairs free of polylysine

If B is the input ratio of lysine/nucleotide before the number of binding sites are saturated there is a linear relationship between B and F:

$B = \beta F$

β = average number of lysine/nucleotide in the polylysine bound regions

therefore, $B = \beta \frac{A_b}{h_b}$ (9)

combining eq. 8 and 9 one gets:

$$B = \beta \left(1 - \frac{A_f}{h_F}\right) \qquad (10)$$

Experimentally, h_f was taken as the hyperchromicities of nucleohistone and salt-treated nucleohistones and DNA before polylysine binding. A_b and A_f was obtained from the derivative melting curves. Fig. 19 shows the plot of eq. 10 for nucleohistone, 0.6M NaCl-treated nucleohistone, 1.6M NaCl-treated nucleohistone and DNA. β is 0.85 for polylysine-nucleohistone and -0.6M NaCl-treated nucleohistone complexes, 0.95 for polylysine-1.6M NaCl-treated

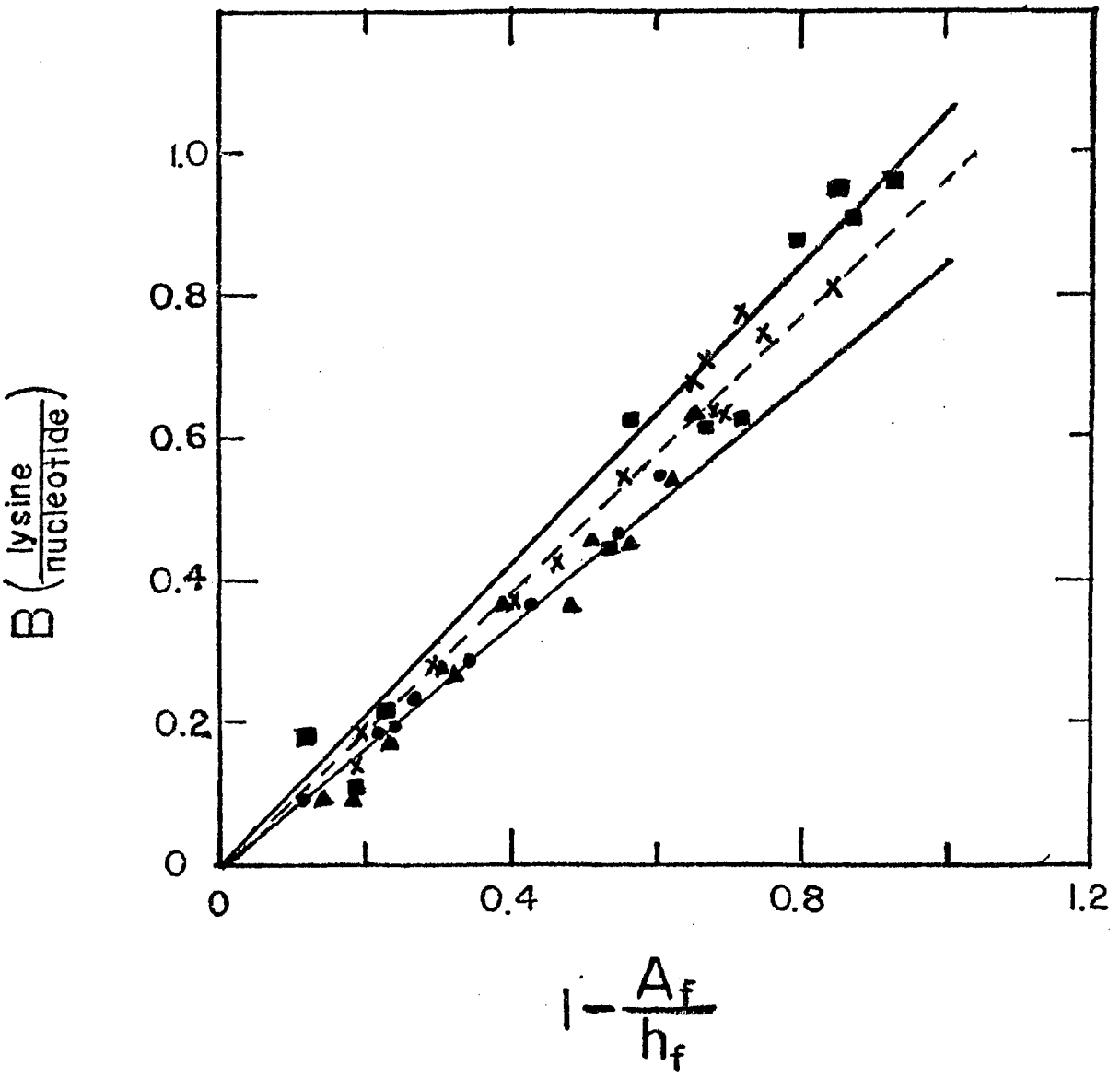

Fig 19. Linear plot of eq. 10. Nucleohistone (●——●), 0.6M NaCl-treated NH (▲——▲), 1.6M NaCl-treated NH (×——×) and DNA (■——■)

nucleohistone complexes and 1.05 for polylysine-DNA complexes. Fig. 20 shows the plot of eq. 9, β/h_b is determined from the slope. Since β is obtained from eq. 10, then h_b of polylysine-nucleohistone, -dehistonized nucleohistones and -DNA complexes can be determined and they are 20, 23.2, 26, and 28.7 respectively.

d. Circular dichroism spectra of the polylysine-nucleohistone, -salt-treated nucleohistone, and -DNA complexes

The CD spectra of polylysine-DNA complexes are shown in Fig. 21. The molecular weight of the poly L-lysine used was 170,000. Pure calf thymus DNA in 0.25mM EDTA, pH 8.0 showed a typical conservative spectrum of the B-form DNA. The $\Delta\varepsilon_m$ at 276 nm is 2.5 $M^{-1}cm^{-1}$. The crossover occurs at 255 nm. There is a negative trough at 245 nm with an amplitude of $-3.0M^{-1}cm^{-1}$. Finally, there is another positive peak at 220 nm with an amplitude of $1.0M^{-1}cm^{-1}$. As more DNA base pairs are bound by polylysine the positive peak is red shifted from 276 nm to 280 nm. Red shift is also observed for the crossover point. However, the CD spectra below 240 nm are independent of polylysine content in the complexes.

The CD spectra of polylysine-DNA complexes are not effected by the difference in chain length of the poly L-lysine. Fig. 22 shows the CD spectra of poly-

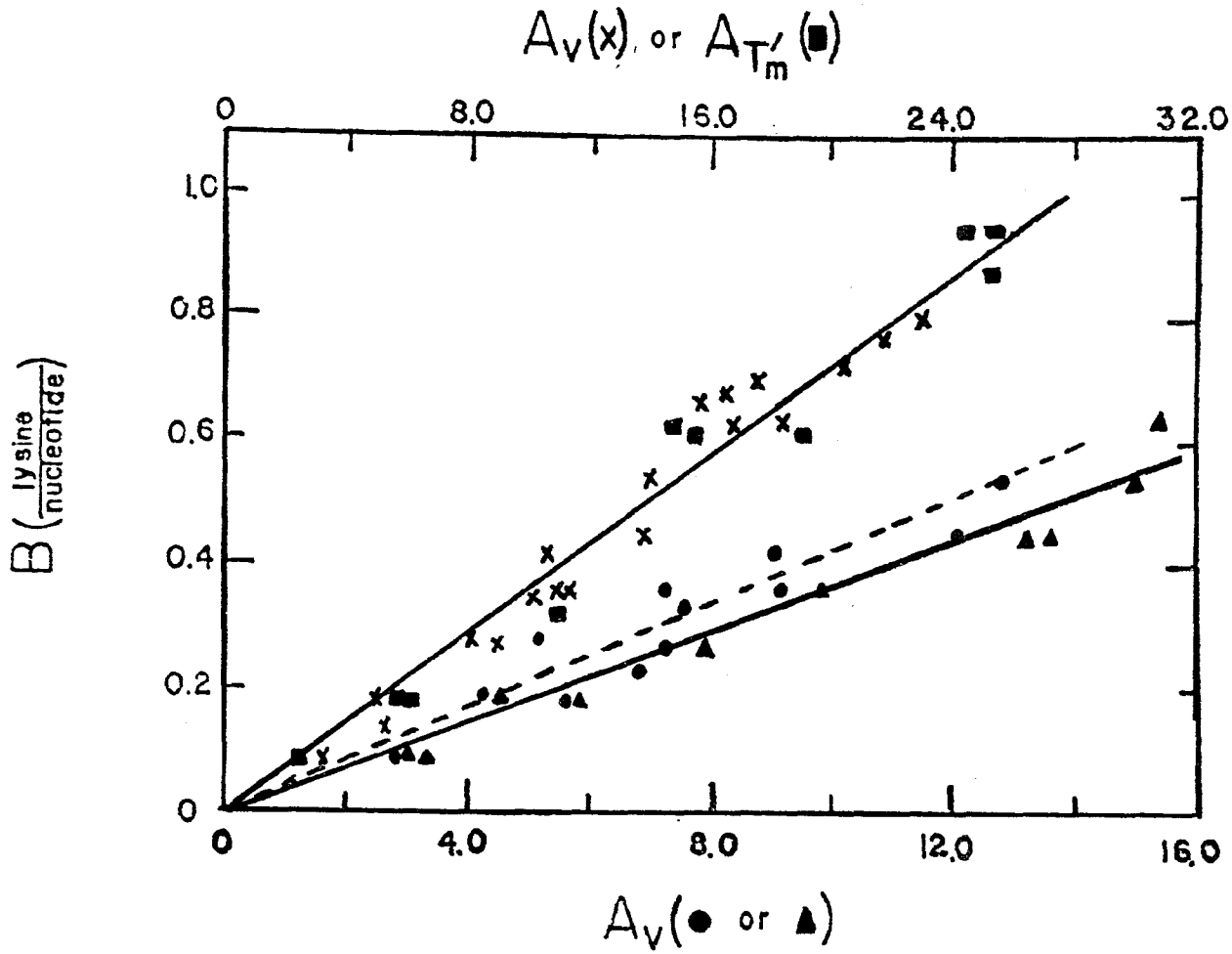

FIGURE 20: Linear plot of eq 9. Nucleohistone (●), 0.6 M NaCl-treated nucleohistone (▲), 1.6 M NaCl-treated nucleohistone (x), and DNA (■).

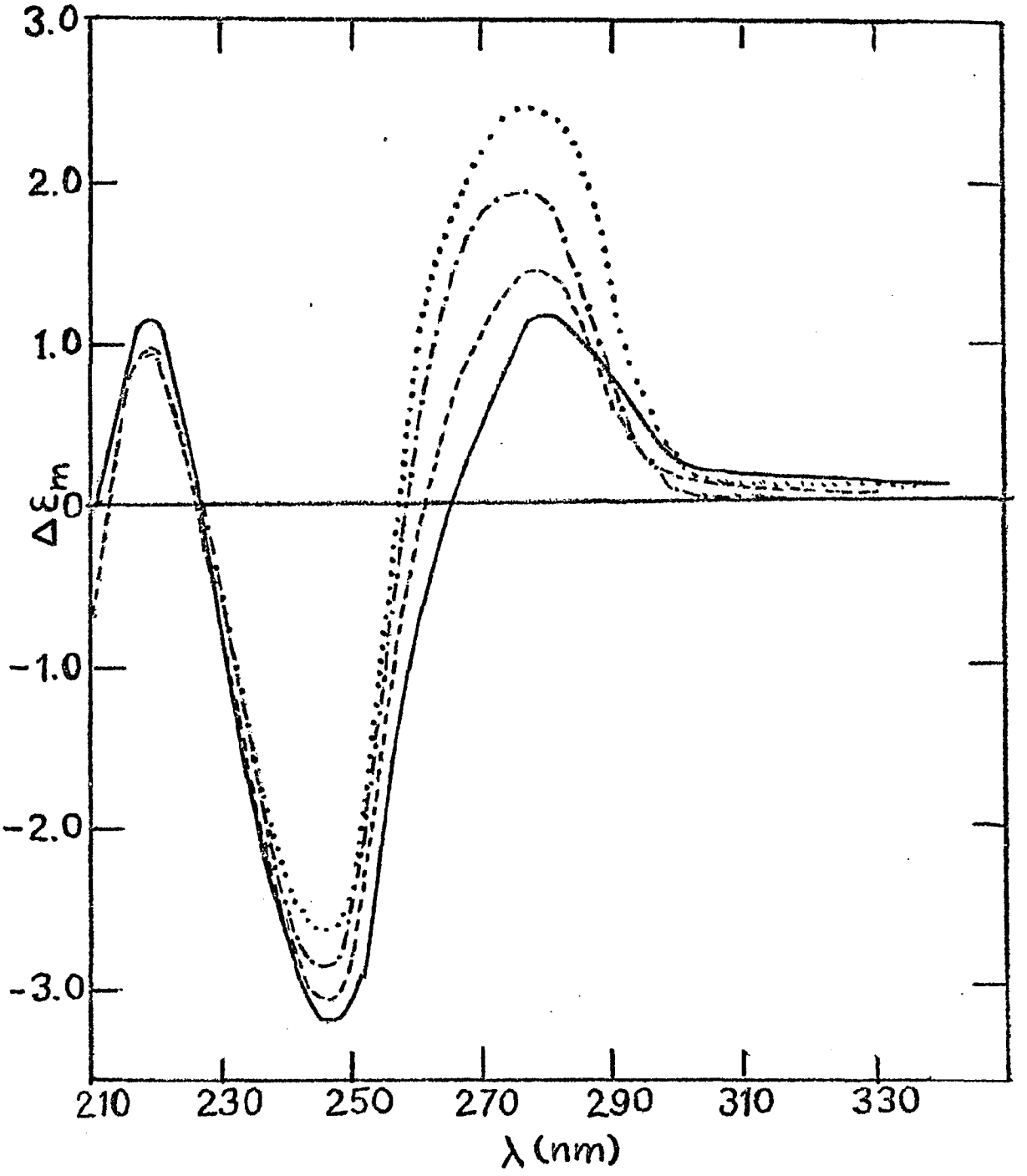

Fig 21. CD spectra of polylysine-DNA complexes. The lysine/nucleotide ratio is 0 (...) 0.27 (-.-), 0.54 (---), and 0.81 (——). The MW of polylysine is 170,000 daltons. Buffer: 0.25mM EDTA, pH 8.0

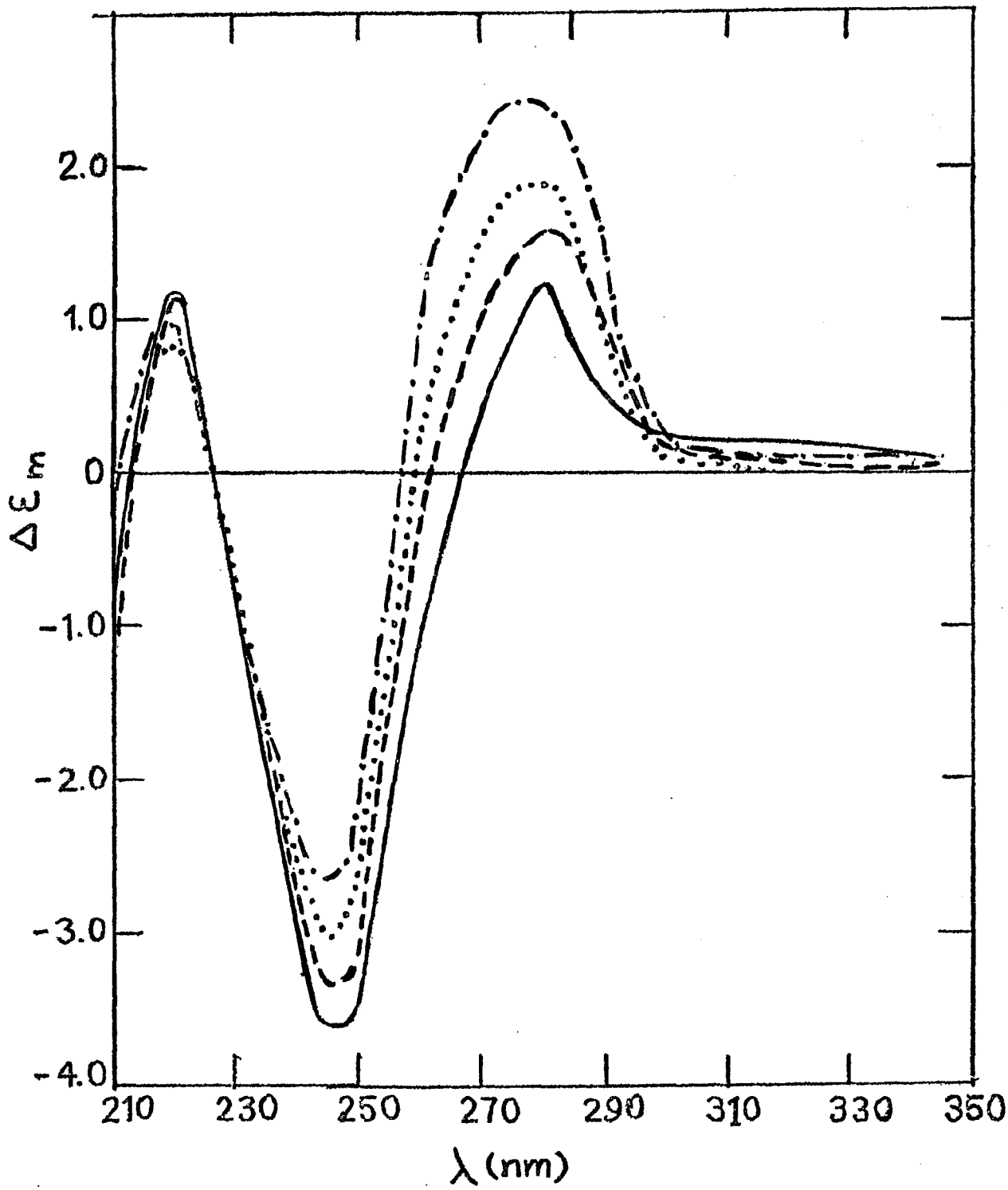

Fig 22. CD spectra of polylysine-DNA complexes. The lysine/nucleotide ratio is 0 (-.-), 0.27 (...), 0.54 (---) and 0.81 (——). The MW of polylysine is 15,500 daltons.
Buffer: 0.25mM EDTA, pH 8.0

lysine-DNA complexes with poly L-lysine of molecular weight of 15,500. The spectra are identical to that of complexes made with polylysine of the higher molecular weight. The changes in the CD spectra is proportional to the input ratio of lysine/nucleotide. This is seen in the difference CD spectra of the complexes in Fig. 23. The difference CD spectrum of the complex is $\Delta\varepsilon_m - \Delta\varepsilon_o$, where $\Delta\varepsilon_m$ is the measured CD and $\Delta\varepsilon_o$ is the CD of pure DNA. The circular dichroism of polylysine-bound DNA base pairs can be calculated from eq. 5 used for the nucleohistone in the previous chapter.

The calculated CD of the polylysine-bound DNA base pairs are shown in Fig. 24. Regardless of the input ratio of lysine/nucleotide the $\Delta\varepsilon_b$ of all the polylysine-DNA complexes are the same. Fig. 24 also shows the CD spectrum of DNA in 6M NaCl. This spectrum is similar to the spectrum of polylysine-covered DNA regions. The effect of polylysine on DNA conformation is similar to that of NaCl effect. This is clearly shown in Fig. 25, where the ratio of positive peak to the negative trough of the CD spectrum ($\Delta\varepsilon_{278}/-\Delta\varepsilon_{246}$) is plotted against lysine/nucleotide ratio and NaCl concentration. The effect of NaCl and lysine/nucleotide input ratio is identical.

Fig. 26 shows the CD spectra of polylysine-nucleohistone complexes. The effects are similar to that of

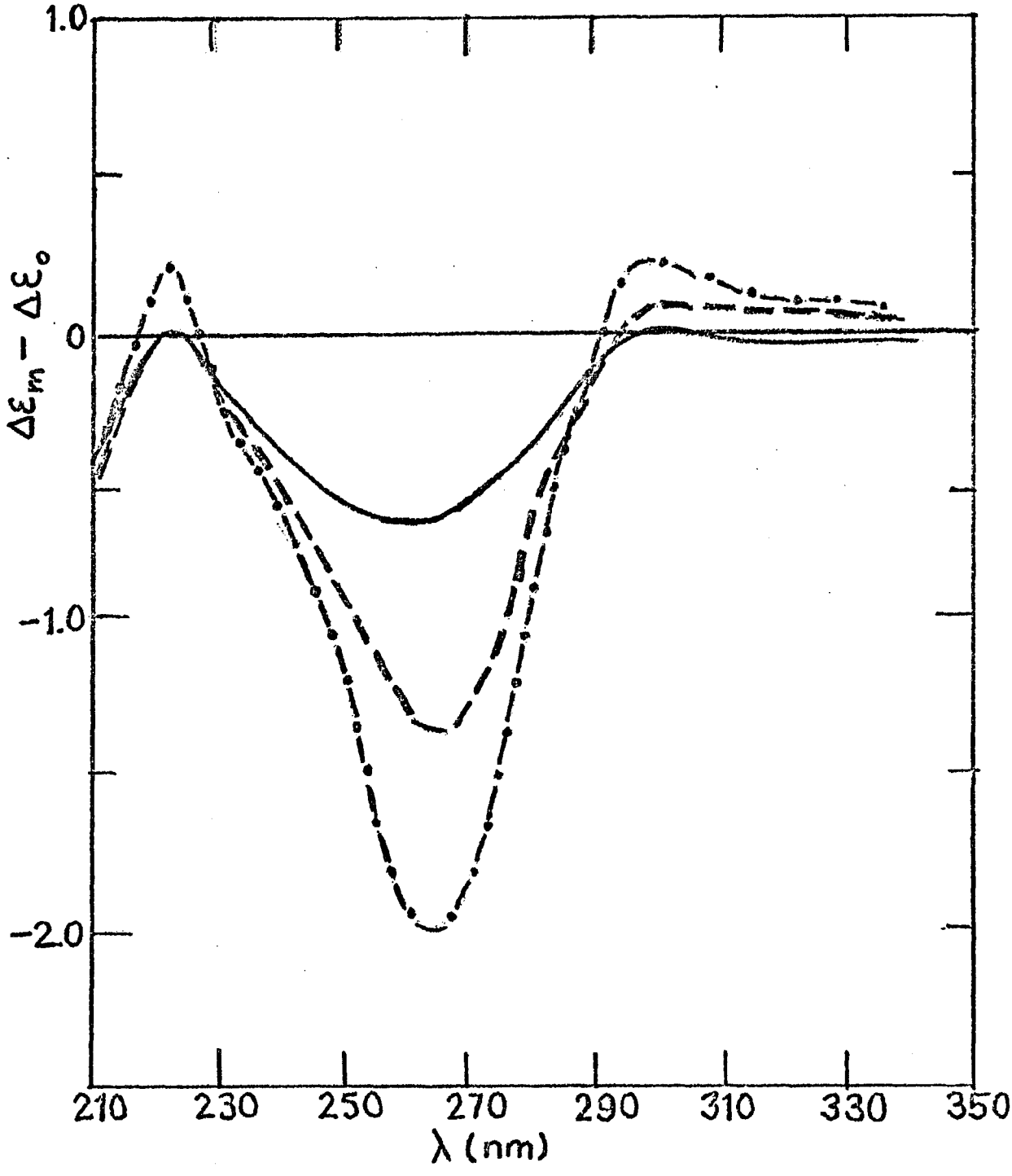

Fig 23. Difference CD spectra of DNA ($\Delta\varepsilon_o$) and polylysine-DNA complexes ($\Delta\varepsilon_m$). The lysine/nucleotide ratio of the complexes is 0.27 (——), 0.54 (---) and 0.81 (-.-)

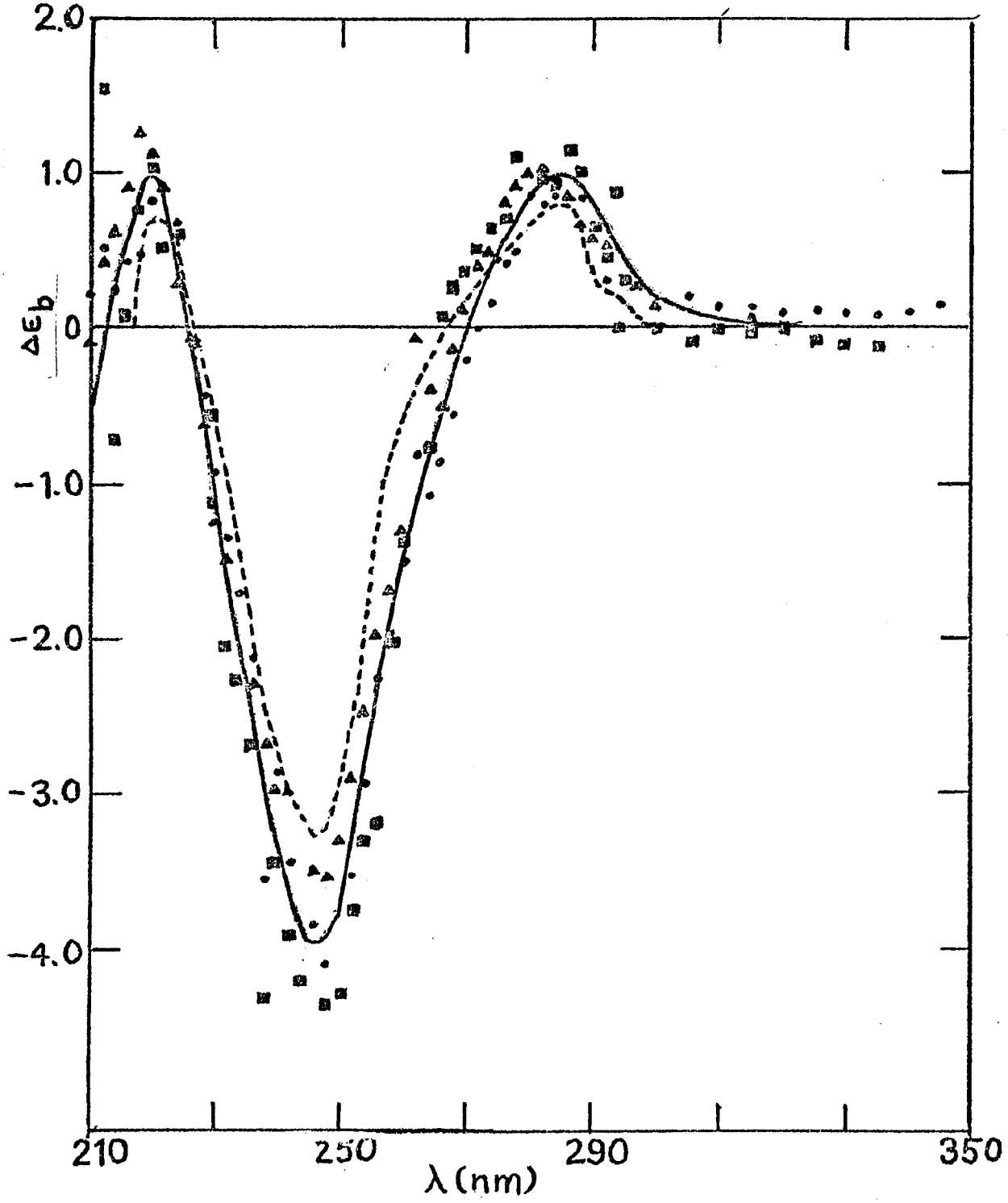

Fig.24. CD spectrum of polylysine-bound base pairs. The lysine/nucleotide ratio is 0.27 (▣), 0.54 (●), and 0.81 (▲). $\Delta\varepsilon_b$ of DNA is 6.0M NaCl is from Tunis-Schneider and Maestre (28). Polylysine=170,000

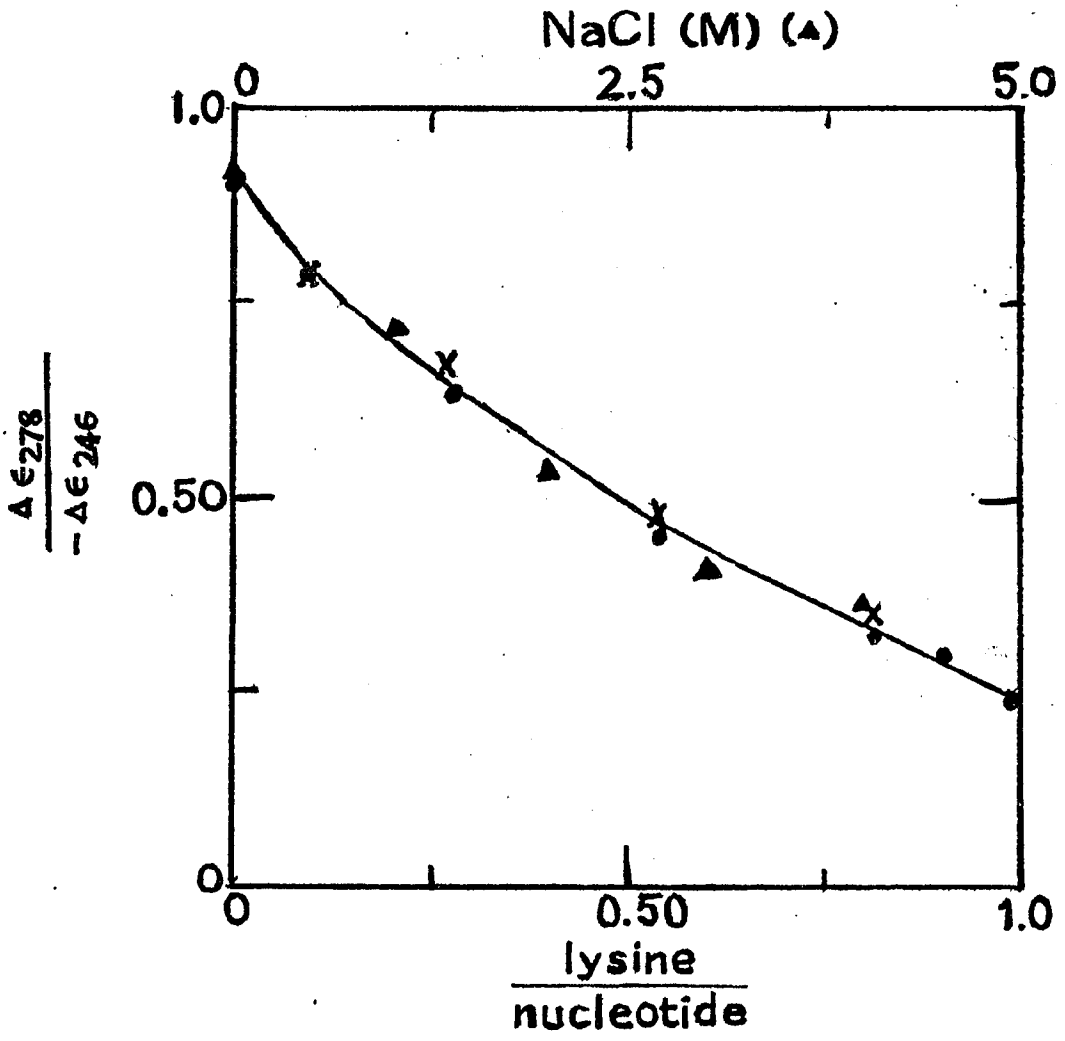

Fig 25. The effect of NaCl and polylysine binding on the CD of DNA. NaCl (▲), polylysine of MW 170,000 (X) and 15,500(●)

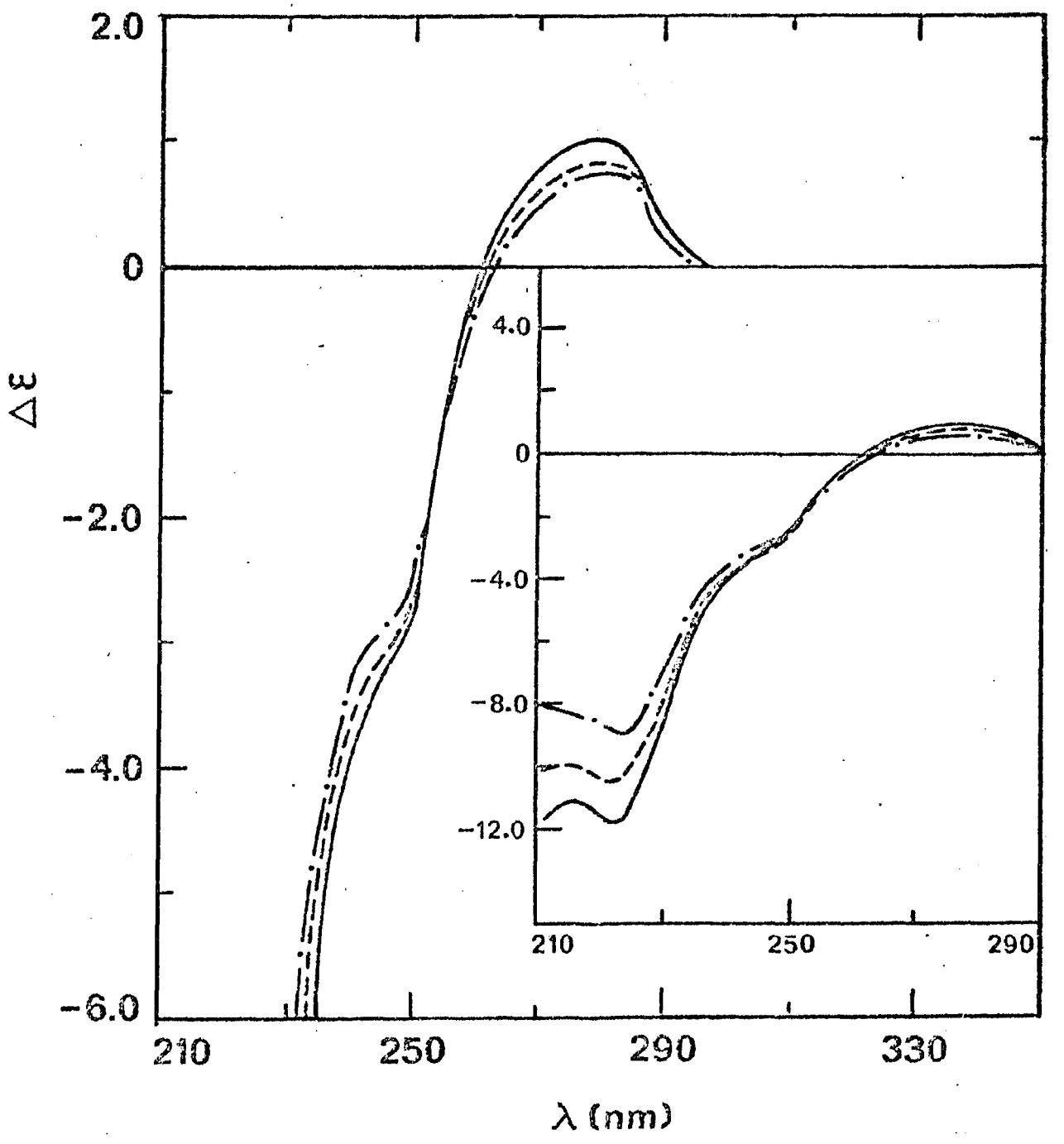

Fig 26. CD spectra of polylysine-nucleohistone complexes. Lysine/Nucleotide ratio is 0 (——), 0.24 (- - -) and 0.42 (-.-). Buffer: 0.25mM EDTA, pH 8.0

DNA-polylysine complexes but on a reduced scale. There is a decrease in the amplitude of the positive peak at 278 nm, a red shift of the crossover point at 260 nm, and a reduction in the negative CD at 220nm. Table 5 gives some of the relevant CD parameters of the polylysine-nucleohistone and -salt treated nucleohistone complexes. The quantitative difference between polylysine-DNA complexes and polylysine-nucleohistone complexes are shown in Fig. 27. This figure gives the dependence of CD changes at 278 nm on the input ratio of lysine/nucleotide. From the thermal denaturation results the input ratio is approximately equal to the fraction of base pairs bound. The CD change is greatest for DNA complexes and smallest for complexes with nucleohistone and 0.6M NaCl-treated nucleohistone. These facts are against the hypothesis of Hanlon et al. (92, 93) that the melting band IV correspond to bound base pairs in the C-form DNA and melting band III correspond to bound base pairs in the B-form. According to this hypithesis polylysine binding will have the same quantitative CD effect on DNA and on nucleohistones since polylysine binding mainly reduces melting band III but not IV.

e. Renaturation of nucleohistone and salt-treated nucleohistones

Renaturation is used here as a tool for the quali-

Table 5

Circular Dichroism Parameters of Polylysine-Nucleohistone Complexes

Nucleohistones (NH)	B($\frac{\text{lysine}}{\text{nucleotide}}$)	$\Delta\varepsilon_{278}$	$\Delta\varepsilon_{220}$	λ_c
NH	0	1.00	-11.50	260.5
	0.18	0.84	-10.45	260.5
	0.24	0.84	-10.40	261.5
	0.42	0.74	- 8.70	262.0
0.6M NaCl -NH	0	1.17	- 9.51	259.5
	0.18	1.00	- 8.99	260.5
	0.42	0.98	- 7.77	261.5
	0.54	0.88	- 6.55	263.0
1.6M NaCl -NH	0	1.95	- 4.74	256.5
	0.18	1.71	- 4.52	258.0
	0.42	1.39	- 3.86	260.5
	0.60	1.03	- 3.42	263.0

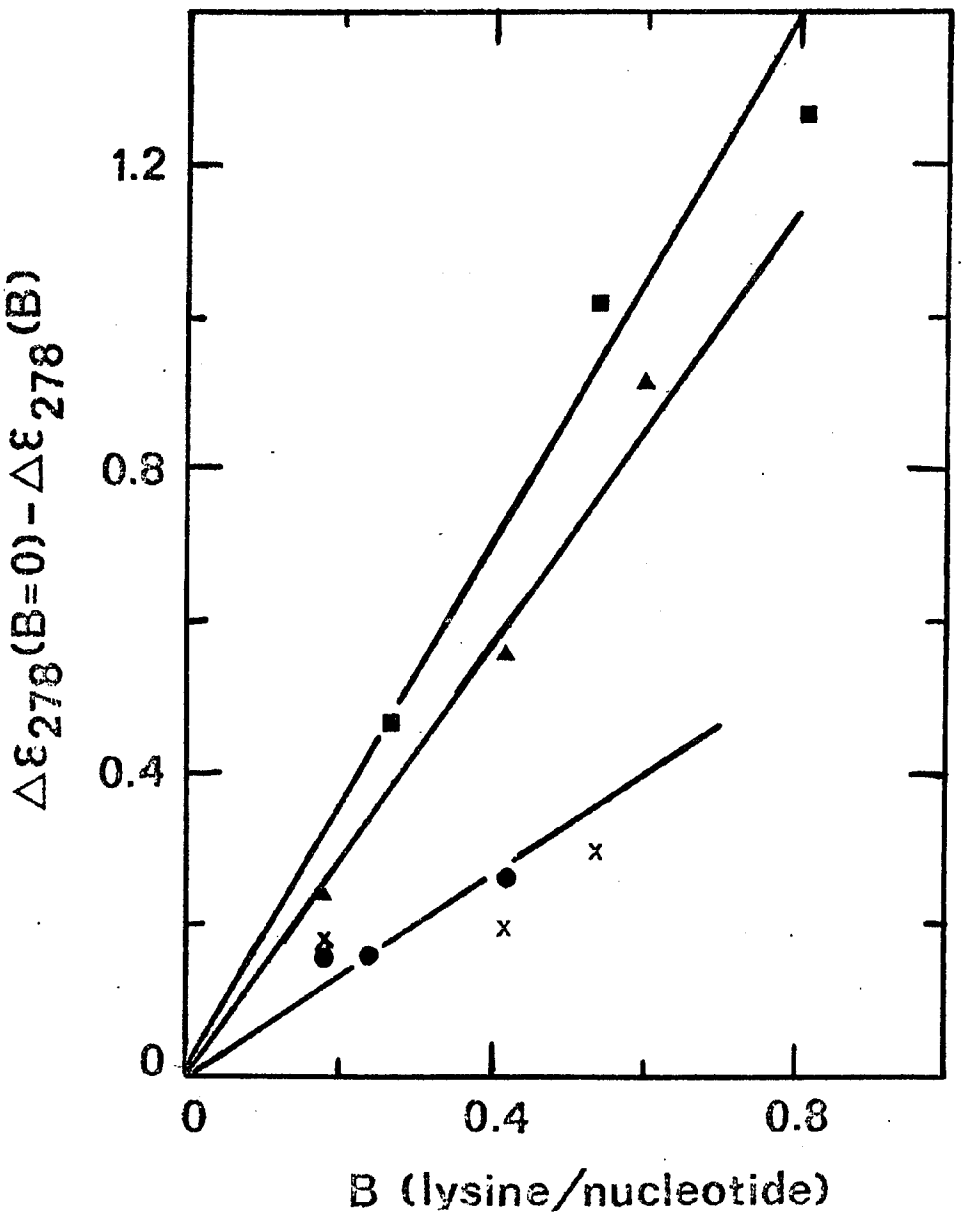

Fig 27. Dependence of CD changes at 278nm on lysine/nucleotide ratio. Nucleohistone (x), 0.6M NaCl-treated NH (●), 1.6M NaCl-treated NH (▲), and DNA (■) complexes with polylysine

tative determination of the size of free DNA regions in nucleohistone. Fig. 28 shows the denaturation and renaturation curves of 1.6M NaCl-treated nucleohistone. The samples are first denatured upto 65°C at which temperature both free DNA regions and very short DNA gaps or DNA base pairs bound by nonhistone proteins are melted. Renaturation then took place at the same rate as denaturation (2/3° per minute). Once the samples are cooled to room temperature at 28°C, they are denatured again upto 92°C. Denaturation of the free base pairs was recorded as $\Delta h_{65°-35°} = h(65°)-h(35°)$, and redenaturation was recorded as $\Delta h'_{65°-35°} = h'(65°)-h'(35°)$. The percent of renaturation is computed as $\Delta h'_{65°-35°} / \Delta h_{65°-35°} \times 100$. Table 6 gives the quantitative results of renaturation. For native nucleohistone there is a 28% renaturation for the melting between 35°-65°C. Since Δh_{65-35} for native nucleohistone is only 8% and is mainly contributed from melting band II at 57°C, the low renaturation value perhaps indicate that most of the melting band II does not come from short, free DNA gaps between histone bound regions, but is from the melting of base pairs bound by nonhistone proteins. The amount of renaturation of free DNA regions for 0.6M NaCl-treated and 1.6M NaCl-treated nucleohistones is 75% and 66% respectively.

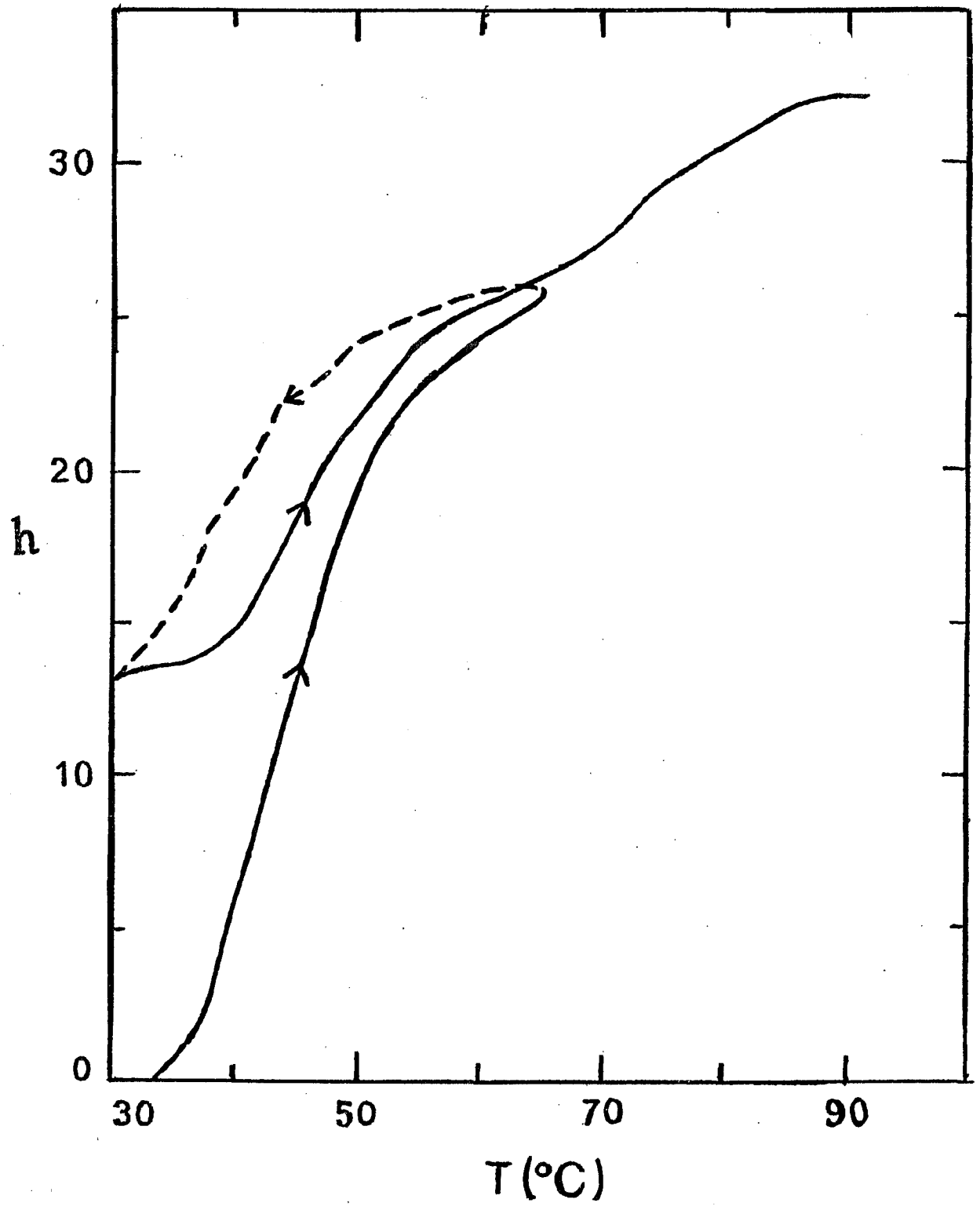

Fig 28. Denaturation (——) and renaturation (---) curves of 1.6M NaCl-treated nucleohistone
Buffer: 0.25mM EDTA, pH 8.0

Table 6

Renaturation of Nucleohistones

Nucleohistones	No Predenaturation $h_{65°-35°}$	Predenatured to 66° C Percent Renaturation (65° - 35° C)
DNA	36.2	14
NH (native)	8.0	28
0.6M NaCl-treated	16.8	75
1.6M NaCl-treated	26.0	60

f. Renaturation of polylysine-nucleohistone complexes

From the thermal denaturation results of polylysine-nucleohistone complexes we know that polylysine bind all but those DNA base pairs bound by the more basic halves of histone in nucleohistone. From the view point of helix-coil transition two questions can be asked:
(a) Will polylysine binding, which keeps the double-helix of the bound base pairs intact, allow the renaturation of histone-bound base pairs to occur more readily?
(b) Will the interruption of polylysine binding by the more basic halves of histones change the renaturation of polylysine-bound DNA base pairs?

To answer the first question, polylysine-nucleohistone complexes were denatured to 92°C, renatured, and redenatured to 105°C. Since histone-bound base pairs show melting at 72° and 82°, the difference hyperchromicity $\Delta h_{85°-65°}$ is used for comparing the renaturation of these base pairs. To answer the second question, polylysine-nucleohistone complexes were denatured upto 105°C, renatured and redenatured. $\Delta h_{T>85°}$ was used to measure renaturation of polylysine-bound base pairs.

Fig. 29 gives the denaturation and renaturation curves of polylysine-nucleohistone complex with an input ratio Of 0.45. The quantitative results are tabulated in Table 7. Increasing the input ratio of lysine/nucleotide causes an increase in the amount of

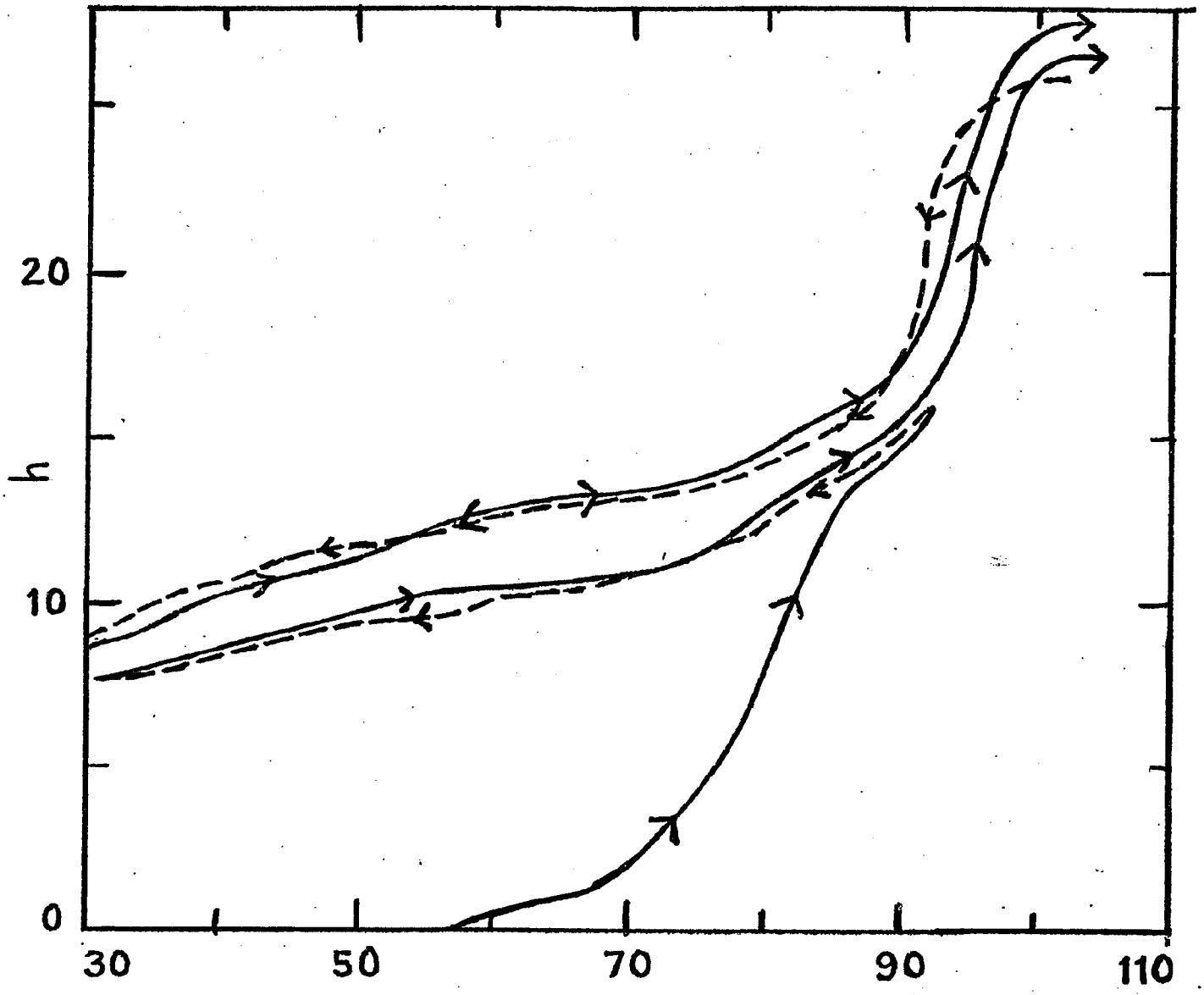

Fig 29. Denaturation (——) and renaturation (---) curves of polylysine-nucleohistone complex, lysine/nucleotide=0.45
Buffer: 0.25mM EDTA, pH 8.0

TABLE VII

Renaturation of Directly Mixed Polylysine-Nucleohistone Complexes[a]

Lysine/ Nucleotide	No Predenaturation			Predenatured to 92°C Percent Renaturation			Predenatured to 105°C Percent Renaturation		
	Δh_{85-65}	$\Delta h_{T>85}$	T_{mV}	(85 − 65°C)	$T > 85$°C	T_{mV}	(85 − 65°C)	$T > 85$°	T_{mV}
0	22.0	1.8	—	8	—	—	8	—	—
0.18	19.0	8.5	96.0	14	71	96.0	11	63	94.5
0.27	17.4	11.3	96.5	20	66	94.0	15	62	93.0
0.45	12.0	17.3	97.0	34	70	95.0	23	67	94.0
0.54	6.7	19.1	98.0	55	69	95.0	45	63	93.5

[a] Mol wt of polylysine = 170,000.

renaturation of histone-bound base pairs at 85°-65°C from 8% to 55% when the complex is predenatured to 92°C. The same effect is observed for histone-bound regions when the complex is predenatured upto 105°C. However, quantitatively the change is smaller from 8% to 45% renaturation. At 105°C there is complete denaturation of polylysine-bound DNA base pairs.

For polylysine-bound DNA base pairs the amount of renaturation remains constant at 70% regardless of the input ratio of lysine/nucleotide when the complexes are predenatured upto 92°C. If the complexes are predenatured up to 105°C the amount of renaturation is 64%, this value is also independent of the input ratio. It is similar to that obtained from polylysine-DNA renaturation (94). Therefore, the interruption of polylysine binding to DNA by histones does not have significant effect on its renaturation.

Discussion

Biphasic melting of polylysine-DNA complexes is a well known phenomenon (60, 68). Biphasic melting is due to the difference in stability between free DNA base pairs and base pairs bound by polylysine. The CD of DNA complexes which depends on the secondary structure can also be classified into two groups: free and bound DNA base pairs. The CD of the bound DNA regions

is similar to that of DNA structure in high salt concentrations. Since NaCl is known to cause dehydration of DNA in the B-form, then polylysine effect on DNA can also be a dehydration effect. This conclusion is further supported by the work done on the effects of ionic strength on the melting of polylysine-DNA complexes (94). The T_m' of polylysine-DNA complexes made by direct mixing is not affected by increase in ionic strength while the T_m' of polylysine-DNA complexes made by reconstitution in a salt gradient dialysis is decreased in the presence of high ionic strength. The authors suggested that such a change is due to the structural change on the polylysine-bound regions caused by the change in ionic strength. The Na^+ ions replace water molecules and bind polylysine-bound regions. Such dehydration could possibily destablize the polylysine-bound regions and lower the T_m'.

In the melting of polylysine-nucleohistone complexes it is shown that polylysine preferentially bind free DNA, and less basic half histone-bound DNA over the more basic half of histone-bound DNA. This is a reasonable result since polylysine interaction with DNA and chromatin is mainly ionic. Based on the thermal denaturation result of polylysine-nucleohistone complexes a model of the melting is proposed in Fig. 30. In a polylysine-

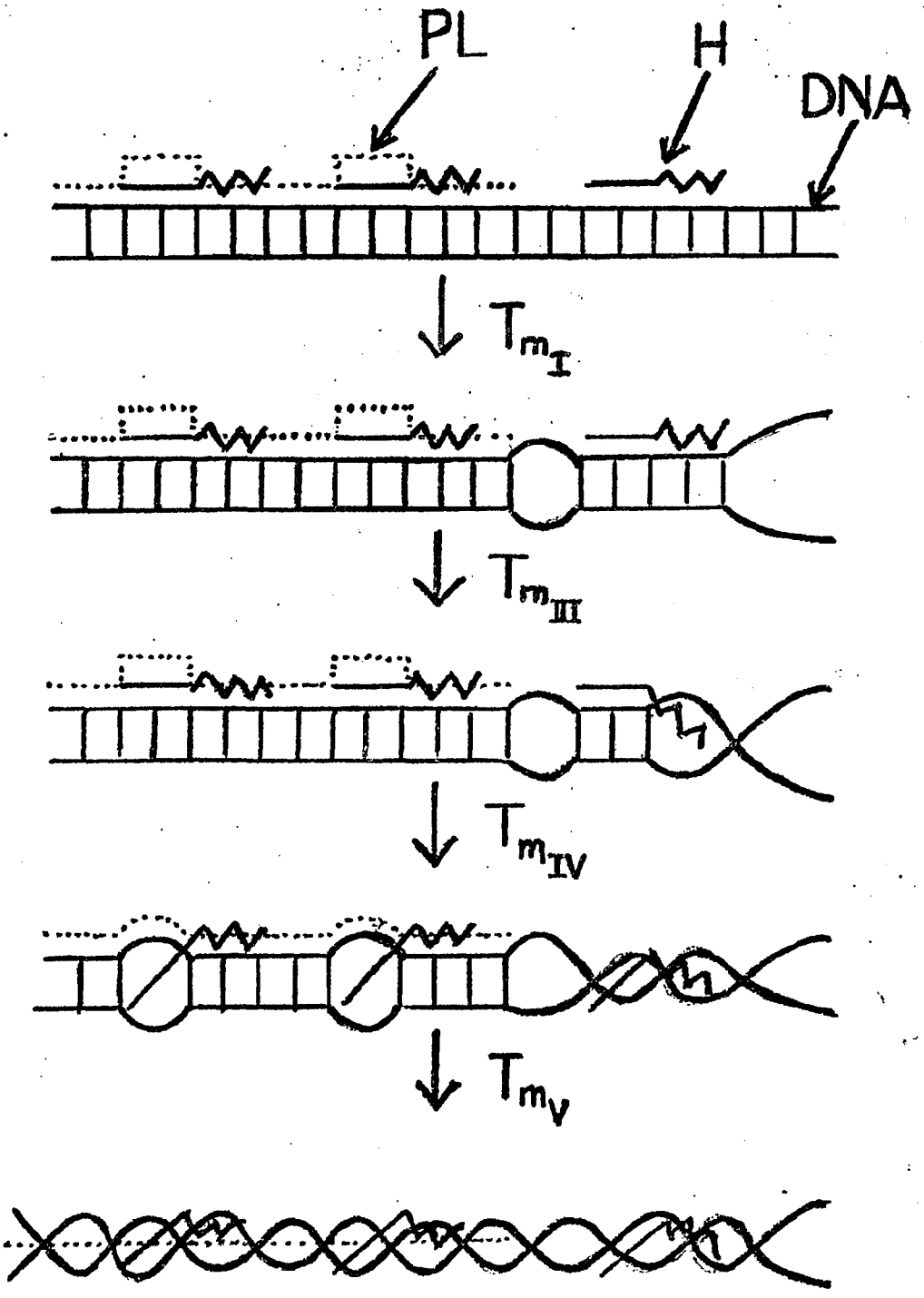

Fig 30. Mechnism of melting of polylysine-nucleohistone complex

nucleohistone complex, polylysine binds to the free DNA regions and to the base pairs bound by the less basic halves of histones. Thermal denaturation of this complex will first melt the free DNA base pairs at 48°C (T_{mI}). The next base pairs to denature are the ones bound by the less basic halves of histones at 72°C (T_{mIII}). The base pairs bound by the more basic halves of histones will be denatured at 82°C (T_{mIV}). Finally at 99°C (T_{mV}) the base pairs bound by polylysine molecules are melted.

From the previous chapter we know that 0.6M NaCl-treated nucleohistone from which histone H1 has been removed has 53% of DNA base pairs bound by histones. The percent of renaturation of its free DNA base pairs is 75% (Table 6) which is similar to renaturation of free DNA bases in directly mixed polylysine-DNA complex with an input ratio of 0.77 (94). This means that the free DNA regions of 0.6M NaCl-treated nucleohistone are not long. With 1.6M NaCl-treated nucleohistone that has 25% of DNA base pairs still bound by histones there is 60% renaturation of the free DNA regions. This implies that the remaining histones are scattered along the DNA molecules and the free DNA regions are also not too long. Therefore, NaCl dissociation of histones from nucleohistones is not a cooperative effect, the removal of histones are by molecules rather than in

large clusters. The renaturation of histone-bound base pairs in native nucleohistone is 8% as compared to 60% of polylysine-DNA complexes (94). This may be due to: (a) Histones are fully dissociated from DNA above 92° C, therefore, renaturation of the two strands of DNA is slow; (b) Histones bind only one of the two strands of DNA after denaturation at 92°C, the two strands are separated and low renaturation results. Polylysine binding to nucleohistones enhances the renaturation of histone bound regions from 8% to 55% when the input ratio of lysine/nucleotide is increased from 0 to 0.54. Therefore, polylysine binding can somehow keep the histones attached to denatured DNA.

Trypsin digests the more basic halves of histones removing melting band IV, while polylysine binding to nucleohistone removes melting band III. The CD results of these two treatments show that the CD changes of the DNA base pairs in the B-form caused by binding of the less basic halves of histones are greater than those affected by the more basic halves. In other words, the binding by the less basic halves has already altered the DNA structure with the resultant reduction of the positive CD at 275 nm so that the binding of polylysine to these regions has much less CD effect on DNA then when it is bound to free DNA regions.

Clark and Felsenfeld (95) titrated chromatin with polylysine followed by nuclease digestion and found that 50% of the DNA in chromatin are accessible to polylysine. They concluded that 50% of the DNA in chromatin is free of protein binding. This is contradictory to the result obtained from the melting of chromatin (chapter III). Melting of chromatin showed that 80% of the DNA in chromatin is bound by proteins. Thermal denaturation of polylysine-nucleohistone complexes showed that polylysine binding to nucleohistone cannot be used as a measure of free DNA regions in chromatin because polylysine can also bind to the DNA base pairs already bound by the less basic halves of histones. This result is supported by the works of (a) Mirsky (96) who showed that the amount of DNA in chromatin succeptible to nuclease depend on both the enzyme concentration and the time allowed for digestion, (b) Itzhaki (97) showed the release of proteins accompanied by nuclease digestion of chromatin.

CHAPTER V

EFFECT OF UREA ON CHROMATIN STRUCTURE

The native strucutre of proteins is thermodynamically the most stable. If a protein structure is partially disrupted it will go back to its native state if appropriate conditions for renaturation are provided. This is also true for DNA. Urea has been widely used as a denaturing reagent in proteins. Urea is used here to test: (1) if the native structure of chromatin is the most stable structure; (2) if the effect of urea on chromatin structure is reversible; and (3) the method of reconstitution of chromatin from DNA, histones and nonhistone proteins by gradient dialysis had been developed by the laboratories of Bonner (98) and Huang (99) and had been widely used as a major method for chromatin reconstitution. Thermal denaturation and CD is used here to test whether the reconstituted chromatins using this method are the same as the native chromatin.

Experimental

Nucleohistone and salt-treated nucleohistones in 0.25mM EDTA, pH 8.0 were prepared by the method

described previously. A stock solution of 8.0M or 10.0M urea (Ultrapure, Schwartz/Mann) was added directly to the nucleohistones to give the appropriate concentrations of urea. The solutions were left at room temperature for ½ hour and then measured for thermal denaturation and CD.

Nucleohistones were dissociated in 5M urea-2M NaCl by dialysis overnight. A continuous gradient of 5M urea-2M NaCl were set up according to the method of Bonner (98). The reconstituted complexes were once again tested by thermal denaturation and CD. An alternative procedure for reconstitution was the stepwise gradient dialysis method (99). Dissociated chromatin in 5M urea-2M NaCl was dialyzed successively in various NaCl concentrations with 5M urea and the salt concentration changed every 1½ hour until the NaCl concentration became 0.1M. Urea was then removed in one step and the samples dialyzed overnight in 0.25mM EDTA, pH 8.0. Dialysis took place at 4°C.

Results

a. Effect of urea on DNA, nucleohistone and salt-treated nucleohistones

Fig. 31 shows the derivative melting curves of DNA and nucleohistone in 0, 3.0 and 5.0M urea. The T_m of DNA decreases with increasing urea concentration. The

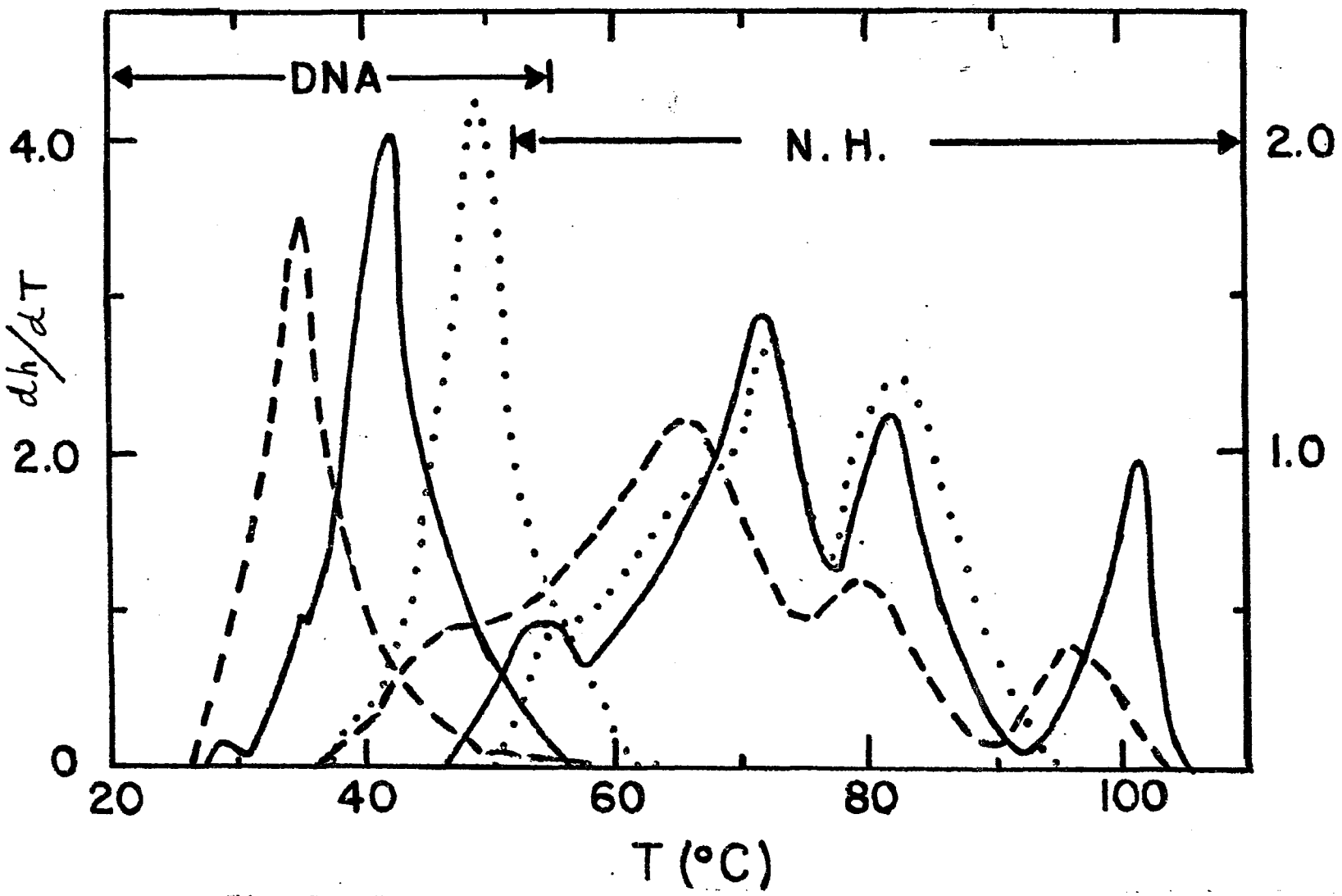

Fig 31. Derivative melting curves of DNA in urea: 0M (...), 3M (——) and 5M (---). Nucleohistone in urea: 0M (...), 3M (——) and 5M (---)

T_m of pure DNA in 0.25mM EDTA is 50°C and is 35°C in the presence of 5.0M urea. This is expected because urea is a denaturing agent. For nucleohistone increasing concentrations of urea induce a new melting band (V) at 97°C. The temperatures of both melting bands III and IV are decreased but the change is greater on melting band III than IV. Since melting bands III, IV, and V are distinguishable the areas of these melting bands can be calculated at different urea concentrations. Fig. 32 shows that there is no change in areas of melting bands I + II and III, but there is a decrease in the area of melting band IV and an increase in that of band V. Since there is no change in the area of melting band I + II, 5 M urea does not cause physical dissociation of histones from DNA. Similar results were obtained for 0.6M NaCl-treated nucleohistone.

Fig. 33 shows the derivative melting profiles of 1.6M NaCl-treated nucleohistone in urea. It is similar to nucleohistone and H1 depleted nucleohistone except that there no melting band V. Since melting band I of free DNA base pairs is easily distinguishable in this partially dehistonized nucleohistone, the effect of urea on T_{mI} can be followed. The change in T_{mI} is identical to that of the change in T_m of pure DNA in urea. Urea does not change the areas of melting bands

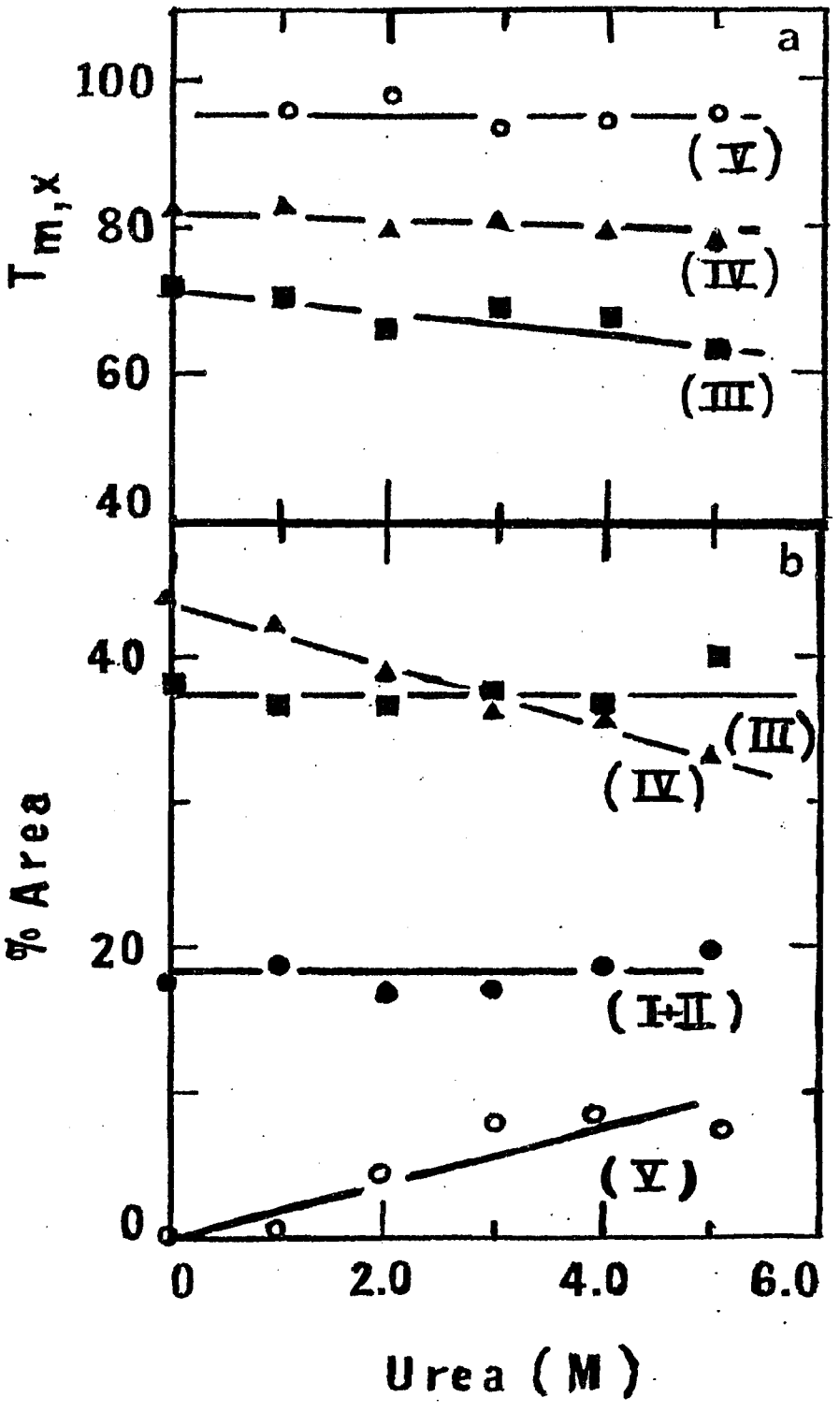

Fig 32. Urea dependence of melting temperature and fraction of area of each melting band in the native nucleohistone

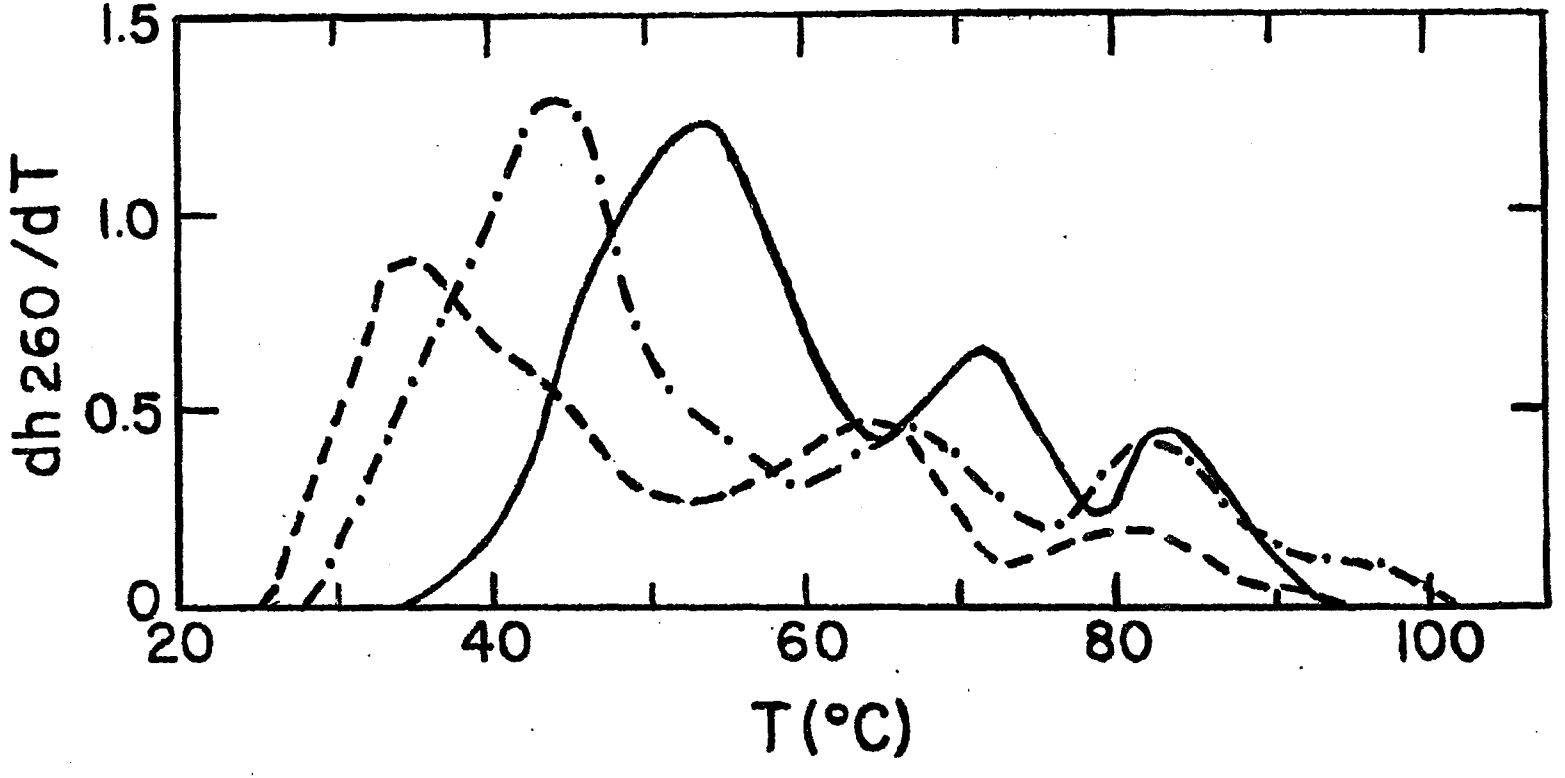

Fig 33. Derivative melting curves of 1.6M NaCl-treated nucleohistone in urea: 0M (—), 3M (—·—) and 5M (---)

in this nucleohistone (Fig. 34).

Figs. 35 and 36 show the effect of urea on the CD of DNA and nucleohistone. For pure DNA, a decrease in the amplitude of the positive CD at 275 nm is observed. There is a slight red shift of the crossover point at 260 nm and no significant change for the CD below 240 nm. For nucleohistone urea causes an increase in the amplitude of the positive peak at 275 nm and reduces the negative band at 220 nm. The observed CD changes of nucleohistone in urea can be due to the fact that urea destroys some α-helical structure of the bound histones; this reduces the conformational effect of histone binding to base pairs giving a greater positive CD band. The destruction of the supercoiled structure of nucleohistone by urea (100, 101) is a result of the above events. To test this, the effect of urea on the CD of NaCl-treated, partially dehistonized nucleohistones was also studied.

The urea effect on the CD spectrum of 0.6M NaCl-treated nucleohistone is very similar to that of native nucleohistone above. There is an increase of the positive band and a decrease of the negative band. The effect of urea on the CD spectrum of 1.6M NaCl-treated nucleohistone (Fig. 37) is quite different from that exhibited by native and 0.6M NaCl-treated nucleohistone. Although 5.0M urea reduces the negative CD at 220nm, indicating the destruction of α-helix of the remaining histones, enhancement of the positive CD band shown with native

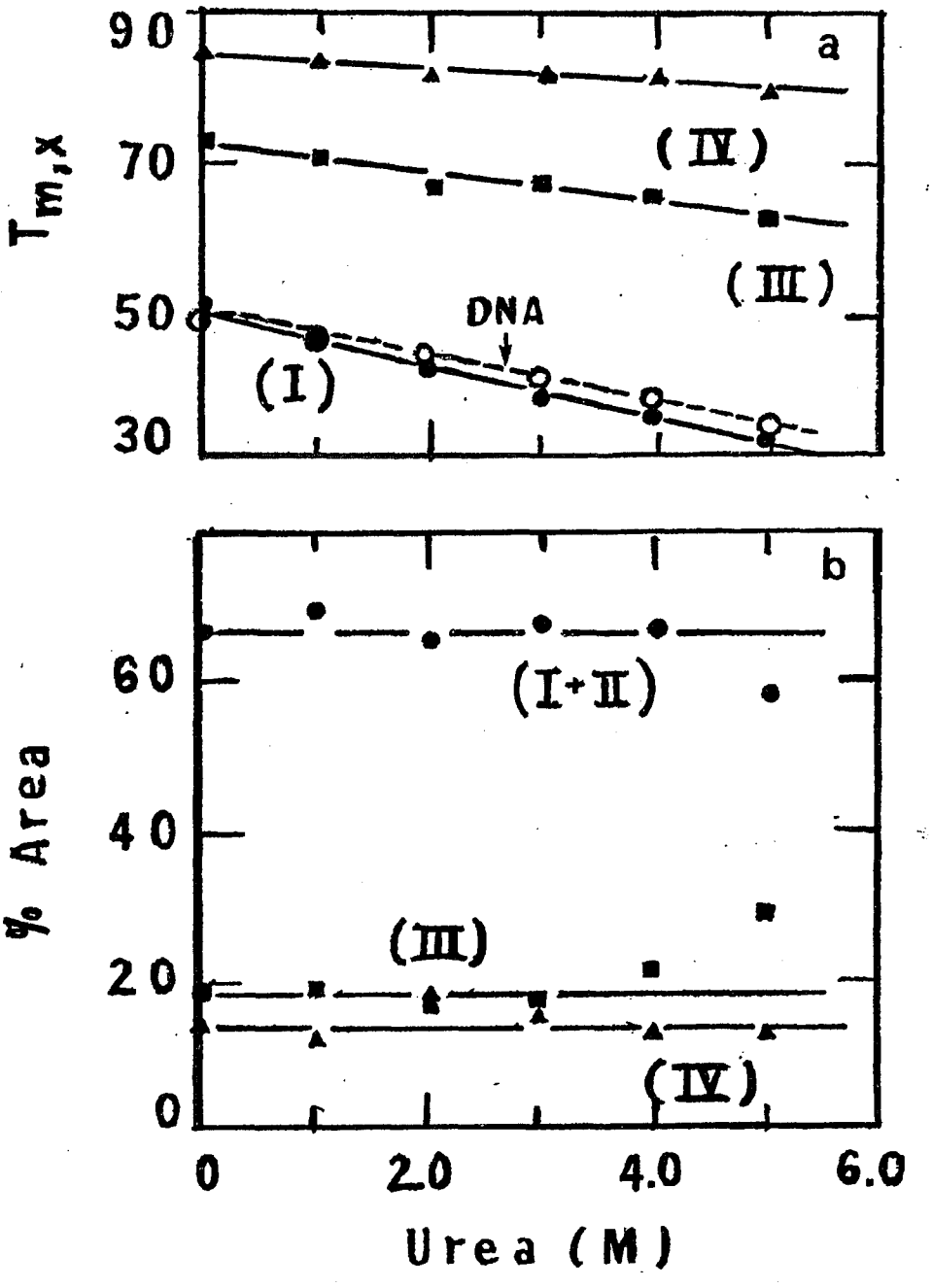

Fig 34. Urea dependence of melting temperature and f action of area of each melting band in 1.6M NaCl-treated NH.

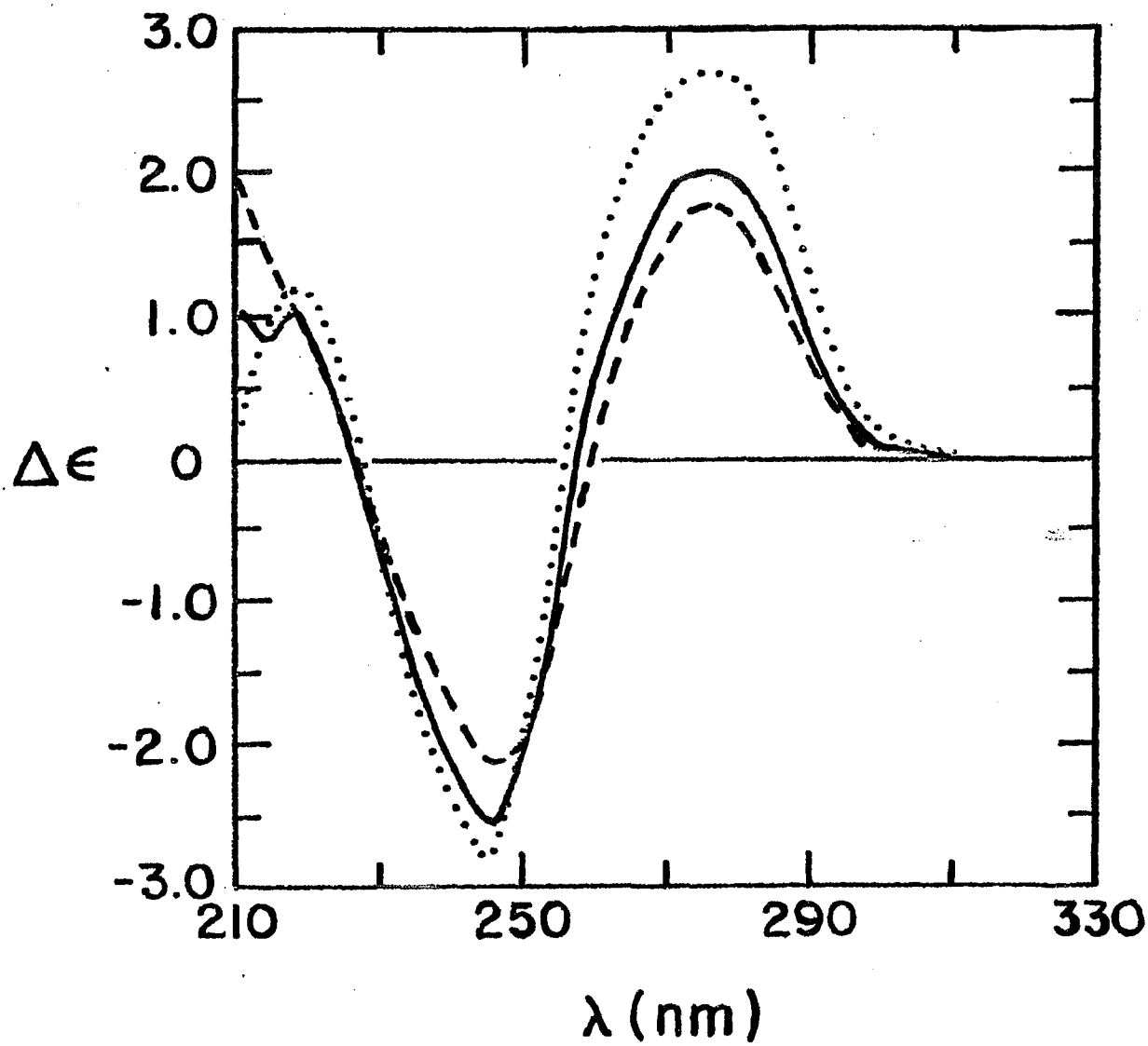

Fig 35. CD spectra of DNA in urea: 0M (...), 3M (——) and 5M (---)

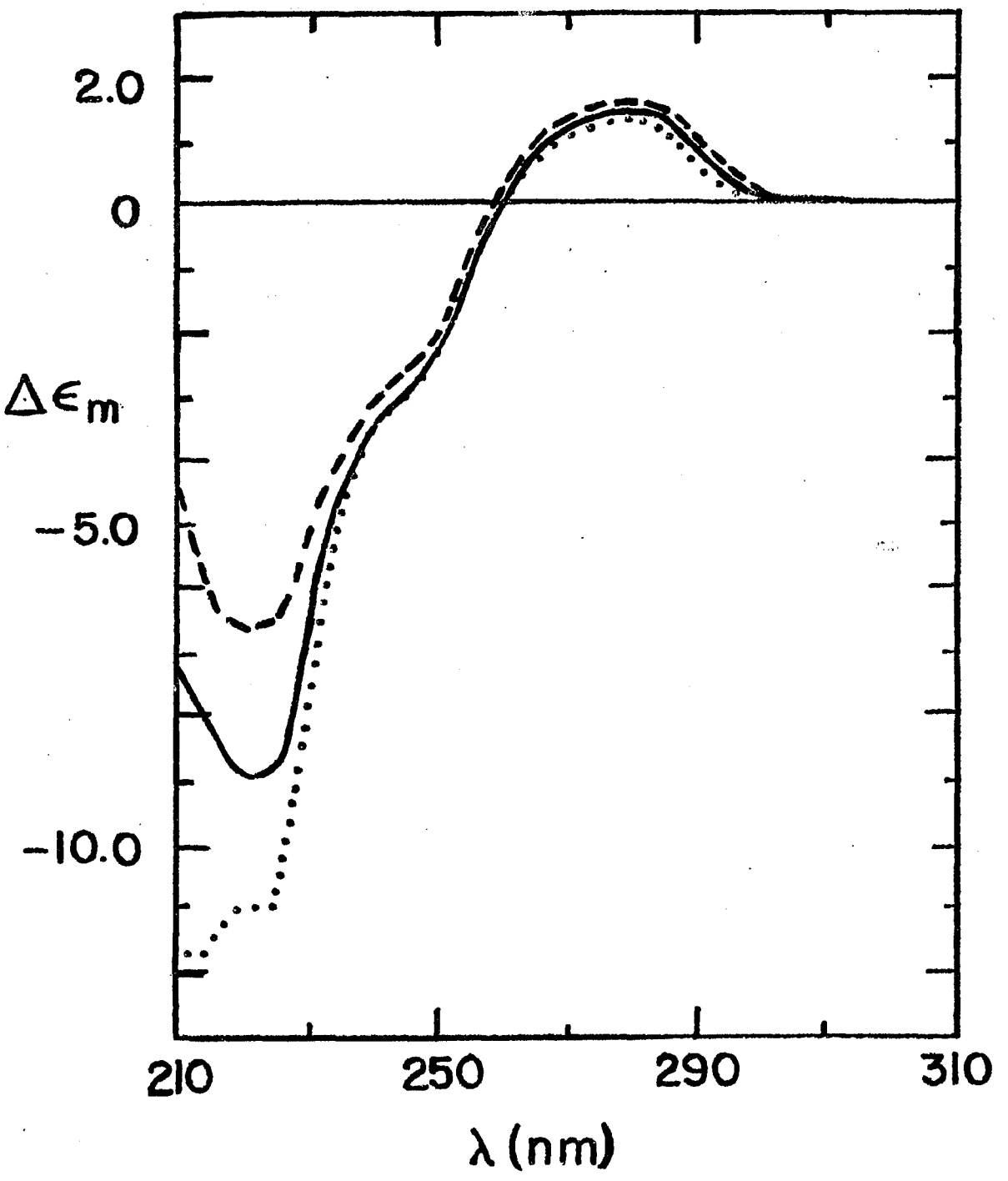

Fig 36. CD spectra of nucleohistone in urea: 0M (...), 3M (——), and 5M (– – –)

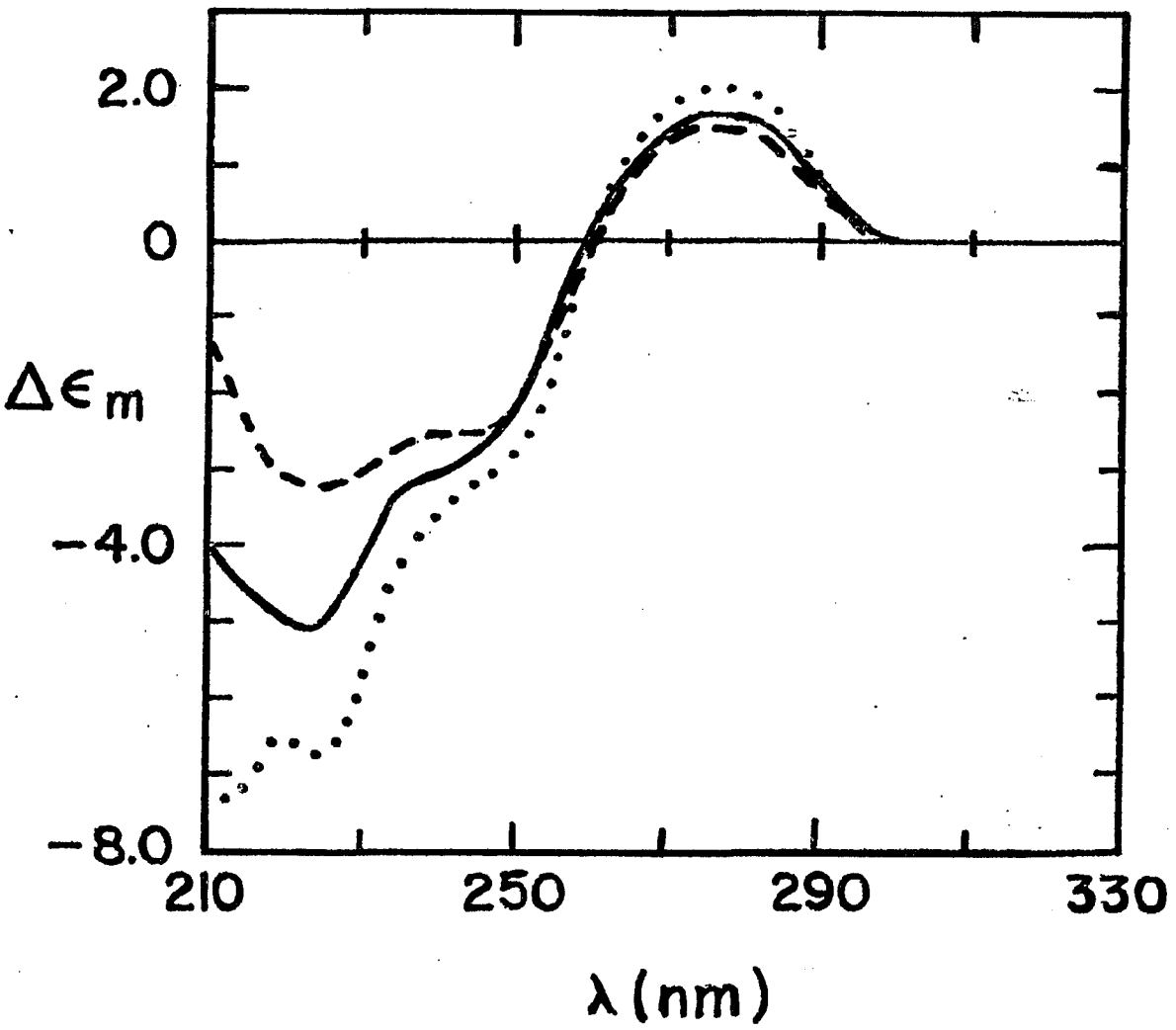

Fig 37. CD spectra of 1.6M NaCl-treated NH in urea: 0.M (...), 3M (——), and 5M (---)

nucleohistone is absent. Instead, the positive CD band at 275 nm of 1.6M NaCl-treated nucleohistone is reduced by urea.

At 220 nm, the CD of nucleohistone and salt-treated nucleohistones is mainly contributed by the bound histones. Fig. 38 gives the change in the CD spectra at 220 nm of the nucleohistones in different urea concentrations. For native and partially dehistonized nucleohistones, $\Delta\varepsilon_{220nm}$ becomes less negative at higher concentration of urea. The reduction is proportional to the urea concentration. For pure DNA, the CD at 220 nm is not changed.

Fig. 39 summerizes the change in CD at 278 nm of nucleohistones in different concentrations of urea. For native and 0.6M NaCl-treated nucleohistones, there is no change in $\Delta\varepsilon_{278nm}$ at concentrations less than 2.0M urea; at concentrations greater than 2.0M increases are observed at this wavelength. Urea effect on $\Delta\varepsilon_{278nm}$ is quite different for 1.6M NaCl-treated nucleohistone. There is a decrease of $\Delta\varepsilon_{278nm}$ up to 3.0M urea, at higher concentrations the trend is reversed.

Since a nucleohistone molecule can generally be classified into two fractions, histone-free and histone-bound base pairs, urea can possibily have different conformational effects on these two classes of base pairs.

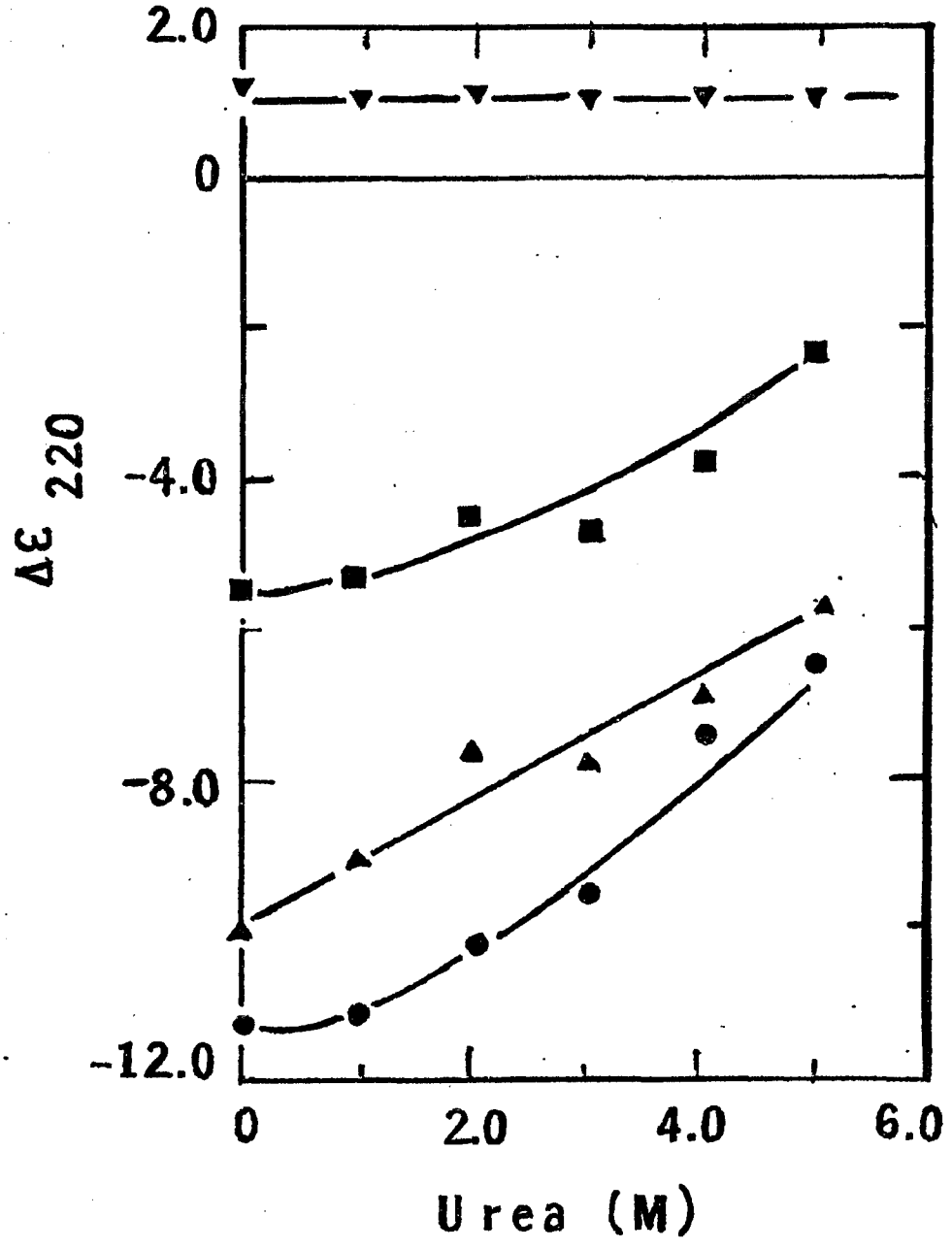

Fig 38. Urea dependence of $\Delta\epsilon_{220}$ of nucleohistones and DNA. Native nucleohistone (●), 0.6M NaCl-treated NH (▲), and 1.6M NaCl-treated NH (■), and DNA (▼)

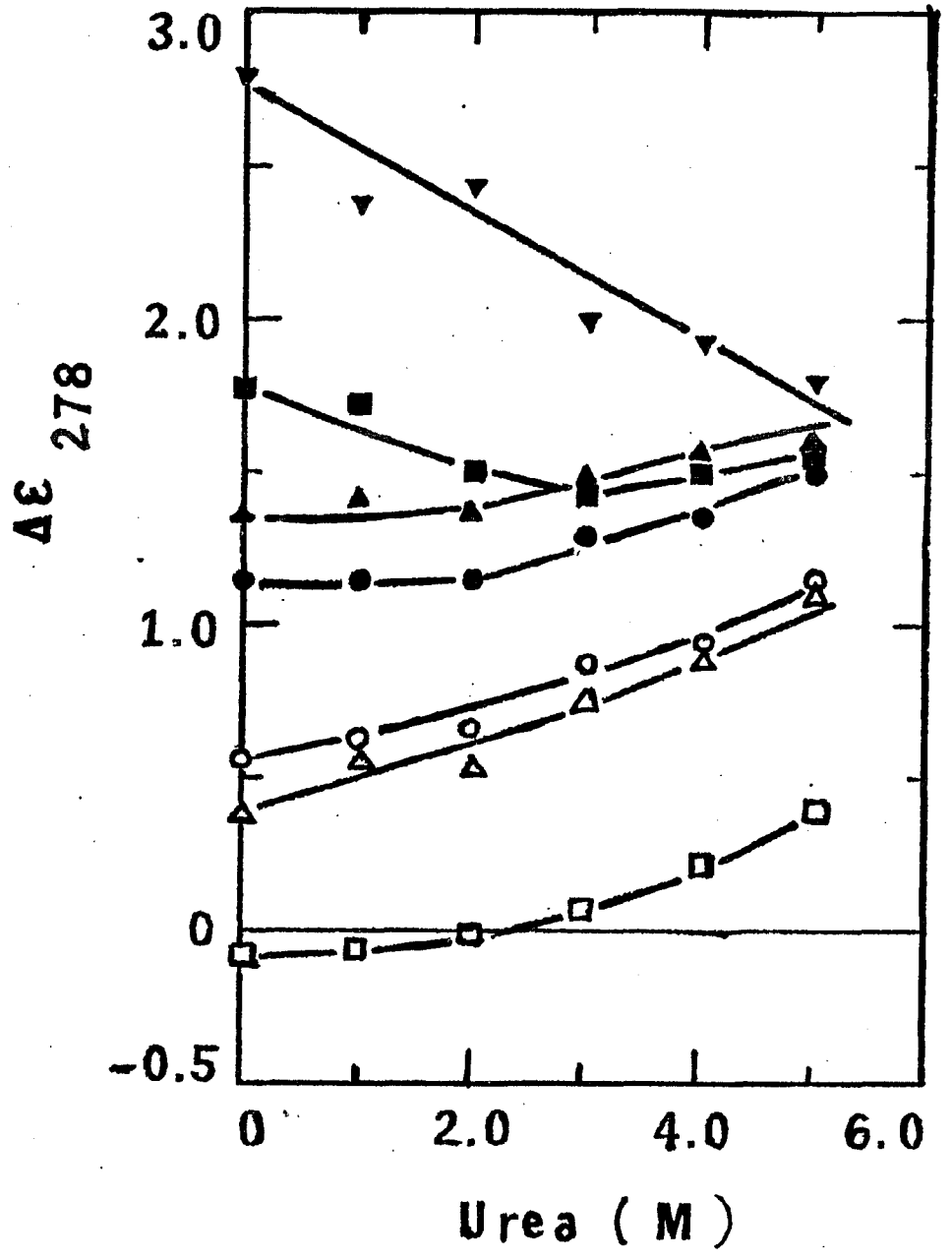

Fig 39. Urea dependence of $_{278}$ of nucleohistones and DNA. Native nucleohistone (o), 0.6M NaCl-treated NH (▲), 1.6M NaCl-treated NH (■), and DNA (▼). Calculated CD at 278nm ($FA\varepsilon_b$) of histone bound base pairs: native nucleohistone (O), 0.6M NaCl-treated NH (Δ), 1.6M NaCl-treated NH (□).

Using eq. 5 with F = 78% for nucleohistone, 60% for 0.6M NaCl-treated nucleohistone and 34% for 1.6M NaCl-treated nucleohistone in this preparation, the CD of bound base pairs ($F\Delta\varepsilon_b$) at 278 nm is calculated for the nucleohistones in different urea concentration. The results are shown in Fig. 39, a consistent increase of $\Delta\varepsilon_{278nm}$ at higher urea concentrations for histone-bound base pairs is seen for all the nucleohistones. Putting together urea effect on $\Delta\varepsilon_{220nm}$ (Fig. 38) and on $F\Delta\varepsilon_b$ at 278 nm (Fig. 39), it is seen that a decrease of $\Delta\varepsilon_{220nm}$ of histones gives an increase of $\Delta\varepsilon_{278nm}$ for histone-bound base pairs. In other words, the destruction of secondary structure of bound histones by urea makes the bound base pairs less tilted.

b. Reversibility of nucleohistone structure in urea

Urea changes the secondary structure of bound histones and the conformation of bound DNA base pairs. In addition, urea changes the thermal stability of histone-bound and histone-free base pairs. To test whether these changes caused by urea are reversible, urea was dialyzed out of the samples. Fig. 40 shows the melting curves of nucleohistone before and after dialyzing out the urea, except for a small change in T_{mIII} the melting curves remain the same. The CD spectrum after dialyzing

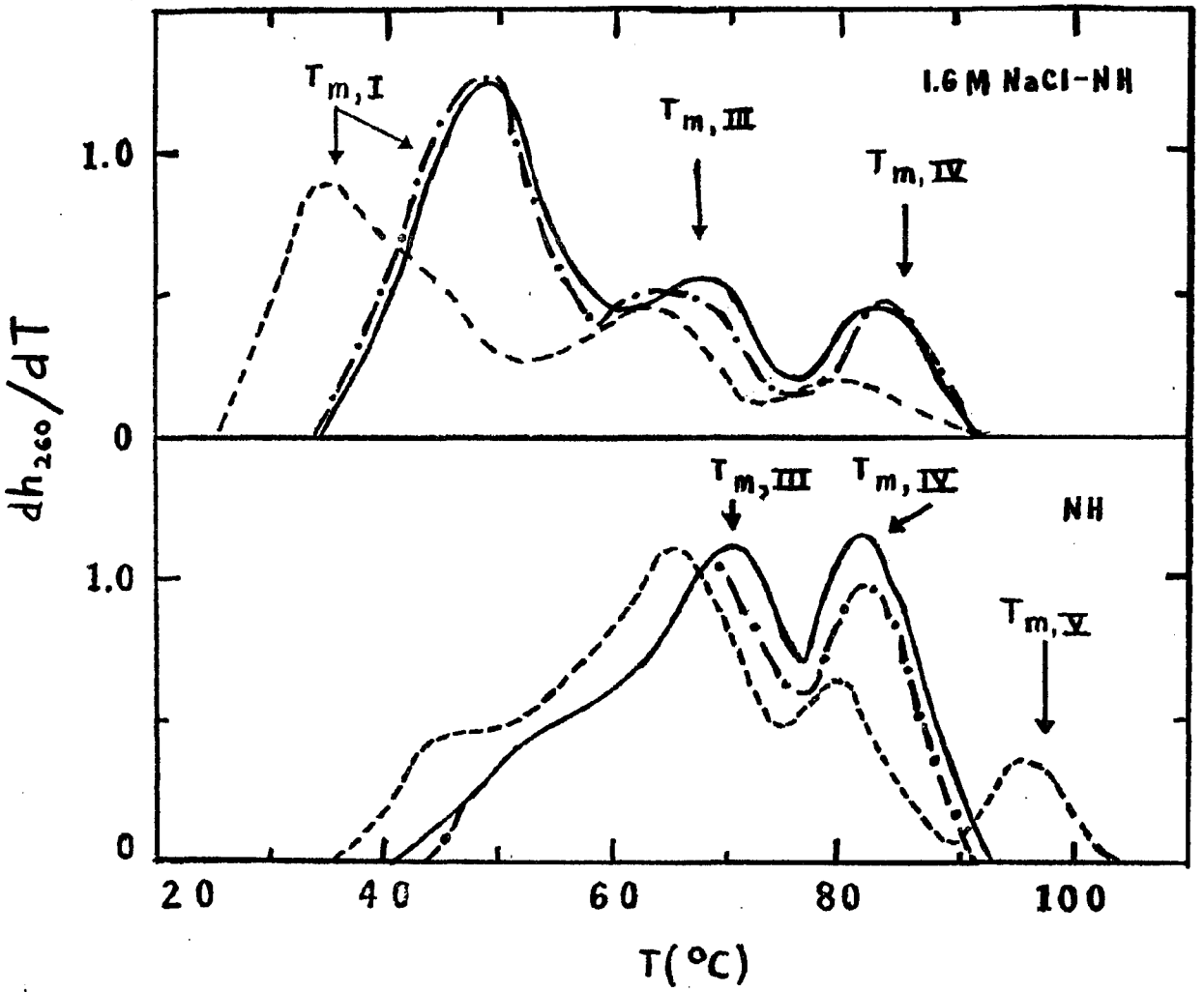

Fig 40. Derivative melting profiles of NH and 1.6M NaCl-treated NH. Controls in EDTA buffer (——), in 5M urea (---), redialyzed into EDTA (-.-)

out the urea also returns to the native spectrum (Fig. 41 a, b). This is also true for salt-treated nucleohistones. This strongly indicates that the structure of native nucleohistone is the most stable one.

c. Reconstitution of nucleohistone and salt-treated nucleohistones using NaCl gradient dialysis in urea

Nucleohistone and salt-treated nucleohistones were dissociated by 5M urea and 2M NaCl and then reconstituted by a continuous NaCl gradient dialysis in urea. Fig. 42 shows the melting curves of native nucleohistone, 0.6M NaCl-treated and 2.5M NaCl-treated nucleohistones before and after reconstitution. Reconstituted nucleohistone and partially dehistonized nucleohistones do not have the same melting profiles as the control nucleohistones. In all cases, there is less melting of the histone-bound regions and more melting of free DNA regions. This could be due to a long dialysis of 48 hours at 4°C in which proteases in chromatin could degrade some of the histones. The CD of the native and reconstituted nucleohistones are shown in Fig. 43. The positive CD peak for the reconstituted nucleohistone is increased from 1.3 $M^{-1}cm^{-1}$ to 2.1 $M^{-1}cm^{-1}$, while the protein CD at 220 nm is reduced from $\Delta\varepsilon_{220nm}$ of 14 to 18.5. The CD changes of the reconstituted salt-treated nucleohistones show similar results as in reconstituted nucleohistone,

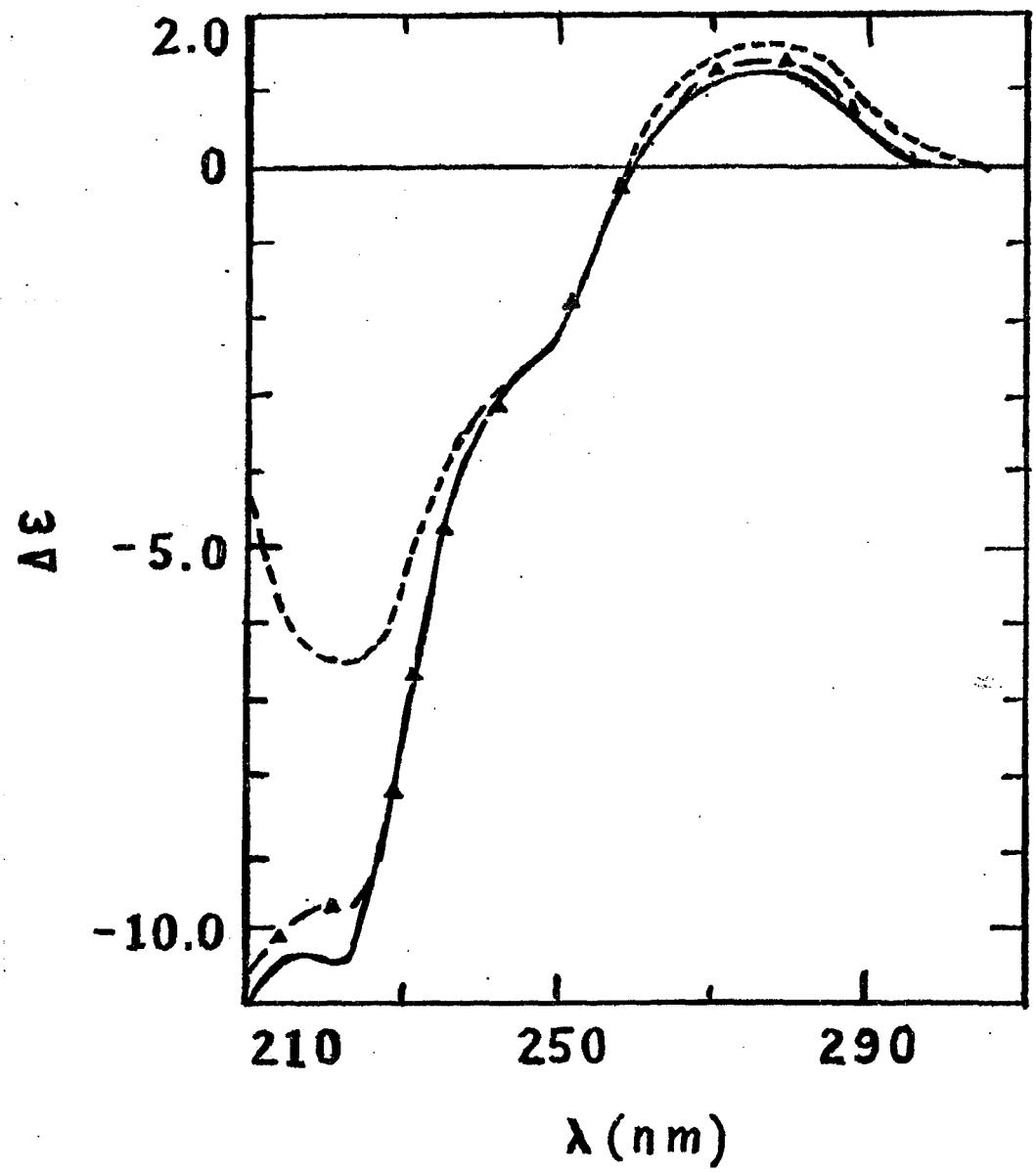

Fig 41a Control nucleohistone. In EDTA buffer (——), in 5M urea (---), redialyzed into EDTA (-▲-)

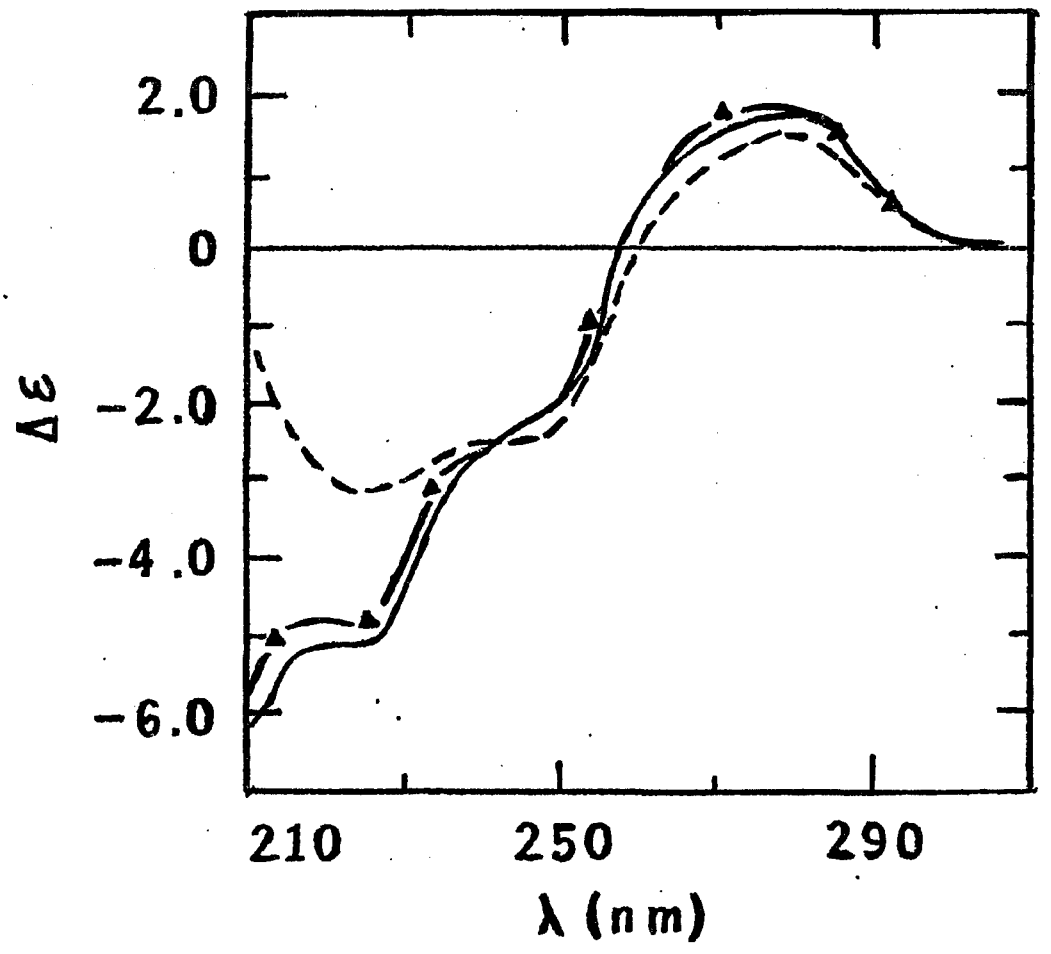

Fig 41b 1.6M NaCl-treated nucleohistone: in EDTA buffer (——), in 5M urea (---) and redialyzed into EDTA (-▲-)

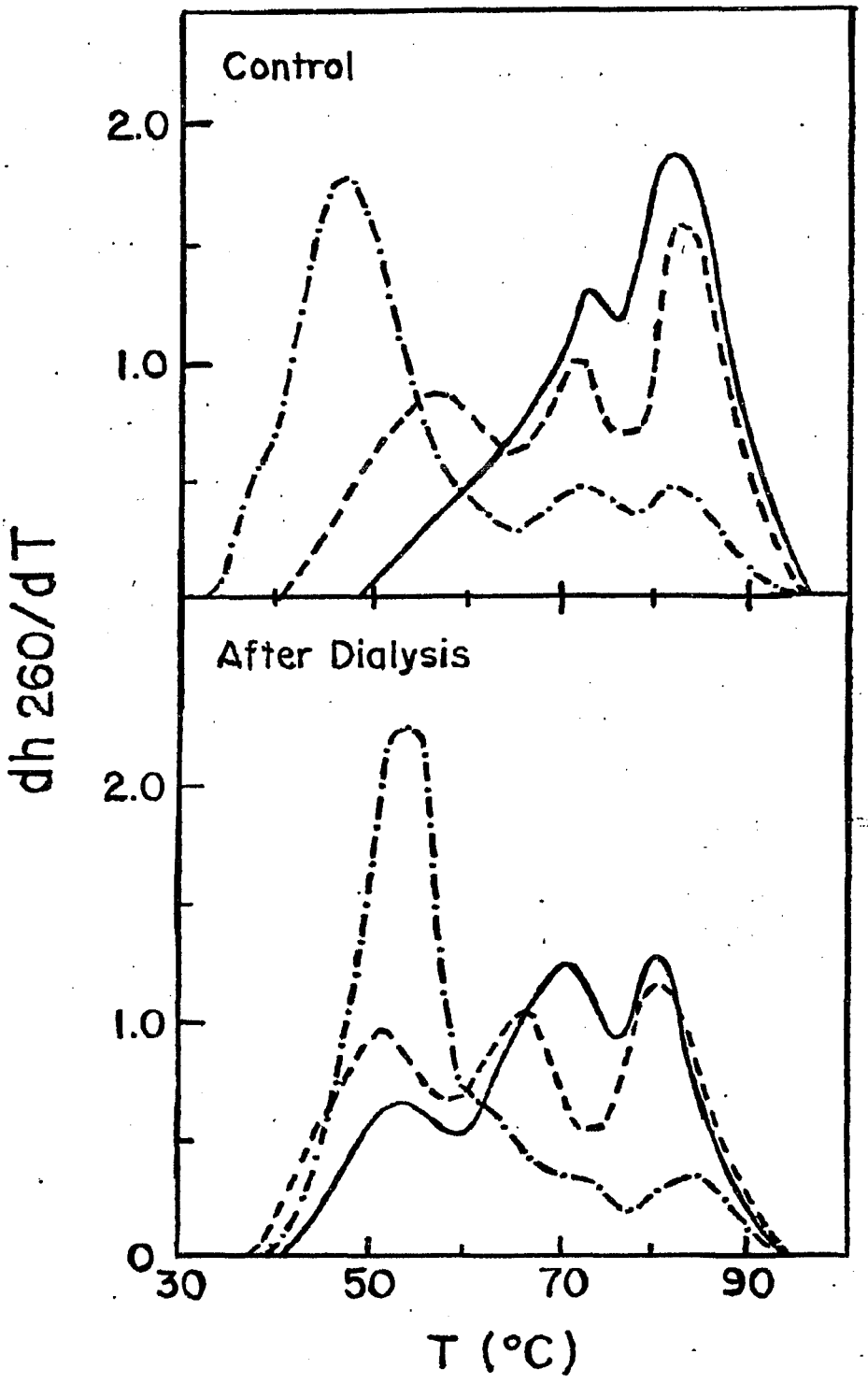

Fig 42 Continuous NaCl gradient reconstitution.
Control: nucleohistone (——), 0.6M NaCl-treated NH (---), and 2.5M NaCl-treated NH (-.-)
Reconstituted samples: nucleohistone (——), 0.6M NaCl-treated NH (---), 2.5M NaCl-treated NH (-.-)

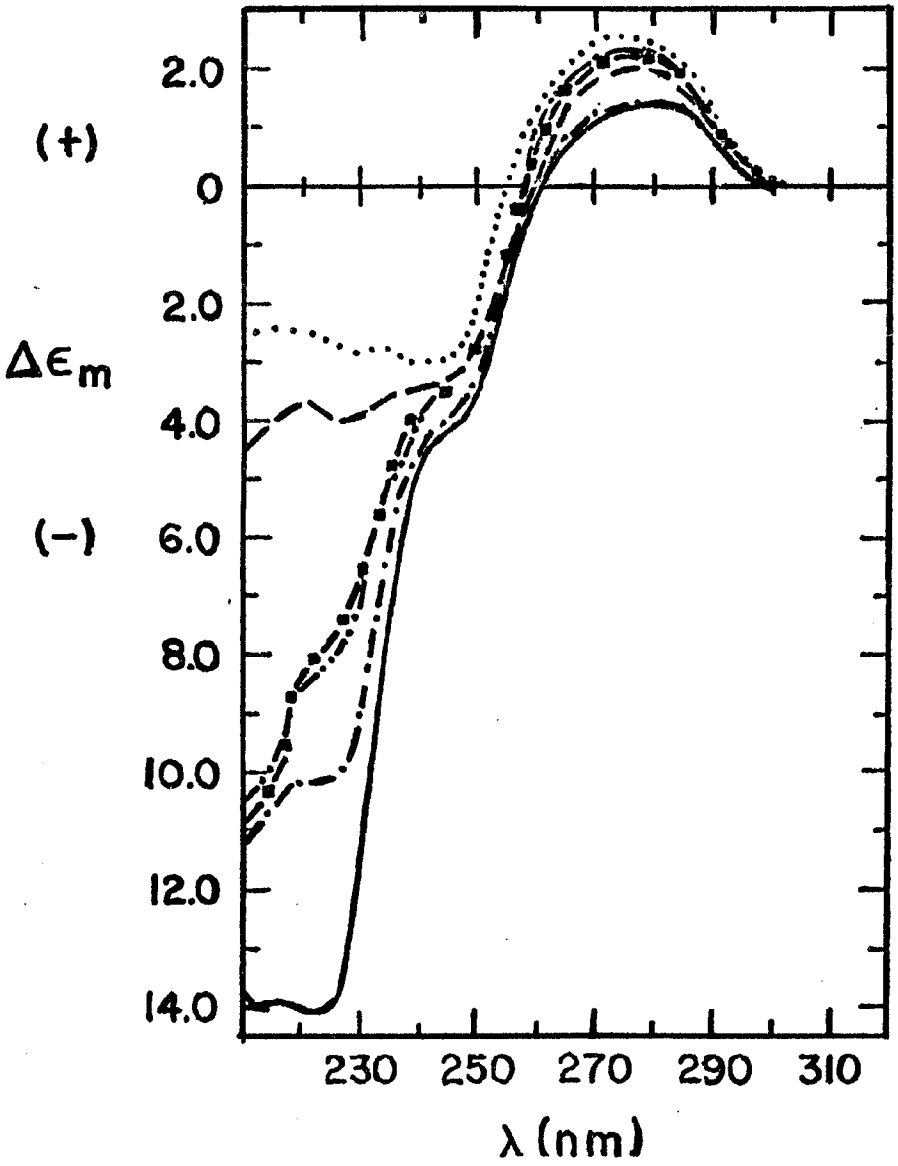

Fig 43 Continuous NaCl gradient reconstitution.
Control: Nucleohistone (——), 0.6M NaCl-treated NH (-.-), 2.5M NaCl-treated NH (- -)
Reconstituted samples: Nucleohistone (-••-), 0.6M NaCl-treated NH (-▪-), 2.5M NaCl-treated NH (...)

but the change for 2.5M NaCl-treated nucleohistone is the least. This may not be surprising since this dehistonized nucleohistone has the smallest amount of histone and therefore has the least amount of histones for proteases to act. Also 2.5M NaCl-treated nucleohistone does not have histone H1 which is the histone most susceptible to proteases.

Theoretically, reconstitution of a complex in a continuous NaCl gradient dialysis a linear NaCl gradient should occur in the complex during the dialysis. In a stepwise NaCl gradient the complex goes through a set of NaCl concentrations and the gradient is not linear. The melting results of the step-wise reconstitution of nucleohistones are shown in Fig. 44. This method of reconstitution does not give better melting curves. There is still a large decrease of the melting area of histone-bound regions, and an increase in the melting of free DNA regions in both reconstituted nucleohistone and in H1 depleted nucleohistone. Reconstituted 2.5M NaCl-treated nucleohistone seemed to give a better melting curve, i.e. similar to the native 2.5M NaCl-treated nucleohistone. Even in this case, there is still a decrease in the area of histone-bound base pairs. The CD results of step-wise reconstituted nucleohistones are given in Fig. 45. Here the positive CD at 278 nm is also greatly increased, while the protein CD at 220nm is reduced. Reconstituted 2.5M NaCl-treated nucleohistone gives a CD spectrum closer

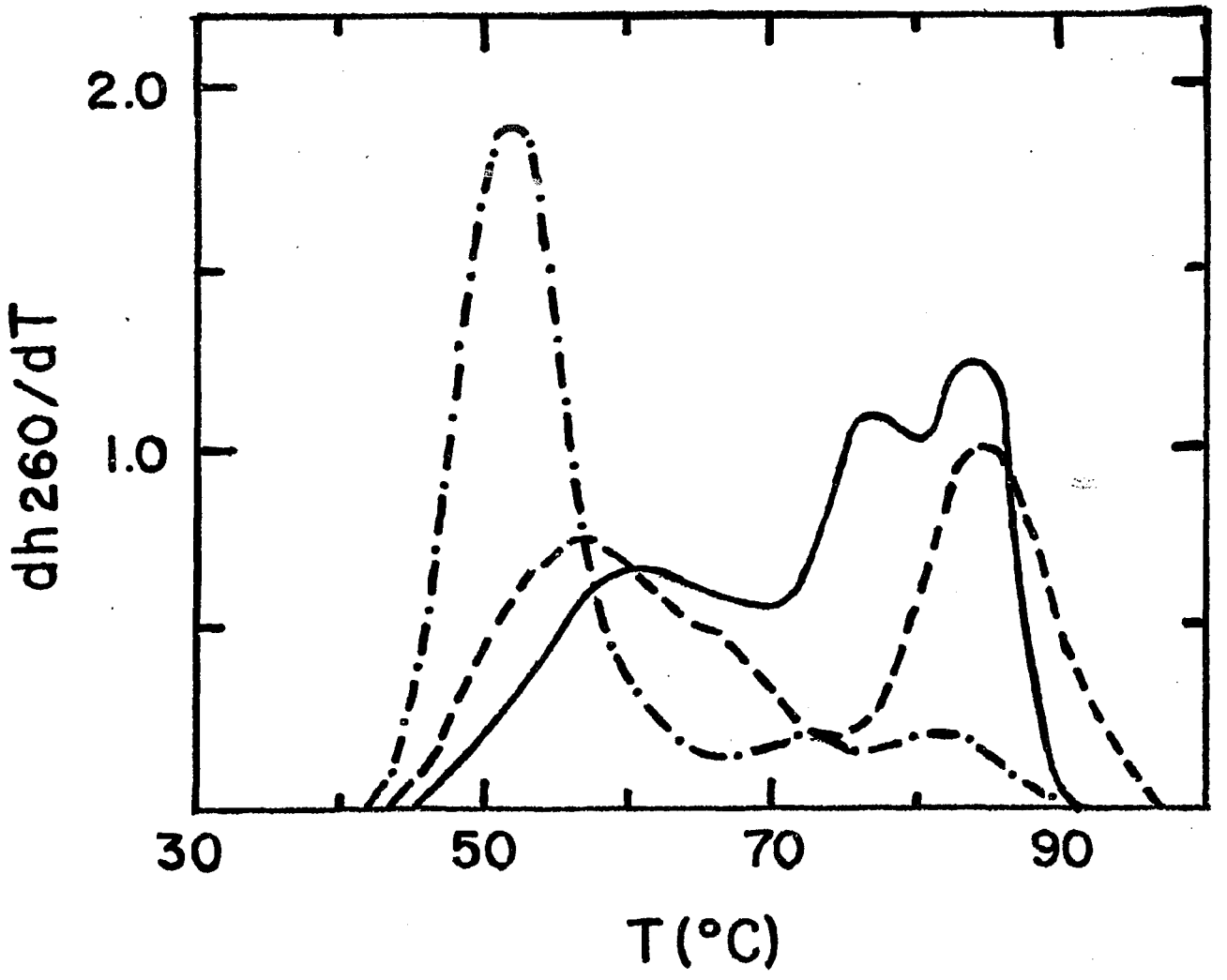

Fig 44 Derivative melting profiles of stepwise NaCl reconstitution. NH (——), 0.6M NaCl-treated NH (– – –), 2.5M NaCl-treated NH (-.-). Control is the same as in Fig 42

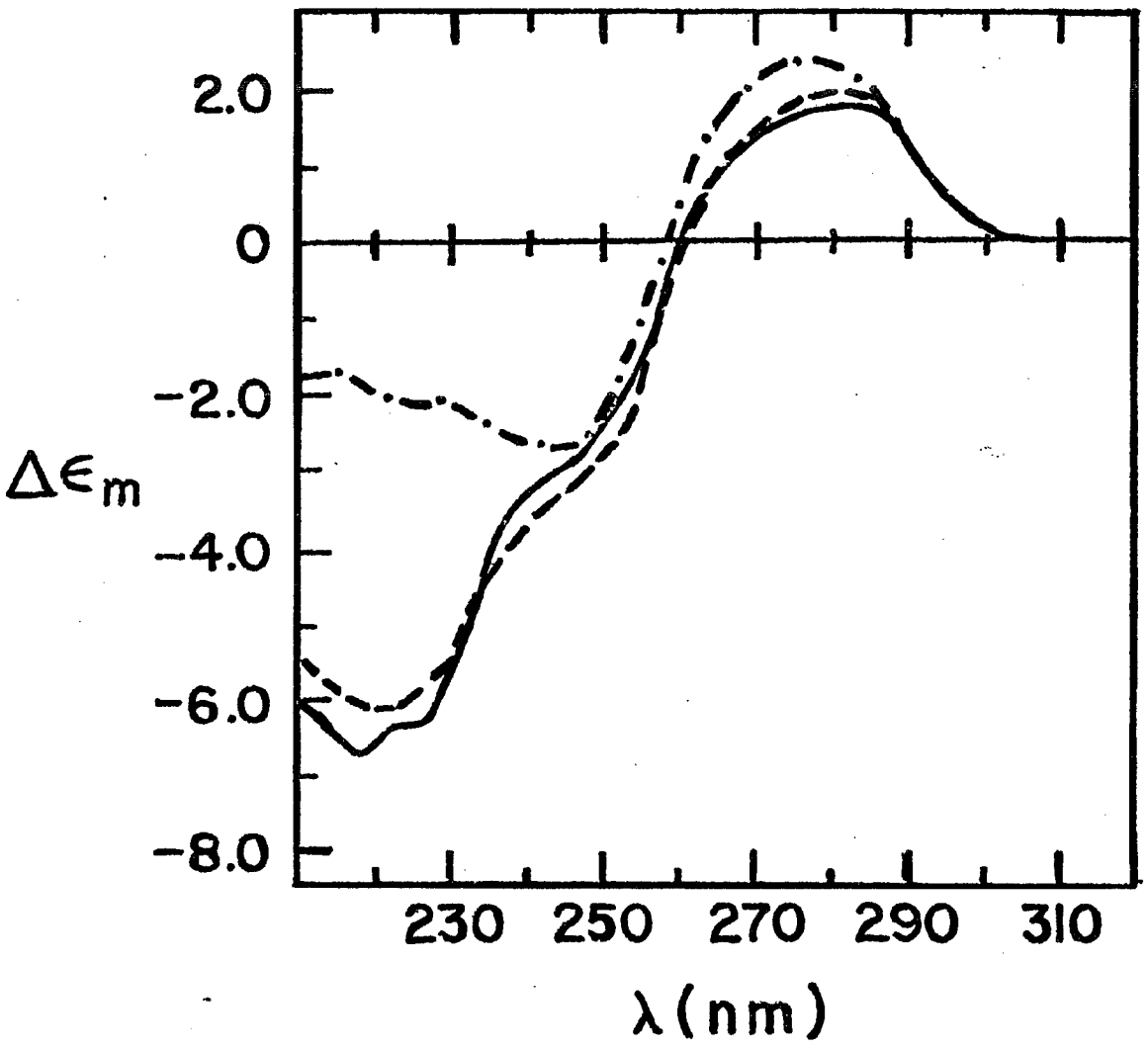

Fig 45 CD spectra of stepwise reconstitution. NH (——), 0.6M NaCl-treated NH (---) and 2.5M NaCl-t treated NH (-.). Control is the same as in Fig 43

to its control. The conclusion is that step-wise NaCl gradient reconstitution of nucleohistones does not improve both the melting and the CD of the reconstituted nucleohistones.

Discussion

Urea acts as a denaturing agent by competing for the hydrogen bonding sites of DNA and thus decrease the probability of formation of intramolecular hydrogen bonds between the bases in the DNA helix (102). The decrease in the T_m of DNA in high urea solution is consistent with the above fact. Shih and Lake (100) and Bartley and Chalkley (101) showed by electrophoresis that urea alone does not fully dissociate histones from DNA in nucleohistone. The constant melting area of melting band I + II in nucleohistone is consistent with these findings. However, T_{mIII} and T_{mIV} for the melting of all nucleohistone and salt-treated nucleohistones are decreased in the presence of urea.

Shih and Lake (100) and Bartley and Chalkely (101) also proposed that a disruption of the supercoiled structure of nucleohistone as the cause for the observed CD changes. This is not in agreement with the results presented here. The theory of helix-coil transition of nucleohistone proposed by Li (78) indicated that the thermal stability of nucleohistones resulted from the direct binding of histones to DNA, irrespective of tertiary structure such as the supercoil. The CD changes

observed in urea must also be due to a direct effect of urea on histone-DNA interaction. If there is a change observed in the supercoil structure, it must be a result of the change in the interaction between histones and DNA in the nucleohistone.

The conformation and thermal denaturation properties of native and partially dehistonized nucleohistones can be reversed after they have been significantly disturbed by urea. In view of the fact that both CD and thermal denaturation measures the conformation of bound histones and the thermal stability of histone-bound base pairs, then native nucleohistone is in tis most stable conformation.

Reconstituted chromatin from both continuous gradient and step-wise gradient dialysis does not show the same melting profile and conformation as that in the native chromatin. Efforts were made to minimize protease reactions by the addition of inhibitors such as bisulfite and phenylmethanesulfonyl fluoride (PMSF) to the reconstitution mixture. The results presented here were reconstitution doen in the presence of these pretease inhibitors. Reconstitution without the inhibitors showed even more degradation of ihistones. The problem of proteases action encountered here is caused by the endogeneous proteases present in chromatin. Reconstituted complexes using pure DNA and histones may not have this problem. One has to be cautious in using reconstituted chromatin as model system for native chromatin. Neither methods of reconstitution tested here yielded a complex identical to native chromatin.

CHAPTER VI

PROTAMINE-DNA, -CHROMATIN, AND -SALT TREATED NUCLEOHISTONE COMPLEXES

Protamine is found in the mature spermatozoa of a great many fish species. It is an interesting molecule to study because during the maturation of spermatids there is a complete displacement of histones by protamine in their chromatin. Protamine is a small protein with 31 amino acid residues among which 67% are arginine. Protamine is used here to complex with nucleohistone in a further attempt in the elucidation of histone-DNA interactions and of chromatin structure.

Experimental

Protamine HCl (Sigma) was dialyzed against 0.25mM EDTA, pH 8.0. Its concentration was determined by ninhydrin using arginine HCl as the standard. Protamine of $1x10^{-4}$M was added dropwise to DNA and nucleohistones for complex formation. In experiments testing replacement of histones by protamine, complexes were made in EDTA then dialyzed into 0.15M NaCl. After 3 changes of buffer the samples were taken out and centrifuged

at 10,000 rpm for 10 minutes. The pellets were redialyzed into EDTA and used for thermal denaturation and CD studies.

Results

a. Titration curve

Fig. 46 shows the precipitation curves of DNA, nucleohistone and salt-treated nucleohistones by protamine. The mid-point of titration for protamine-DNA complex was 1.35 amino acid residues per nucleotide, similar to the result obtained by Yu et al. (61). The mid-point of titration occured at 0.6, 0.9 and 1.2 amino acid residues per nucleotide for nucleohistone, 0.6M NaCl-treated and 1.6M NaCl-treated nucleohistone, respectively. The increase in the mid-point of precipitation curve for nucleohistones with more histones removed indicates that protamine binds DNA in nucleohistones in a manner similar to that of polylysine.

b. Thermal denaturation of protamine-DNA, -nucleohistone, and salt-treated nucleohistone complexes

Figs. 47-50 show the melting profiles of protamine-DNA, -nucleohistone and-salt-treated nucleohistone complexes. The protamine-bound base pairs in the DNA-protamine complexes have a T_m' of 90°C. After the binding of protamine to nucleohistone, melting bands I, II and III are entirely suppressed. There is only a broad melting band at 90°C at high input ratio of protamine. At low

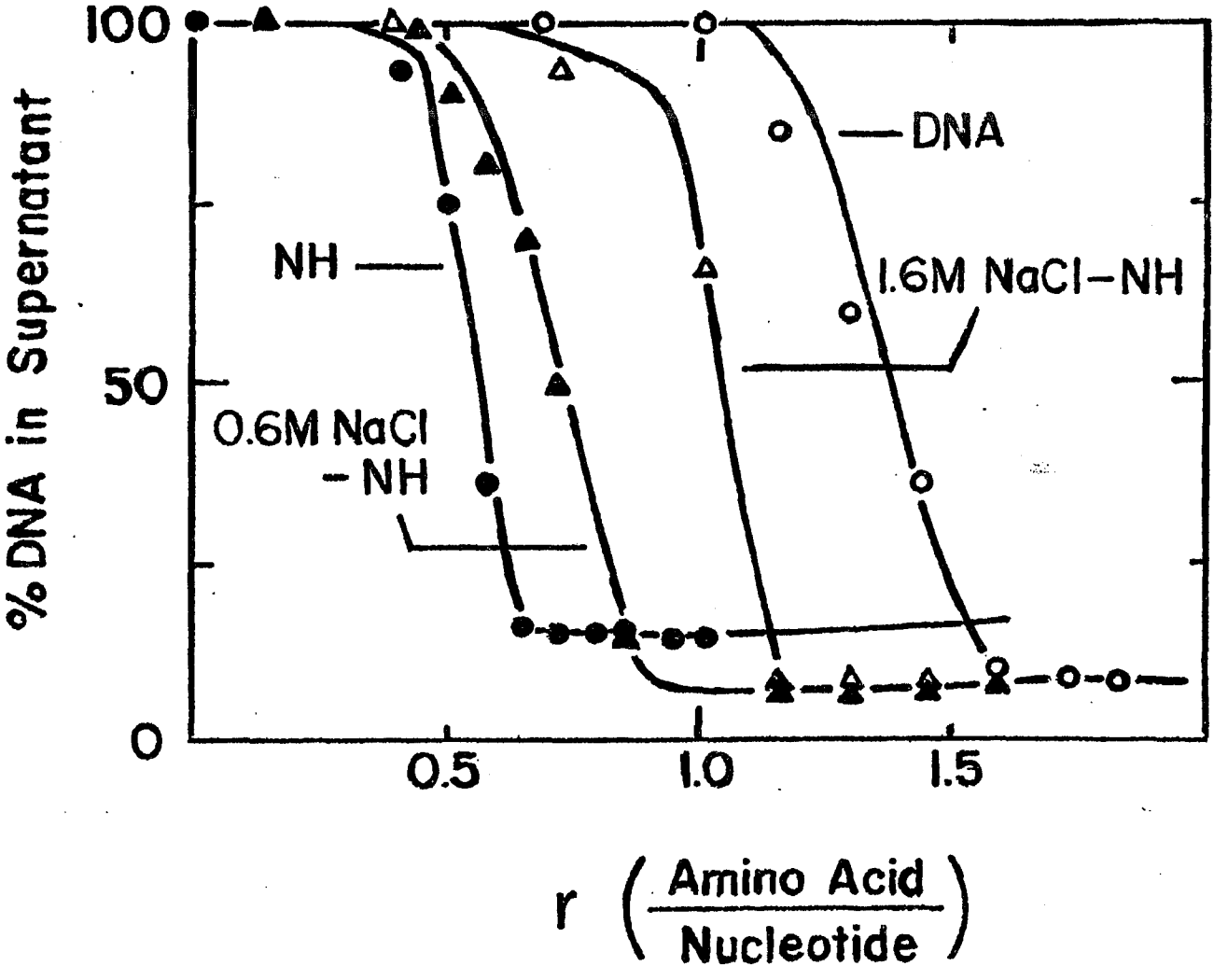

Fig 46 Titration curves of nucleohistones and DNA with protamine. NH (●), 0.6M NaCl-treated NH (▲), 1.6M NaCl-treated NH (△) and DNA (○)
Buffer: 0.25mM EDTA, pH 8.0

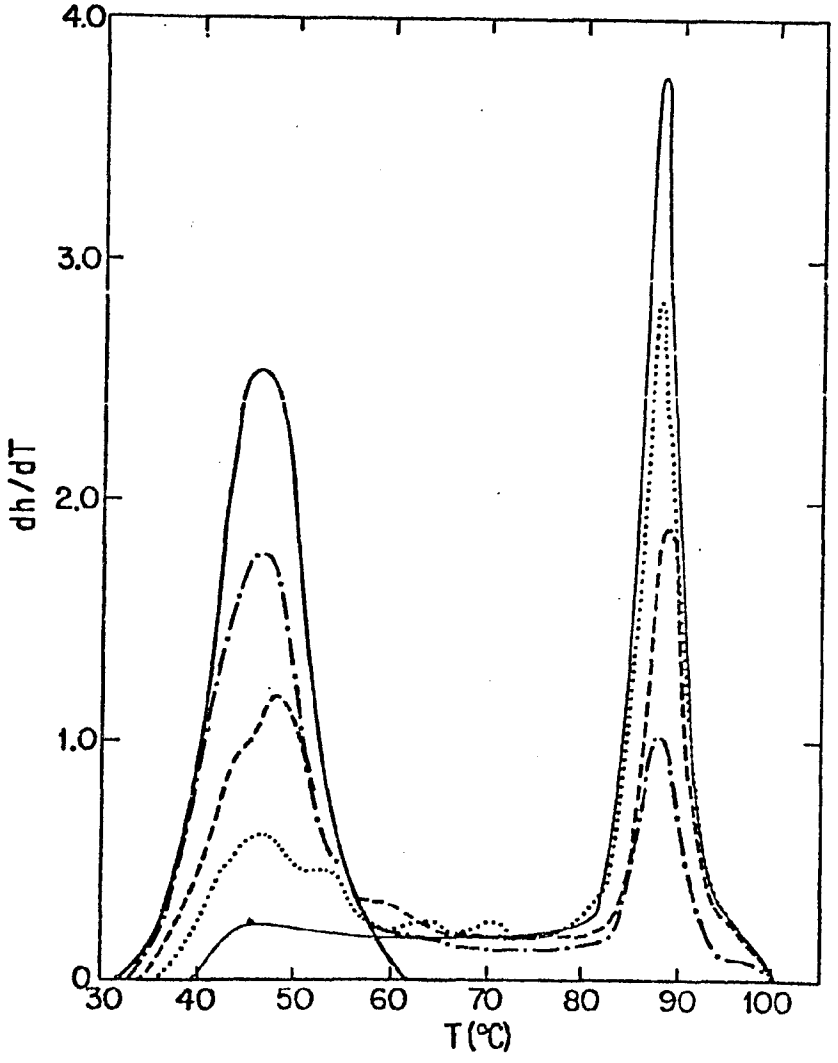

Fig 47 Derivative melting curves of protamine-DNA complexes. r=0 (——), r=0.2 (-.-), r=0.4 (---), r=0.6 (...) and r=0.8 (——)
Buffer: 0.25mM EDTA, pH 8.0

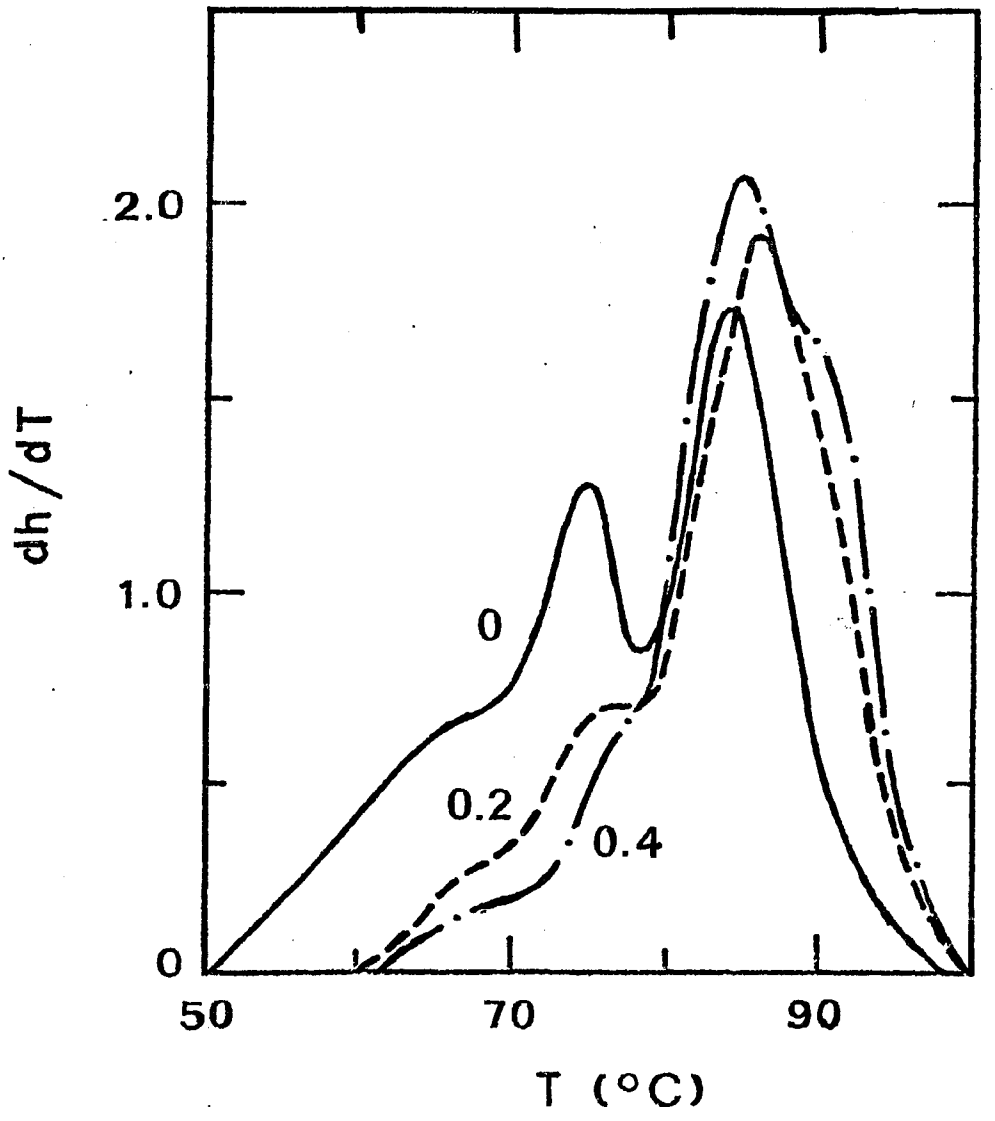

Fig 48 Derivative melting curves of protamine nucleohistone complexes. r=0 (——), r=0.2 (---) and r=0.4 (—·—)
Buffer: 0.25mM EDTA, pH 8.0

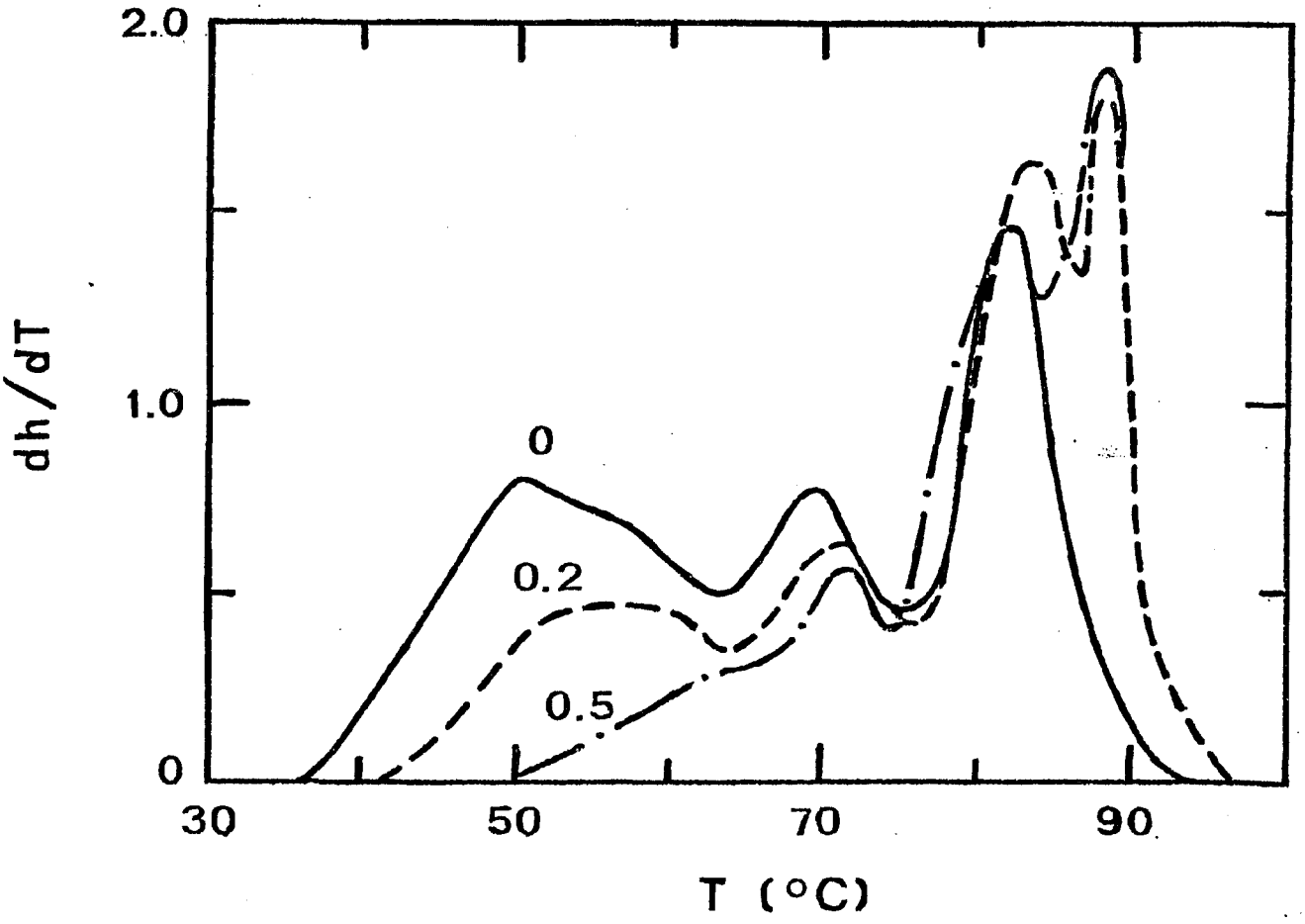

Fig 49 Derivative melting curves of 0.6M NaCl-treated nucleohistone. r=0 (—), r=0.2 (---) and r=0.5 (—.—)
Buffer: 0.25mM EDTA, pH 8.0

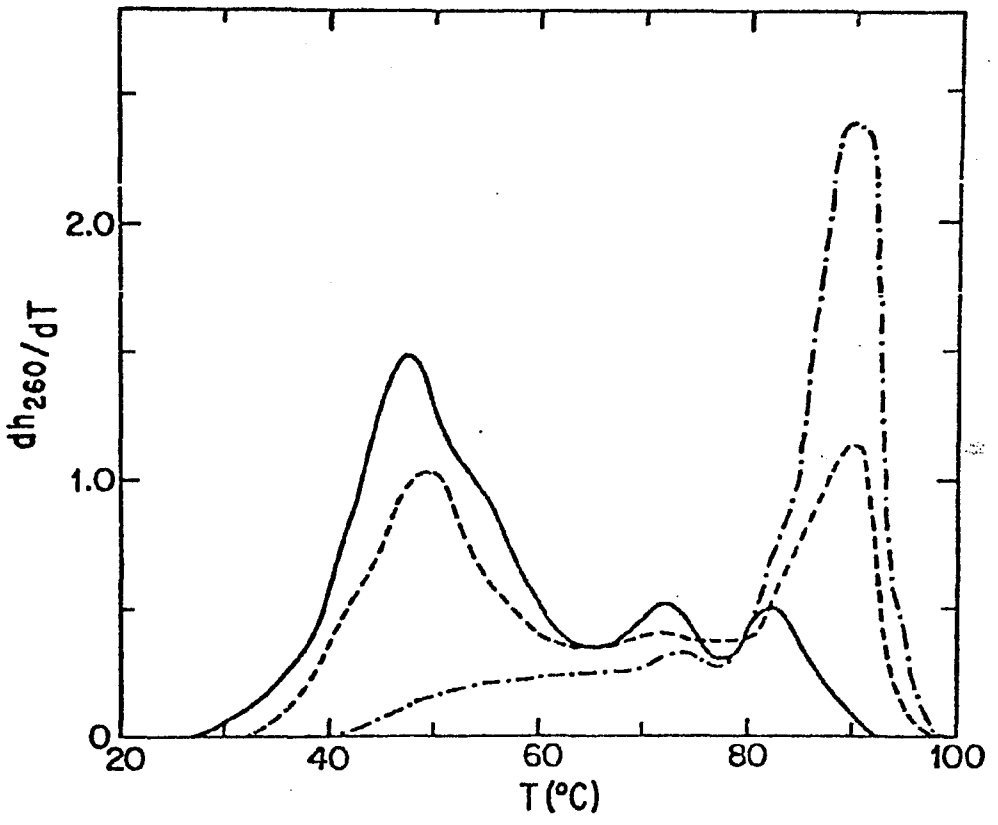

Fig 50 Derivative melting curves of protamine-1.6M NaCl-treated NH. r=0 (——), r=0.1 (---) and r=0.3 (-.-)
Buffer: 0.25mM EDTA, pH 8.0

input ratios a shoulder of melting band III can still be detected, with a broadening of melting band IV. T_{mIV} is shifted from 82°C to 86°C. At higher input ratios, melting band III disappears completely with the appearance of a shoulder near 90° C. This means that protamine like polylysine not only bind to the free DNA regions in nucleohistone but can also bind the base pairs already bound by the less basic halves of histones.

For 0.6M NaCl-treated and 1.6M NaCl-treated nucleohistone complexes, the binding of protamine to the free DNA base pairs is seen readily with a decrease in the area of melting band I. The area of melting band III decreases with increasing input ratio of protamine but the effect on melting band IV cannot be resolved because it becomes a broad band which overlaps with the melting of protamine-bound DNA.

c. Circular dichroism of protamine-DNA, -nucleohistone and -salt-treated nucleohistone complexes

Figs. 51-54 show the CD spectra of protamine-DNA, -nucleohistone, and -salt-treated nucleohistone complexes. The effect of protamine on the CD spectrum of DNA is similar to that reported by Yu et al. (61). The effect of protamine binding to DNA is to reduce the amplitude of the positive peak at 278 nm. There is a slight red shift of the cross-over point as protamine input ratio

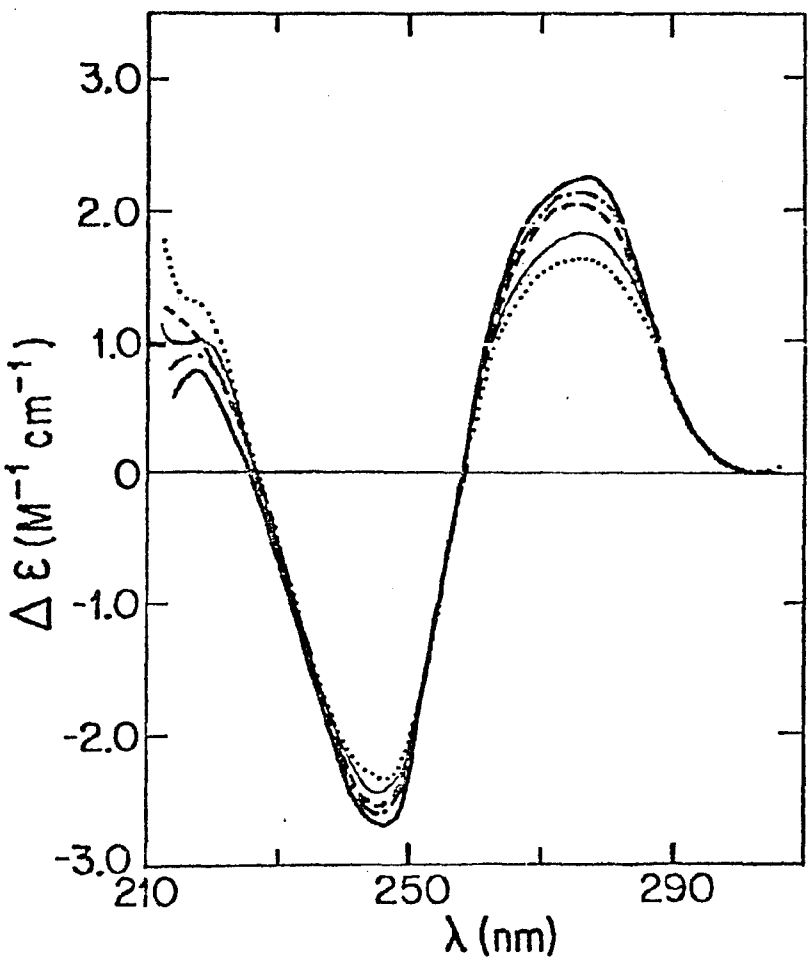

Fig. 51 CD spectra of protamine-DNA complexes. r=0 (——), r=0.2 (-.-), r=0.4 (---), r=0.6 (——) and r=0.8 (...) in EDTA buffer

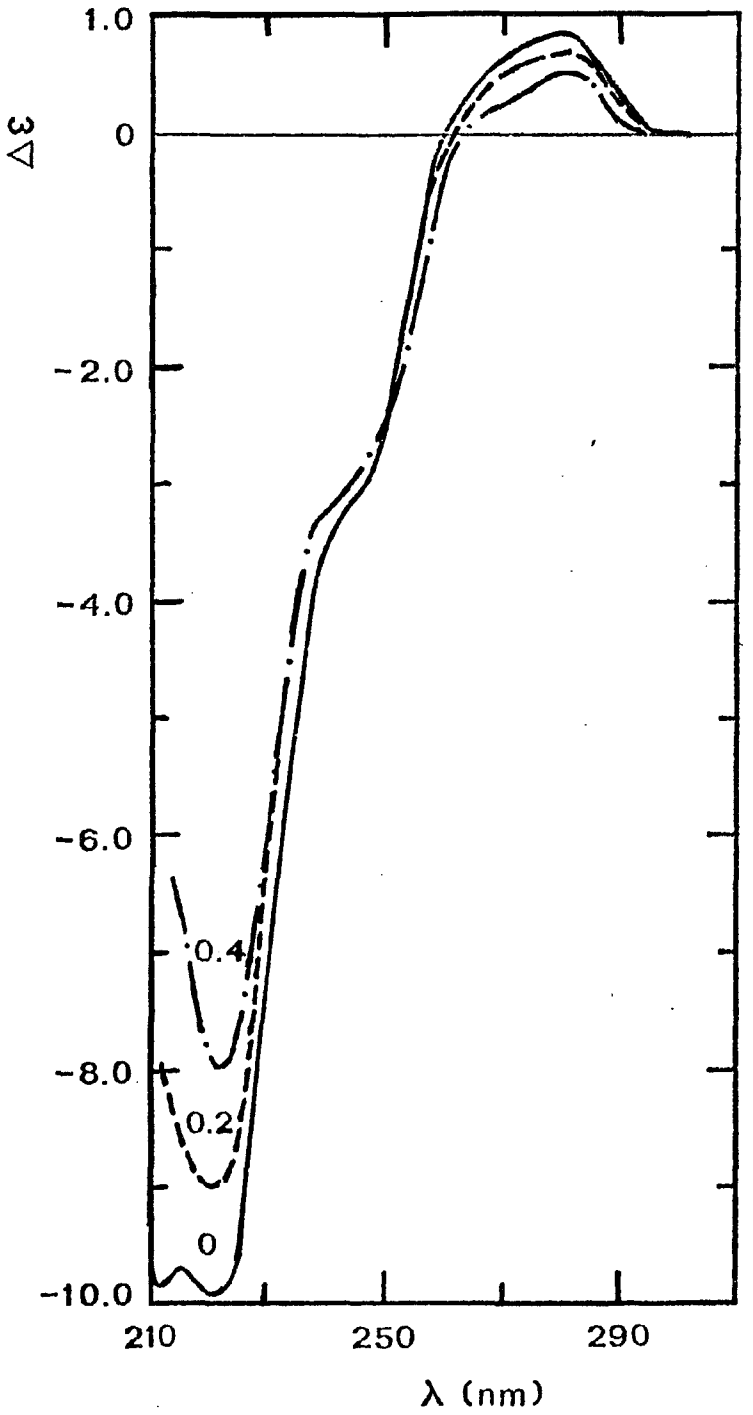

Fig 52 CD spectra of protamine-nucleohistone complexes. r=0 (—), r=0.2(- - -) r = 0.4 (—·—)

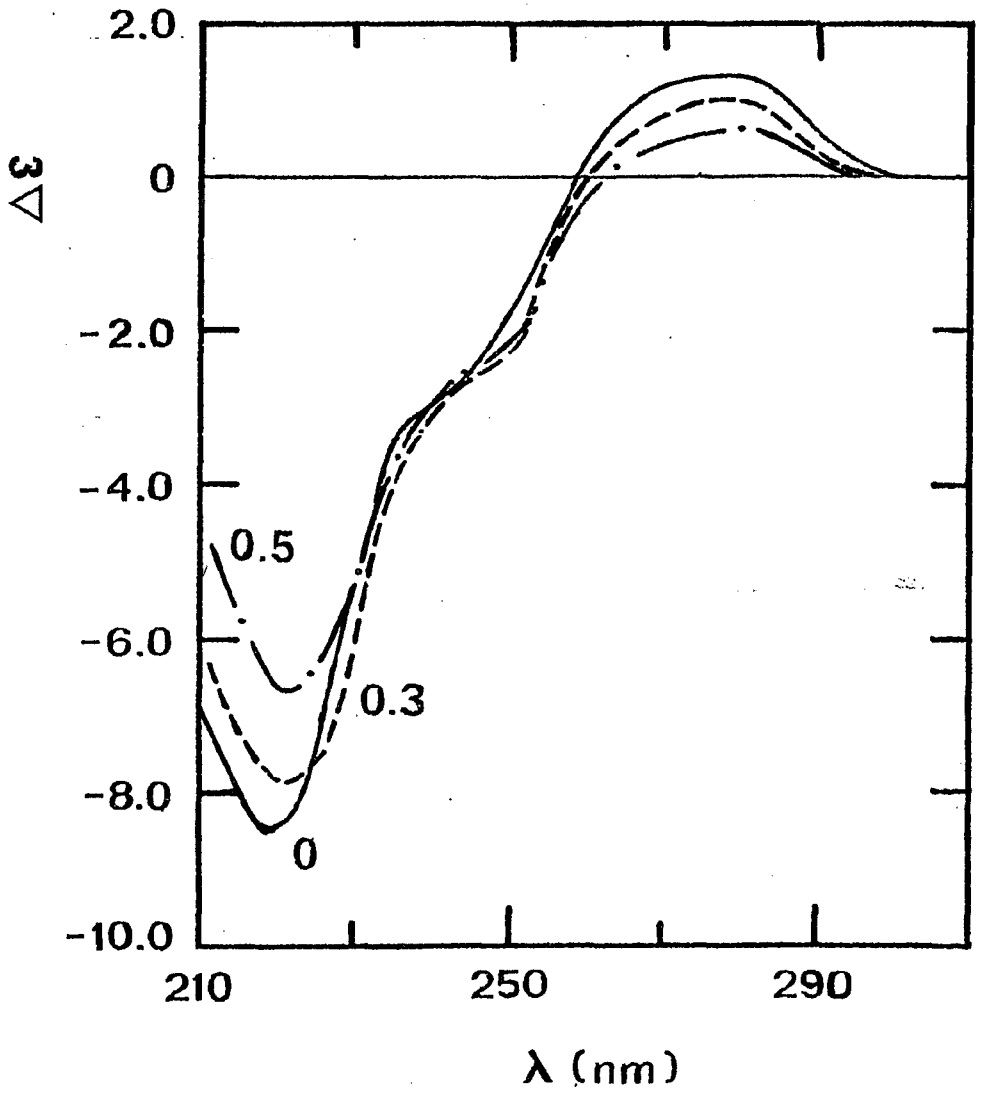

Fig 53 CD of protamine-0.6M NaCl-treated nucleohistone complexes. r=0 (——), r=0.3 (– – –), and r=0.5 (–·–) in EDTA buffer

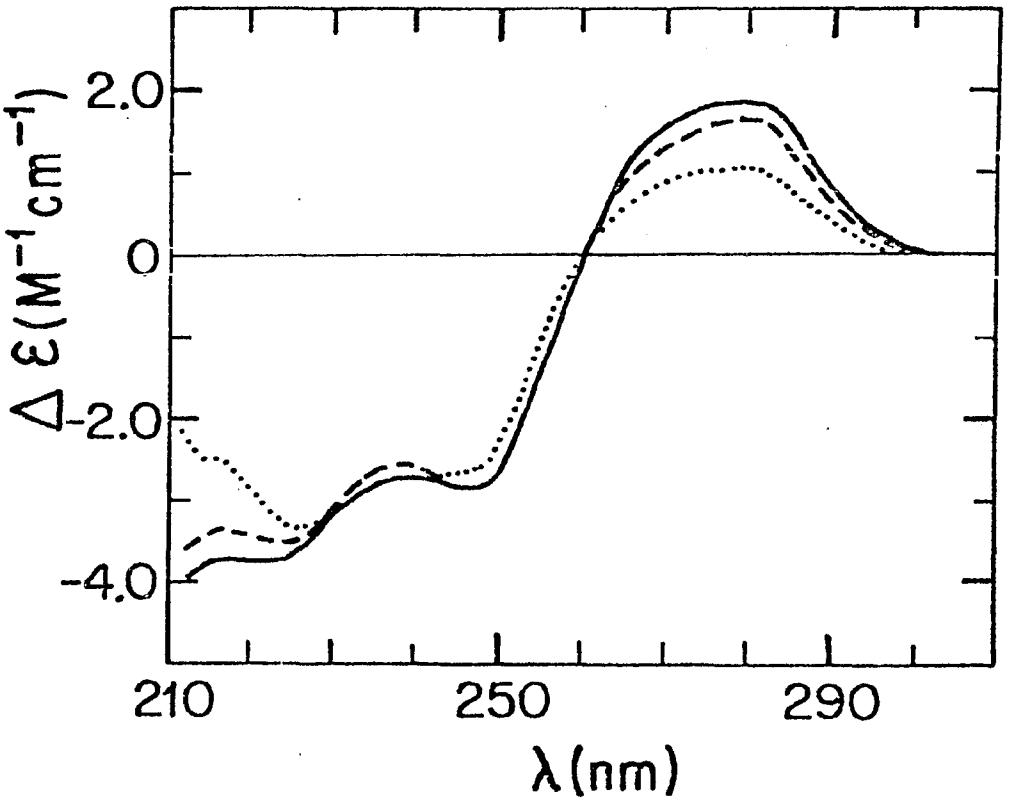

Fig 54 CD of protamine-1.6M NaCl-treated NH complexes. r=0 (——), r=0.1 (---) and r=0.3 (...) in EDTA buffer

increases, and no change is seen on the negative CD below 240 nm. Because of the distinct melting band of protamine-bound base pairs in protamine-DNA complexes (Fig. 47) the CD of protamine-bound base pairs can be calculated. It has been observed that the effect on DNA conformation by protamine binding is similar to that of polylysine binding. Protamine, too, shows a dehydration effect on the DNA conformation when it binds to the DNA.

The effects of protamine on the CD spectra of nucleohistone and histone H1 depleted nucleohistone (Figs. 52, 53) are similar. Protamine binding to these nucleohistones causes a decrease in the amplitude of the positive CD peak at 278 nm. This is expected if protamine is to have some dehydration effect on those DNA base pairs which are bound by protamine. The DNA base pairs become more distorted towards C-form DNA. The CD of the protein region at 220 nm is reduced after protamine binding. This result suggests that protamine binding to nucleohistone may cause the release of some histones and the loss of their secondary structure.

The effect of protamine binding on the CD spectra of 1.6M NaCl-treated nucleohistone is similar to that of other nucleohistones at 278 nm with a decrease in the amplitude. However, the CD at 220 nm is not changed after binding. At 1.6M NaCl both lysine-rich and the

slightly lysine-rich histones are removed. The change in the protein CD at 220 nm after protamine binding in nucleohistone and 0.6M NaCl-treated nucleohistone suggests that protamine binding may cause preferential removal of the lysine and slightly lysine rich histones. I.6M NaCl-treated nucleohistone contains mainly the arginine rich histones shows no change in the protein CD with protamine binding suggesting that protamine does not displace arginine rich histones. This conclusion is substantiated by the works of Evin et al. (103) and Marushige and Dixon (104). These authors found during in vitro studies of spermatogenesis the lysine rich histones are removed before the arginine rich histones.

c. Histone displace ment by protamine:

In order to see whether histones are displaced by protamine and what effect would this displacement cause on nucleohistone conformation, protamine-nucleohistone complexes were made and dialyzed into an intermediate ionic strength of 0.15M NaCl, similar to the ionic strength in living cells. If histones are replaced by protamine, they should be dissociated and remain in the supernatant after centrifugation. Since only a small quantity is involved, ordinary methods to determine the histones in the supernatant, such as electrophoresis is not adequate. Consequently, the

experiments were designed to collect the pellets, redialyze the pellets back to 0.25mM EDTA, pH 8.0 buffer and measure its CD and melting properties.

Figs. 55a and 55b show, respectively, the melting and CD results of the control nucleohistone before and after being exposed to 0.15M NaCl. Even though the melting results show some difference in the nucleohistone after the treatment of high ionic strength, the CD spectrum is not effected. The small change seen in the melting curves after dialysis may be due to slight degradation of proteins in nucleohistone during the dialysis in 0.15M NaCl.

Fig. 56 show the melting curves of protamine-nucleohistone complexes at r=0.3 and 0.4. At these input ratios the complexes remain in solution in EDTA buffer, i.e. they have not reached precipitation point. The results in Fig. 56 show no consistent difference before and after treatment of the complexes by 0.15M NaCl. This indicates that 0.15M NaCl does not force histones to dissociate from DNA after protamine binding in nucleohistone.

Fig. 57 shows the effect of dialysis into 0.15M NaCl on the CD spectra of protamine-nucleohistone complexes with r=0.3 and 0.6. The supernatant of the complexes after dialysis showed no DNA absorption,

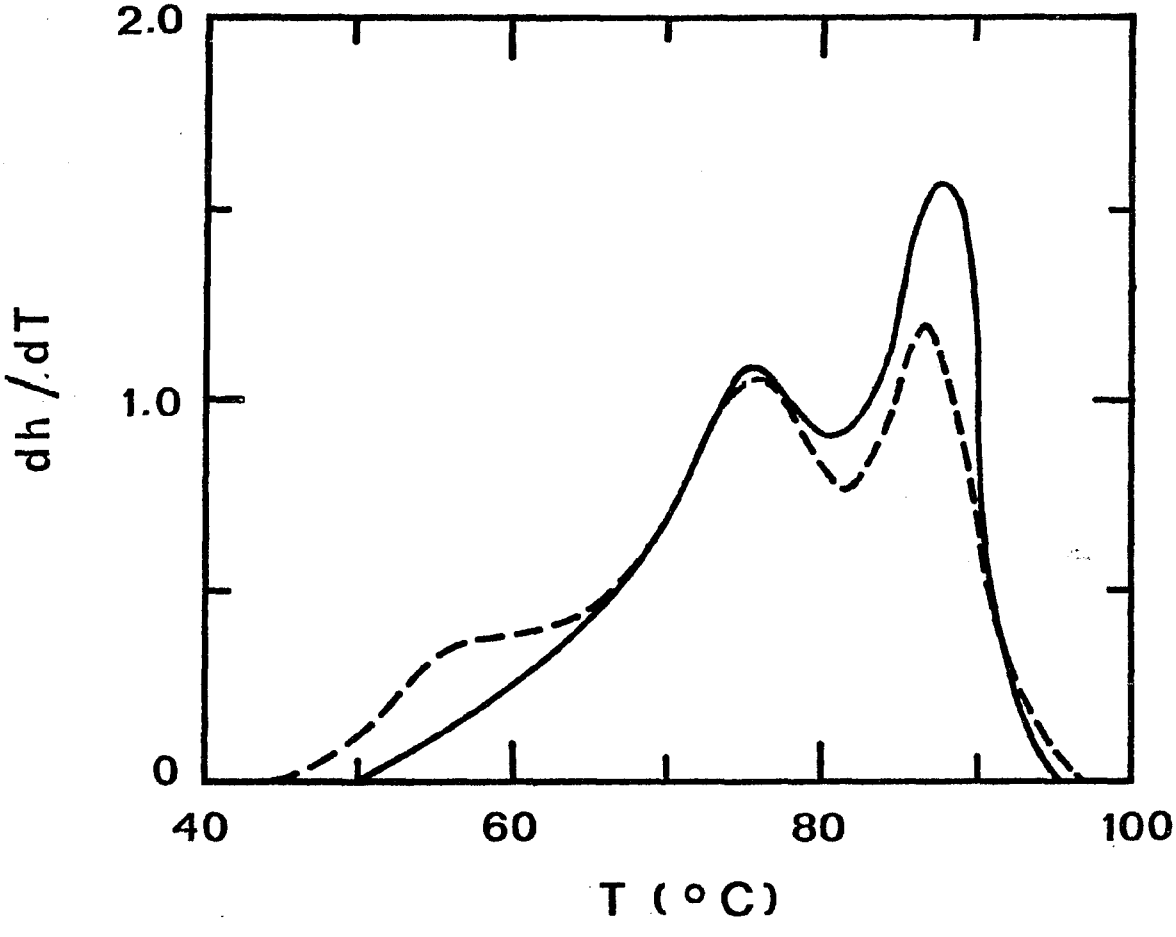

Fig 55a Derivative melting curves of nucleohistone in (a) 0.25mM EDTA buffer (——), (b) dialyzed into 0.15M NaCl then redialyzed back into EDTA buffer (---)

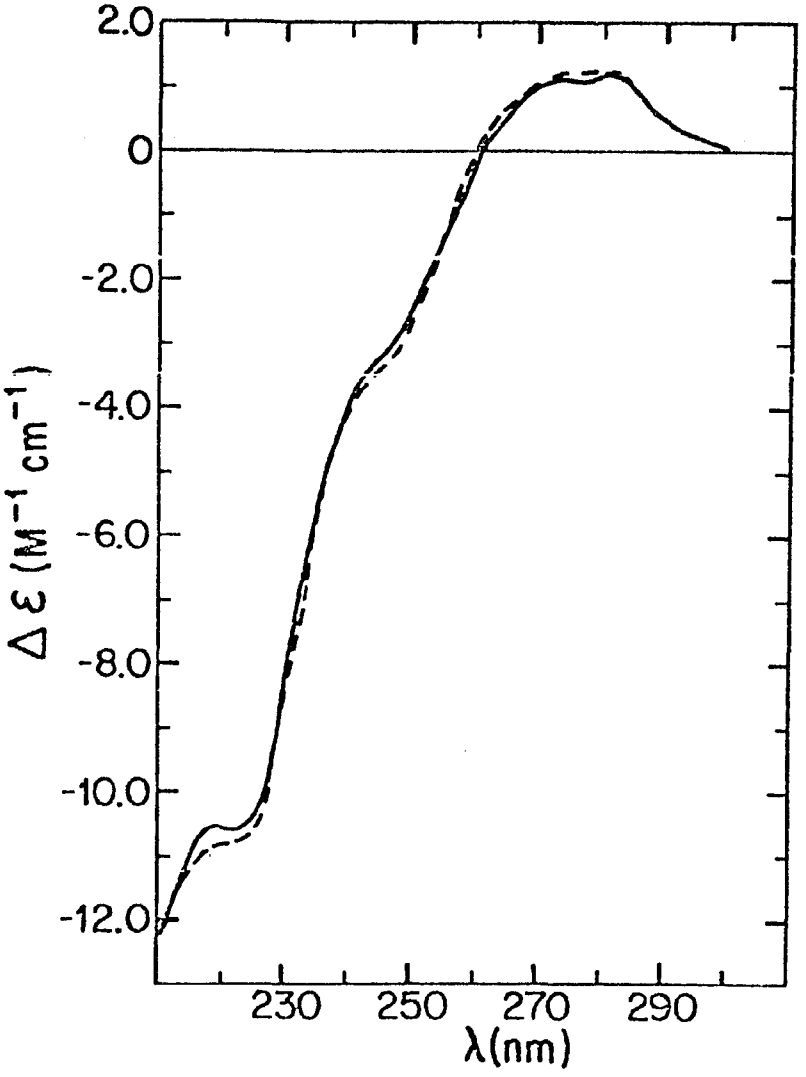

Fig 55b CD spectra of nucleohistone in (a) 0.25mM EDTA buffer (——), (b) dialyzed into 0.15M NaCl then redialyzed back into EDTA buffer (---)

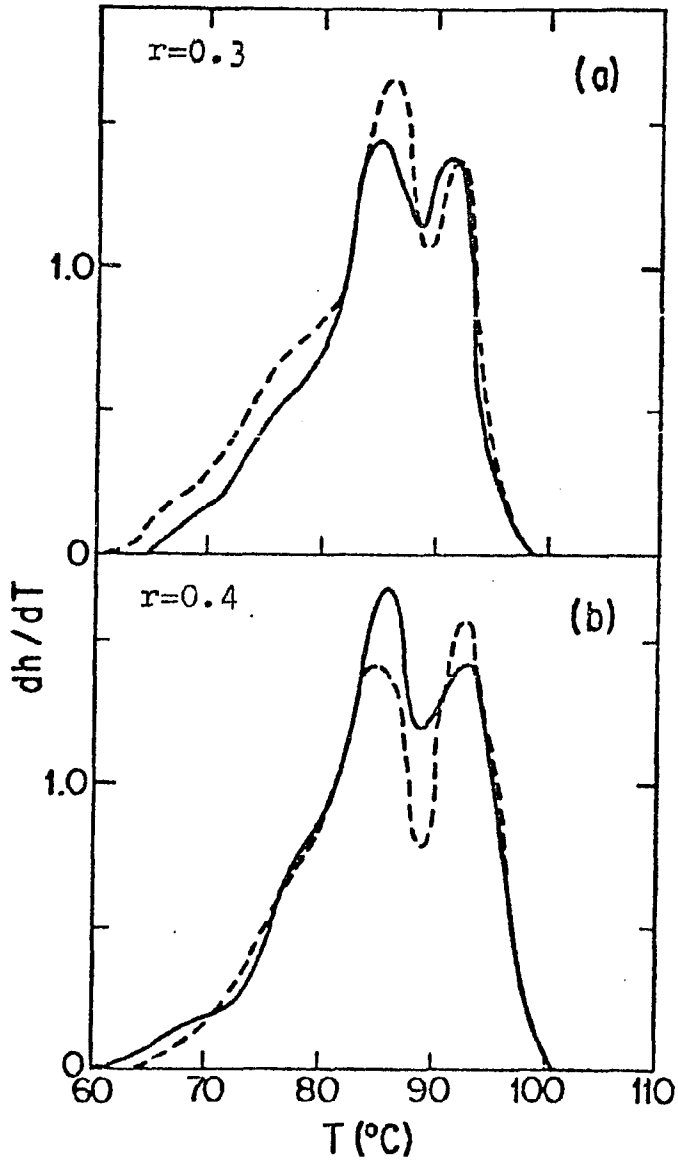

Fig 56 Derivative melting curves of protamine-nucleohistone complexes of r=0.3 and 0.4. Complex in 0.25mM EDTA buffer (——), complex dialyzed into 0.15M NaCl then redialyzed back into EDTA buffer (---)

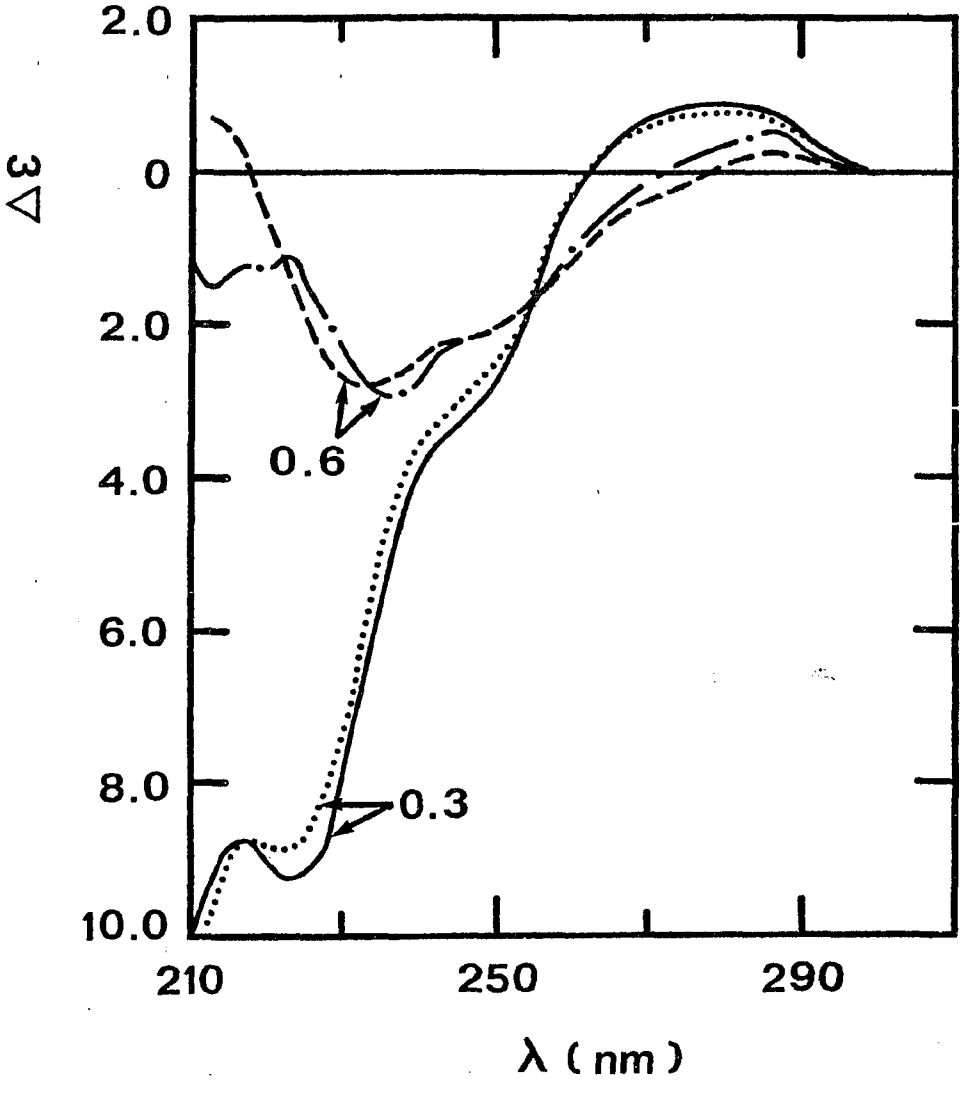

Fig 57 CD spectra of protamine-nucleohistone complexes at r=0.3 and 0.6
r=0.3 in EDTA buffer (——), dialyzed into 0.15M NaCl then redialyzed into EDTA buffer (·····).
r= 0.6 in EDTA buffer (—·—), dialyzed into 0.15M NaCl then redialyzed into EDTA buffer (---)

and consequently no thermal and CD were done on them. The pellets of the complexes gave CD spectra that were not significantly different from that of the complexes before 0.15M NaCl treatment. This result suggests that the replacement of histones by protamine at very low ionic strength (0.25mM EDTA) is a function of the input ratio of protamine in chromatin and the physiological ionic strength of 0.15M NaCl does not facilitate further histone replacement.

Discussion

Protamine stabilized DNA base pairs to a lesser extent than polylysine. Protamine-DNA complexes have T_m' of 90°C while polylysine-DNA complexes have T_m' of 99°C. This difference is due to the fact that protamine contains mainly polyarginine residues. However, polyarginine-DNA complexes show two T_m's at 91° and 100°C.

Protamine has the same effect on DNA conformation as polylysine. Protamine binding cause the dehydration of DNA and distorts the B-conformation of DNA. Protamine binding to nucleohistone causes a reduction of both the DNA conformation at 278 nm and the protein conformation at 220 nm. The results imply that histones may be displaced during protamine binding. However, the displacement is not facilitated by 0.15M NaCl.

CHAPTER VII

DISCUSSION

The theory of helix-coil transition in DNA has been treated in detail by Sheraga (102), Poland and Sheraga (105), Crothers et al. (106), and Crothers (75). Here, only a brief qualitative description of helix-coil transition will be presented.

Helix-coil transition in DNA can be described as a two state process at the nuclostide level. A base pair is considered to be either a "closed", double helical region, or an "open", random coil region. The simplest model of DNA allows interaction only between nearest neighbor base pairs, and can be described by two parameters: a stability constant, or equilibrium constant for the transfer of a base pair from a coil region to the end of a helical region, and a nucleation parameter, which measures the additional energy required to initiate a new helical region in the middle of a coiled region. The cooperativity transition of DNA from a helical to a coiled state occurs because it is easier

to extend a preexisting helical region than to start a new helical region, and it is also easier to extend prexisting reandom coil than to break a base pair in a helical region. Thus, cooperative transitions favor long stretches of intact helix, or of random coil. Crothers and Zimm (74) predicted that the main stabilizing interaction in DNA should be the stack ing energy of the base pairs. However, studies on single stranded poly rA and poly rU by Leng and Felsenfeld (65) and Brahms et al. (107) resulted in the conclusion that for DNA the main origins of cooperativity of melting comes from the conformations of the denatured or unfolded state, rather than in the interactions present in the helix.

Helix-coil transition presented so far is only applicable to DNA. Little theoretical work was done on the helix-coil transition of DNA in a DNA-protein complex. The binding to DNA of basic proteins such as polylysine, polyarginine and histones, resulted in a biphasic or multiphasic melting transitions. Such melting curves could not be interpreted until a theoretical model of thermal denaturation of nucleoproteins was presented (78). The basic assumption of Li's model is that protein-bound base pairs melt independently from its neighboring base pairs. Thus, biphasic or multiphasic melting curves in a nucleoprotein represent the independent helix-coil transition in

protein-free and -bound regions.

This theoretical model was shown to work very well when applied to nucleohistone (chapter III), polylysine-DNA and polylysine-nucleohistone complexes (chapter IV). Thermal denaturation results showed that all nucleohistones, irrespective of the size, give the same melting profiles. The melting profile of a nucleohistone measures the thermal stability of histone-free and histone -bound regions. These regions are primarily determined by the irreversible ionic interaction between the phosphates of DNA and the basic amino acids of histones. The higher order structure which may depend upon the size of nucleohistones seems to be less important. The interaction between histones and DNA gives the pattern of melting seen for nucleohistone, namely the higher melting bands at 72° and 82°C. This assignment is supported by the melting results of salt-treated nucleohistones: the removal of histones by NaCl in the NaCl-treated nucleohistones showed a progressive decrease in the area of melting at 72° and 82° C with an increase in the melting at low temperature corresponding to free DNA regions.

The above interpretation of the melting of nucleohistone is substantiated by circular dichroism studies of nucleohistone. For nucleohistone, the CD above 240 nm reflect the DNA conformation and the CD

below 240 nm reflects histones or protein conformation. When histones are removed by salt the CD of the resulting salt-treated nucleohistone showed increase in the DNA conformation and decrease in the histone conformation. The concept of separating a nucleoprotein into protein-free and -bound base pairs successfully used in thermal denaturation can also be applied to the conformational aspects of nucleoprotein, namely circular dichroism. The CD of a nucleoprotein can also be divided inot two parts, the CD of protein-bound base pairs and that of protein-free base pairs. Using this concept the CD of protein-bound DNA base pairs was calculated for polylysine-DNA complexes (chapter IV) and for histone-bound DNA in chromatin (chapter III).

Based upon the derivative melting profiles it was calculated that the fraction of base pairs bound by histones in chromatin is 80%. This agrees with the results obtained from DNA-RNA hybridization results of chromatin. The average number of amino acid residues per nucleotide in histone-bound regions is found to be 3.7 ± 0.4 amino acid residue per nucleotide or about 7 amino acid residues per base pair in calf thymus nucleohistone.

Every histone isolated from eukaryotic cells has an asymmetrical distribution of basic amino acids along its molecule. One half contains more basic amino

acids and the other half contains more hydrophobic amino acids. Because of this fact, the two melting bands at 72° and 82° C in nucleohistone are assigned to base pairs bound by the less and the more basic halves of histones respectively. With this assignment the melting results of polylysine-nucleohistone complexes (chapter IV) suggest that polylysine can bind to DNA base pairs already bound by the less basic halves of histones. This can be accomplished if the less basic halves of histones bind the major groove of DNA while polylysine binds to the minor groove, a suggestion made by Li et al. (88) based on trypsin digestion of nucleohistone and the CPK molecular models.

From the melting curves of polylysine-DNA complexes (chapter IV), 1.0 lysine per nucleotide was obtained in the polylysine-bound regions. This agrees with the results obtained from the binding studies of Latt and Sober (64). Polylysine-DNA complex studied by CD were used as a model for histone-DNA complexes. The changes of the CD spectra seen in reconstituted DNA-histone complexes (48, 49) and in chromatin are in the same general trend seen in DNA-polylysine complexes. Polylysine cause a dehydration of the DNA molecule, thus distorting the normal B-conformation of DNA in solution to a C-form. Histones have the same effect on DNA conformation in chromatin.

A combination of the CD results of trypsin-treated chromatin and polylysine-nucleohistone binding leads to the conclusion that the two halves of histones contribute differently to the CD of chromatin. The less basic halves of histones have more α-helical content than the more basic halves. This is reasonable in view of the fact that the more basic halves of histones have more positive charges and are more tightly bound to DNA while the less basic halves have more hydrophobic residues to form α-helix.

Studies of protamine interaction with chromatin was carried out as an extension of polylysine-DNA complexes and histone DNA interactions in nucleohistone. As far as the conformation is concerned protamine binding to nucleohistone is similar to polylysine binding. Both systems show similar melting effect on DNA base pairs bound by the less basic halves of histones. However, protamine binding causes the overlap of the melting of base pairs bound by the more basic halves of histones and the base pairs bound by protamine. Interestingly enough, protamine , which contains 67% arginine does not give the same melting profile in its DNA complexes as in polyarginine-DNA complexes (61). Polyarginine bound base pairs show two T_m's while protamine- and polylysine-bound base pairs give only one melting band at T_m'. Exactly how polylysine or polyarginine

bind to DNA is not known at present.

At present, two widely accepted models of chromatin structure have been proposed: the supercoil structure of chromatin (53, 54) and the nucleosome structure of chromatin (55). Pardon et al. (108) postulated from X-ray studies that the nucleoprotein-DNA complex in chromatin existed in a supercoil state. On the other hand, based on electron micrograph studies Olins and Olins (55) and other workers proposed that chromatin existed in a beaded structure. Each bead contains a double stranded DNA stretch of approximately 140 to 200 base pairs long and an octamer of two each of the four histones excluding histone H1. However, the compact beaded structure of chromatin reported by Olins and Olins (55) could possibly be induced by formaldehyde fixation of the chromatin. Recently, Polacow et al. (109) showed, using formaldehyde-fixed chromatin and H1-depleted chromatin, that formaldehyde fixation of chromatin cause condensation of histone-bound regions within the subunits of chromatin. Oudet et al. (110) showed that formaldehyde fixation of chromatin also yielded nucleosomes with a reduced dimension.

Crick and Klug (111) proposed that DNA within the chromatin subunit is in the kinky helix state. In the kinky helix, segments of DNA in the B-conformation are connected by kinks of two adjacent unstacked base pairs. The kinky helix was proposed on the basis that

the packing of 200 base pairs of DNA into a nucleosome of 60 to 100Å in diameter required large amount of energy and that nature favors B-form DNA. As pointed out in the introduction of this dissertation DNA can exist in many states or conformations depending on the salt and the relative humidities. The binding of polylysine and protamine to DNA causes a B to C transition in DNA conformation (chapters IV and VI). In native chromatin the conformation of DNA is between that of B and C form DNA as shown by circular dichroism (chapter III). Li (112) also pointed out that physically there is ample space in the chromatin subunit for DNA (200 base pairs) to fold if the dimension of nucleosomes (130Å in diameter) (110) is used.

Many reports on histone-histone interactions have appeared in literature. A histone core consisting of 8 histones (2 of each kind of histones excluding H1) was found in the PS particles by van Holde and co-workers (113). Li et al. (114) found dimers of histone H4 in solution. Kornberg and Thomas (115, 116) isolated tetramers of $(H3)_2(H4)_2$ in chromatin treated with nuclease. Using chemical cross-linking reagents they were also able to isolate an octamer of $(H2A)_2(H2B)_2(H3)_2(H4)_2$. Martison and McCarthy (117) also using a chemical crosslinker found that histones H2B and H4 are close to each other in chromatin.

The exact interaction of histone subunits with DNA in chromatin is not clear at present. Van Holde et al.

(113) proposed a model of chromatin with a histone octamer core with the DNA wounded on the outside. The binding of histone H1 to DNA was not considered. This model of chromatin was supported by neutron diffraction data of Baldwin et al. (58). Considering the results of thermal denaturation and circular dichroism of chromatin, chromatin-polylysine complexes presented in this dissertation, and trypsin treated chromatin Li (118) proposed a more detailed model of chromatin structure. He proposed that chromatin can exist in two states, a supercoil state and a compact, nucleosome state. These two structures of chromatin can be in equilibrium with each other. The primary subunit of histones are parallel dimers of $(H2A)_2$, $(H2B)_2$, $(H3)_2$ and $(H4)_2$. These parallel dimers of histones bind DNA in such a way that their less basic halves bind to the major groove and the more basic halves bind to the minor groove of DNA. Octamers of histones can be formed from the hydrophobic interactions of the nonpolar regions of two tetramers $(H3)_2(H4)_2$ and $(H2A)_2(H2B)_2$. Histone H1 bind approximately 30-40 base pairs and serves to link two octamers of the above histones. The binding of the subunits to DNA cause a structural distortion of DNA as seen from the CD results presented here. Depending on the external conditions such as pH, ionic strength etc., chromatin can exist either as a coiled structure or a compact nucleosome structure. This model suggests that

the nucleosome structure is a major structure of chromatin but it is not the only structure. In addition, it provides a detailed description of histone-histone interactions and histone-DNA interactions which were not discussed in other models.

REFERENCES

1. Dingman, C.W., and Sporn, M.B., (1964) J. Biol. Chem., 239, 3483
2. Messineo, L., (1962) Arch. Biochem. Biophys., 96, 479
3. Phillips, D,M.P., and Clarke, M., (1970) J. Chromatogr., 46, 321
4. Teller, D.C., Kinkade, J.M., and Cole, R.D., (1965) Biochem. Biophys. Res. Commun., 20, 739)
5. Haydon, A.J., and Peacocke, A.R., (1968) Biochem. J., 110, 243
6. Delange, R.J., Fambrough, D.M., Smith E.L., and Bonner, J., (1969) J. Biol. Chem. 244, 5669
7. Phillips, D.M.P., (1968) Biochem. J., 107, 135
8. Blazsek, V.A., and Bukaresti, L., (1964) Experienta 20, 369
9. Ord, M.G., and Stocken, L.A., (1967) Biochem. J., 102, 631
10. Phillips, D.M.P., and Simson, P., (1962) Biochem. J., 82, 236
11. Reid, B.R., and Cole, R.D., (1964) Proc. Natl. Acad.Sci. US., 51, 1044
12. Murray, K., (1965) Ann. Rev. Biochem., 34, 209
13. Phillips, D.M.P., (1963) Biochem. J., 87, 258
14. Huang, R.C.C., and Bonner, J., (1962) Proc. Nat. Acad. Sci. US., 48, 1216
15. Allfrey, V.G., Littau, V.C., and Mirsky, A.E., (1963) Proc. Natl. Acad. Sci. US., 49, 414

16. Laurence, D.J.R., Phillips, D.M.P., and Butler, J.A.V., (1966) Arch. Biochem. Biophys., 113, 338

17. Laurence, D.J.R., Simson, P., and Butler, J.A.V., (1963) Biochem. J. 87, 200

18. Davison, P.F., and Butler, J.A.V., (1954) Biochim. Biophys. Acta., 15, 439

19. Stevely, W.S., and Stocken, L.A., (1966) Biochem. J., 100, 20

20. Adler, A. J., Schaffhausen, B., Langan, T.A., and Fasman, G.D., (1971) Biochemistry, 10, 909

21. Monod, J., Changeus, J.P., and Jacob, F., (1963) J. Mol. Biol., 6, 306

22. Elgin, S.C.R., and Bonner, J., (1970) Biochemistry, 9, 4440

23. Shirey, T., and Huang, R.C.C., (1969) Biochemistry, 8, 4138

24. Benjamine, W., and Gellhorn, A., (1968) Proc. Natl. Acad. Sci. US., 59, 262

25. Platz, R.D., Kish, V.M., and Kleinsmith, L.J., (1970) FEBS Lett., 12, 38

26. MacGillivray, A.J., Carroll, D., and Paul, J., (1971) FEBS Lett.,.13, 204

27. Kleinsmith, L.J., Heidema, J., and Carroll, A., (1970) Nature, 226, 1025

28. Spelsberg, T.C., and Hnilica, L.S., (1970) Biochem. J., 120, 435

29. Gilmour, R.S., and Paul, J., (1970) FEBS Lett., 9, 242

30. McCarthy, B.J., and Church, R.B., (1970) Ann. Rev. Biochem. 39, 318

31. Spelsberg, T.C., Steggles, A.W., O'Malley, B.W., (1971) 246, 4188

32. Spelsberg, T.C., Steggles, A.W., Chytil, F., and O'Malley, B.W., (1972) J. Biol. Chem., 247, 1368

33. Tsai, S.Y., Tsai, M.J., Schwartz, R., Kalime, M., Clark, J.J., and O'Malley, B.W., (1975) Proc. Natl. Acad. Sci. US., 72, 4228

34. Huang, R.C.C., and Bonner, J., (1965) Proc. Natl. Acad. Sci. US., 54, 960

35. Bonner, J., Chalkley, R.G., Dahmus, J., Fambrough, D., Fujimura, F., Huang, R.C.C., Huberman, J., Jensen, R., Marushige, K., Ohlenbusch, H., Olivera, B.M., and Widholm, J., (1968) Methods in Enzymology, 12b. Academic Press, New York.

36. Jacobson, R.A., and Bonner, J., (1968) Biochem. Biophys. Res. Commun., 33, 716

37. Dahmus, M., and McConnell, D., (1969) Biochemistry, 8, 1534

38. Mayfield, J.E., and Bonner, J., (1971) Proc. Natl. Acad. Sci. US., 68, 2652

39. Holmes, D., and Bonner, J., (1973) Biochemistry, 12, 2330

40. Tunis-Scheider, J.J.B., and Maestre, M.F., (1970) J. Mol. Biol. 52, 521

41. Davis, D.R., (1967) Ann. Rev. Biochem., 36, 321

42. Watson, J.D., and Crick, F.H.C., (1953) Nature, 171, 964

43. Arnott, S., (1970) Progr. Biophys. Mol. Biol., 21, 267

44. Tuan, D.Y.H., and Bonner, J., (1969) J. Mol. Biol., 45, 59

45. Bradbury, E.M., Crane-Robison, C., Goldman, H., Rattle, H.W.E., and Stephens, R.M. (1967) J. Mol. Biol. 29, 507

46. Shih, T.Y., and Fasman, G.D., (1971) Biochemistry 10, 1675

47. Adler, A.J., and Fasman, G.D., (1971) J. Phys. Chem. 75, 1516

48. Leffak, IM., Hwan, J.C., Li, H.J., and Shih, T.Y., (1974) Biochemistry, 13, 1116

49. Hwan, J.C., Leffak, I.M., Li, H.J., Huang, PC., and Mura, C., (1975) Biochemistry, 14, 1390

50. Permogorov, V.I., Debabov, V.G., Sladkova, I.A., Rebentish, B.A., (1970) Biochim. Biophys. Acta, 199, 556

51. Simpson, R.T., and Sober, H.A., (1970) Biochemistry, 9, 3103

52. Littau, V.C., Burdick, C.J., Allfrey, V.G., and Hirsky, A.E., (1965) Proc. Natl. Acad. Sci. US., 54, 1204

53. Richards, B.M., Pardon, J.F., and Hirst, E., (1970) Biochem. J., 117, 59

54. Richards, B.M., and Pardon, J.F., (1970) Exp. Cell Res. 62, 184

55. Olins A.L., and Olins, D.E., (1974) Science, 183, 330

56. D'Anna, J.A., and Isenberg, I., (1974) Biochemistry, 13, 4987 and 4992

57. Weintraub, H., and Van Lente, F (1974) Proc. Natl. Acad. Sci. US., 71, 4249

58. Baldwin, J.P., Boseley, P.G., Bradbury, E.M., and Ibel, K., (1975) Nature, 253, 245

59. Sober, H.A., Schlossman, S.F., Yaron, A., Latt., S.A., and Rushizky, G.W., (1966) Biochemistry, 5, 3608

60. Carroll, D., (1972) Biochemistry, 11, 421

61. Yu, S., and Li, H.J., (1973) Biopolym. 12, 2777

62. Pinkston, M.F., and Li, H.J., (1974) Biochemistry, 13, 5227

63. Santella, R.M., and Li H.J., (1974) Biopoly. 13, 1909

64. Latt, and Sober, H.A., (1967) Biochemistry 6, 3307

65. Leng, M., and Felsenfeld, G., (1966) Proc. Natl. Acad. Sci. US., 56, 1325

66. Shapiro, J.T., Stannard, B.S., and Felsenfeld, G., (1969) Biochemistry, 8, 3233

67. ibid.

68. Olins, D.E., Olins, A.L., and von Hippel, P.H., (1967) J. Mol. Biol. 24, 157

69. Lees, C.W., and Von Hippel, P.H., (1968) Biochemistry, 7, 2480

70. Li, H.J., Chang, C., Weiskopf, M., (1972) Biochem. Biophys. Res. Commun. 47, 883

71. Shih, T.Y., and Bonner, J., (1969) Biochim. Biophys. Acta, 182, 30

72. Panyim, S., Ph.D dissertation.

73. Li, H.J., and Bonner, J., (1971) Biochemistry, 10, 1461

74. Crothers, D.M., and Zimm, B.H., (1964) J. Mol. Biol. 9, 1

75. Crothers, D.M., (1968) Biopolym. 6, 1391

76. Tsubio, M., Matsui, K., and Tsao, P.O.P. (1966) J. Mol. Biol. 15, 256

77. Ohlenbush, H.H., Oivera, B.M., Tuan, D., and Davidson, N. (1967) J. Mol. Biol. 25, 229

78. Li, H.J., (1973) Biopolym. 12, 287

79. Nelson, R.C., and Johnson, W.C. Jr., (1971) Biochem. Biophys. Res. Commun. 41, 211

80. Green, G., and Mahler, H.R., (1971) Biochemistry, 10, 2200

81. Haynes, K., Garrett, R.A., and Gratzner, W.B., (1970) 9, 4410

82. Chang, C., Weiskopf, E., and Li, H.J., (1973) Biochemistry, 12, 3028

83. Marmur, J. (1961) J. Mol. Biol. 3, 201

84. Ivanov, V.I., Michenkova, L.E., Schyolkina, A.K., and Poletayev, A.I., (1973) Biopolym., 12, 89

85. Schildkraut, C., and Lifson, S., (1965) Biopolym. 3, 195

86. Yu, S., and Li, H.J., submitted.

87. Ansevin, A.T., Hnilica, L.S., Spelsberg, T.C., and Kahn, S.L., (1971) Biochemistry 10, 4793

88. Li. H.J., Chang, C., Evagelinou, Z., and Weiskopf, M., (1975) Biopolym. 14, 211

89. Paul, J., and Gilmour, R.S., (1966) J. Mol. Biol. 16, 242

90. Bonner, J., Dahnus, H.E., Fambrough, D., Huang, R.C.C., Marushige, K., and Tuan, D.Y.H., (1968) Science, 159, 49

91. Li, H.J., Chang, C., and Weiskopf, M., (1973) Biochemistry, 12, 1763

92. Hanlon, S., Johnson, R.S., and Chan, A., (1974) Biochemistry, 13, 3963

93. Hanlon, S., Hohnson, R.S., and Chan,A., (1974) Biochemistry, 13, 3972

94. Li, H.J., Chang, C., Weiskopf, M., Brand, B., Rotter, A., (1974) Biopolym., 13, 649

95. Clark, R.J., and Felsenfeld, G., (1971) Nature New Biology, 229, 101

96. Mirsky, A.E., (1971) Proc. Natl. Acad. Sci., US 68, 2945

97. Itzhaki, R.F., (1971) Biochem. J. 125, 221

98. Huang, R.C.C., Bonner, J., and Murray,K., (1964) J. Mol. Biol. 8, 54

99. Bekhor, I., Kung, G.M., and Bonner, J., (1969) J. Mol. Biol., 39, 351

100. Shih, T.Y., and Lake, R.S., (1972) Biochemistry, 11, 4811

101. Bartley, J.A., and Chalkley, R., (1973) Biochemistry, 12, 428

102. Sheraga, H.A. Protein Structure (1961) p. 125. Acad. Press, NY

103. Evin, K., Konigsher, P., and Cole, D.R., (1970) Biochem. J. 141, 389

104, Marushige, K., and Dixon, G.H., (1971) J. Biol. Chem 18, 5799

105. Poland, D., and Sheraga, H.A., (1966) J. Chem. Phys. 45, 1456

106. Cohen, R.T., and Crothers, D.M., (1970) Biochemistry, 9, 2533

107. Brahams, S., and Ris, H., (1971) J. Mol. Biol. 55, 325

108. Pardon, J.F. and Wilkins, M.H.F., (1967) Nature, 215, 508

109. Polacow, I., and Li, H.J., submitter

110. Oudet, M., Cross-Bellard, and Chambon, P., Cell, 4, 281

111. Crick, F.H.C., and Klug, A., (1975) Nature, 255, 530

112. Li, H.J., "Chromatin Structure- A Model" presented in Molecular Biology of the Mammalian Genetic Apparatus- Its Relationship to Cancer, Aging and Medical Genetics. Ed. P.O.P. Tso, Associated Scientific Publishers. In press.

113. Van Holde, K.E., Sahasrabuddhe, C.G., and Shaw, B.R., (1974) Nucleic Acid Research, 1, 1579

114. Li, H.J., Wickett, R., Craig, A.M., and Isenberg, I., (1972) Biopolym., 11, 375

115. Kornberg, R.D., (1974) Science, 184, 868

116. Kornberg, R.D., and Thomas, J.D., (1974) Science, 184, 865

117. Martison, H.G., and McCarthy, B.J., (1975) Biochemistry, 14, 1073

118. Li, H.J., (1975) Nuc. Acids Res. 2, 1275